

**THE EFFECT OF CRYSTALLINE PHASE MORPHOLOGY ON THE STRUCTURE
AND PROPERTIES OF POLYPROPYLENE IMPACT COPOLYMERS**

by

TEBOHO SIMON MOTSOENENG (B.Sc. Hons.)

Submitted in accordance with the requirements for the degree

MASTER OF SCIENCE (M.Sc.)

Department of Chemistry

Faculty of Natural and Agricultural Sciences

at the

UNIVERSITY OF THE FREE STATE (QWAQWA CAMPUS)

SUPERVISOR: Prof AS Luyt

CO-SUPERVISOR: Prof AJ van Reenen, University of Stellenbosch

December 2012

DECLARATION

We, the undersigned, hereby declare that the research in this thesis is Mr Motsoeneng's own original work, which has not partly or fully been submitted to any University in order to obtain a degree.

TS Motsoeneng

Prof AS Luyt

DEDICATION

This work is dedicated to my mother (Elisa Motsoeneng), and my father (Joseph Motsoeneng) for their consistent support throughout all these years of my academic training, and not forgetting the entire Motsoeneng family.

ABSTRACT

The present study covers the preparation and the characterisation of β -nucleated impact polypropylene copolymer (NA-IPC), and its fractions prepared through temperature rising elution fractionation (TREF). Calcium stearate (CaSt), as well as pimelic (Pim) and adipic (Adi) acids, were doped into IPC as a mono- or bi-component nucleating agents (NAs) at varying mass ratios. The non-isothermal crystallisation kinetics, and the effect of the NAs on the morphology, thermal and mechanical properties were investigated. However, only thermal properties of the fractions were investigated on. DSC and XRD results revealed that IPC nucleated with Pim and Pim-CaSt nucleants induced up to 90% β -crystals, while Adi and Adi-CaSt formed only about 17% β -crystals. This was associated with the strong nucleation efficiency (NE) of Pim. The 110C and 120C fractions treated with Pim-based NAs were the only fractions that formed β -crystals, probably due to their higher isotacticity. The non-isothermal crystallisation kinetics showed that the crystallization of IPC and NA-IPC followed a three-dimensional growth with athermal nucleation mechanism. The SEM images showed no changes in the distribution and size of the rubber phase after treatment with NAs. FTIR showed that none of the NAs chemically reacted with IPC, and the chemical structure of the polymer was thus intact during the treatment. Formation of β -crystals in the samples with Pim and Pim-CaSt improved the impact strength by more than 50%. However, incorporation of Adi, CaSt, and Adi-CaSt nucleants had little effect on the impact resistance of IPC. The tensile properties such as Young's modulus, yield stress and stress at break changed very little for the nucleated samples. On the other hand, the elongation at yield and at break increased. This is an indication of the strong ductility of IPC caused by the formation of β -crystals. The glass transition temperatures shifted slightly to higher temperatures with increasing β -crystal contents, due to the immobilization of the chains in the amorphous phase in the vicinity of the β -lamellae.

TABLE OF CONTENTS

	Page
DECLARATION	i
DEDICATION	ii
ABSTRACT	iii
TABLE OF CONTENTS	iv
LIST OF ABBREVIATIONS	vii
LIST OF TABLES	ix
LIST OF FIGURES	x
CHAPTER 1 (GENERAL INTRODUCTION)	1
1.1 Background	1
1.2. Objectives of the study	5
1.3 Thesis outline	5
1.4 References	6
CHAPTER 2 (LITERATURE REVIEW)	9
2.1 Introduction	9
2.1.1 Classification of nucleating agents, production, and utilities	9
2.2 β -nucleated isotactic polypropylene (β -NA-iPP)	10
2.2.1 Preparation and morphology	10
2.2.2 Thermal properties	11
2.2.3 Mechanical properties	13
2.3 β -nucleated isotactic polypropylene blends	14
2.3.1 Preparation and morphology	14
2.3.2 Thermal properties	16
2.3.3 Mechanical properties	18
2.4 References	19

CHAPTER 3 (MATERIALS AND METHODS) 26

3.1	Materials	26
3.1.1	Impact polypropylene copolymer (IPC)	26
3.1.2	Pimelic acid	26
3.1.3	Adipic acid	26
3.1.4	Calcium stearate	26
3.1.5	Acetone	26
3.1.6	Irganox 1010 and Irgafos 168 (antioxidant)	27
3.2	Preparation of IPC nucleated samples	27
3.2.1	Dissolution of nucleating agents	27
3.2.2	Blending of nucleating agents and IPC	27
3.3	Preparation of TREF fractions	28
3.3.1	Temperature rising elution fractionation (TREF)	28
3.3.2	Blending of nucleating agents and TREF fractions	29
3.4	Sample analysis	30
3.4.1	Differential scanning calorimetry (DSC)	30
3.4.2	Thermogravimetric analysis (TGA)	31
3.4.3	Dynamic mechanical analysis (DMA)	31
3.4.4	Tensile testing	32
3.4.5	Impact testing	32
3.4.6	Scanning electron microscopy (SEM)	33
3.4.7	Fourier transform infrared (FTIR) spectroscopy	33
3.4.8	Wide angle x-ray diffraction (WAXD)	34
3.5	References	34

CHAPTER 4 (RESULTS AND DISCUSSION) 36

4.1	Differential scanning calorimetry (DSC)	36
4.1.1	Unfractionated IPC	36
4.1.2	Fractionated IPC	42
4.1.3	Nonisothermal crystallisation behaviour	44
4.2	Wide angle x-ray diffraction	50
4.3	Fourier transform infrared (FTIR) spectroscopy	53

4.4	Scanning electron microscopy (SEM)	56
4.5	Thermogravimetric analysis (TGA)	60
4.6	Tensile and impact properties	63
4.7	Dynamic mechanical analysis (DMA)	66
4.8	References	68
CHAPTER 5 (CONCLUSIONS)		71
ACKNOWLEDGRMENTS		73
APPENDICES		75

LIST OF ABBREVIATIONS

3988	1,3:2,4-bis(3,4-dimethylbenzylidene)
ABS	Acrylonitrile-butadiene-styrene
Adi	Adipic acid
α -iPP	Alpha crystals in isotactic polypropylene
α -NA	Alpha nucleating agent
ATR	Attenuated total reflectance
β -iPP	Beta crystals in isotactic polypropylene
β -NA	Beta nucleating agent
β -NA-iPP	β -nucleated isotactic polypropylene
CaSt	Calcium stearate
CMR648	Commercial name of impact polypropylene copolymer
ΔE	Crystallisation activation energy
$\Delta H_{m,\alpha}$	Melting enthalpies of the α -crystals
$\Delta H_{m,\beta}$	Melting enthalpies of the β -crystals
DMA	Dynamic mechanical analysis
DSC	Differential scanning calorimetry
E	Young's modulus of elasticity
EO	Metallocenic ethylene-octene copolymer
EPDM	Ethylene-propylene-diene terpolymer
EPR	Ethylene-propylene rubber
EVA-g-MA	Maleic anhydride grafted poly(ethylene-co-vinyl acetate)
FTIR	Fourier transform infrared
γ -phase	Gamma crystalline phase
HPN-68	Heptane dicarboxylate
IPC	Impact polypropylene copolymer
iPP	Isotactic polypropylene
IR	Infrared
K_{DSC}	Amount of β -crystals calculated from DSC
K-resin	Styrene-butadiene
K_{XRD}	Amount of β -crystals calculated from XRD
MA	Maleic anhydride

MFR	Melt flow rate
NA11	sodium 2,2'-methylene-bis(4,6-di-tert-butylphenyl) phosphate DCHT N,N'-dicyclohexylterephthalamide
NA-iPP	Nucleated isotactic polypropylene
NAs	Nucleating agents
NE	Nucleation efficiency
PA	Polyamide
PB	Polybutadiene
Pim or PA	Pimelic acid
POE-g-MA	Maleic anhydride grafted poly(ethylene octane)
PP	Polypropylene
PP-g-GMA	Glycidyl methacrylate grafted polypropylene)
PVCH	Poly(vinylcyclohexane)
PVDF	Poly(vinylidene-fluoride)
SAN	Styrene-acrylonitrile
SEBS	Styrene-ethylene butylene-styrene triblock copolymer
SEM	Scanning electron microscopy
SMSs	Super-molecular structures
T_c	Crystallisation peak temperature
T_{c1}	Crystallisation peak temperature of the non-nucleated sample
T_{c2max}	Crystallisation peak temperature of the self-nucleated polymer
T_{cNA}	Crystallisation peak temperature of the nucleated sample
TEM	Transmission electron microscopy
T_g	Glass transition temperature
TGA	Thermogravimetric analysis
TREF	Temperature rising elution fractionation
$T_{\alpha1}$	Melting peak temperatures of the α -polymorphs
$T_{\beta1}$	Melting peak temperatures of the β -polymorphs
WBG	Rare earth nucleating agents
w_{IPC}	Weight fraction of IPC
X_{DSC}	Total crystallinity calculated from DSC
XRD	X-ray diffraction
X_{XRD}	Total crystallinity calculated from XRD

LIST OF TABLES

		Page
Table 3.1	Mass ratios of the respective nucleating agents and the total mass of the IPC matrix in the blends	27
Table 4.1	Crystallisation peak temperatures (T_c), and melting peak temperatures of the β - and α - polymorphs ($T_{\beta 1}$ and $T_{\alpha 1}$), in IPC	37
Table 4.2	Summary of the DSC melting and crystallisation results of the investigated samples	42
Table 4.3	Crystallisation half-life ($t_{1/2}$) at different cooling rates for neat and nucleated IPC	48
Table 4.4	Nonisothermal crystallisation kinetics parameters determined by the Ozawa-Avrami and Kissinger methods	50
Table 4.5	Summary of the XRD crystalline phase parameters of the investigated samples	53
Table 4.6	TGA results of all the samples	62
Table 4.7	Summary of tensile and impact results for pristine IPC and the nucleated samples	64

LIST OF FIGURES

		Page
Figure 3.1	Schematic representation of separation mechanism of TREF	29
Figure 4.1	The nucleation efficiency of IPC nucleated with individual and compounded nucleating agents	37
Figure 4.2	DSC heating curves of IPC nucleated with individual (Pim, CaSt) and compounded nucleants	38
Figure 4.3	DSC heating curves of IPC nucleated with individual (Adi, CaSt) and compounded nucleants	39
Figure 4.4	DSC cooling curves of IPC nucleated with individual (Pim, CaSt) and compounded nucleants	41
Figure 4.5	DSC cooling curves of IPC nucleated with individual (Adi, CaSt) and compounded nucleants	41
Figure 4.6	DSC heating curves of nucleated and non-nucleated 80C, 90C, and 100C fractions	43
Figure 4.7	DSC heating curves of nucleated and non-nucleated 110C, 120C, and 140C fractions	44
Figure 4.8	DSC cooling curves of the pristine IPC during non-isothermal crystallisation at different cooling rates	46
Figure 4.9	DSC cooling curves of IPC nucleated with a bi-component Pim-CaSt (1:2) nucleant during non-isothermal crystallisation at different cooling rates	47
Figure 4.10	Crystallisation peak temperatures of pure and nucleated IPC at different cooling rates	47
Figure 4.11	Relative degree of crystallinity versus crystallisation time for pristine IPC	49
Figure 4.12	Relative degree of crystallinity versus crystallisation time for IPC/Pim-CaSt (1:2)	49
Figure 4.13	XRD spectra of nucleated and non-nucleated IPC with individual (Pim, CaSt) and compounded nucleants	51
Figure 4.14	XRD spectra of nucleated and non-nucleated IPC with individual (Adi, CaSt) and compounded nucleants	52
Figure 4.15	FTIR spectra of individual and compounded nucleating agents	53

Figure 4.16	FTIR spectra of IPC samples prepared in the absence and presence of individual and compounded Pim and CaSt	54
Figure 4.17	FTIR spectra of IPC samples prepared in the absence and presence of individual and compounded Adi and CaSt	55
Figure 4.18	SEM micrographs of unetched (a) pristine IPC, (b) IPC/Pim, (c) IPC/Pim-CaSt (1:2), and (d) IPC/Pim-CaSt (1:3)	56
Figure 4.19	SEM micrographs of unetched (a) IPC/CaSt, (b) IPC/Adi, (c) IPC/Adi-CaSt (1:2), and (d) IPC/Adi-CaSt (1:3)	57
Figure 4.20	SEM micrographs of etched (a) pristine IPC, (b) IPC/Adi, (c) IPC/Pim, and (d) IPC/CaSt	58
Figure 4.21	SEM micrographs of etched (a) pristine IPC, (b) IPC/Pim, (c) IPC/Pim-CaSt (1:2), and (d) IPC/Pim-CaSt (1:3) samples	59
Figure 4.22	TGA curves of IPC and the individual nucleating agents	60
Figure 4.23	TGA curves of pristine IPC and IPC nucleated with individual (Pim, CaSt) and compounded nucleants	61
Figure 4.24	TGA curves of pristine IPC and IPC nucleated with individual (Adi, CaSt) and compounded nucleants	62
Figure 4.25	Charpy impact strength of pristine IPC and all the nucleated IPC samples	63
Figure 4.26	Elongation at break of pristine IPC and all the nucleated IPC samples	64
Figure 4.27	Young's modulus of pristine IPC and all the nucleated IPC samples	65
Figure 4.28	DMA $\tan \delta$ curves for pure IPC and the nucleated (Pim, CaSt) samples	66
Figure 4.29	DMA $\tan \delta$ curves for pure IPC and the nucleated (Adi, CaSt) samples	67
Figure 4.30	DMA loss modulus curves for pure IPC and the nucleated (Pim, CaSt) samples	67

CHAPTER 1

GENERAL INTRODUCTION

1.1 Background

Isotactic polypropylene (iPP) is a semicrystalline commodity polymer which, by virtue of its nature, is described as a polymorphic material. In essence, it possesses several crystallographic forms, namely monoclinic (α), trigonal (β), triclinic (γ), and smectic forms. The α -modification is a thermodynamically stable and very common crystalline phase of iPP. The trigonal form is known by its metastable character and has excellent properties compared to the other crystalline phases. The triclinic phase is normally established in low-molecular weight iPP and in propylene random copolymers under very high pressure conditions. The smectic mesophase is a middle phase between the ordered and disordered (amorphous) phases [1-5]. The polymorphs (α , β , γ and smectic phase) of polypropylene have a certain structural feature in common, because they share three helical (3_1) conformations in the crystal lattice structure. The structural instability of the beta form can generate supermolecular structures (SMSs) in a certain range of crystallisation temperatures. The features of the β -modification are readily affected by the crystallisation conditions, the presence of inappropriate particles, and the melting history of the sample [2,3,5,6].

β -hedrites, identified by their hexagonal configuration (hexagonites), can be found in β -nucleated resins at reasonably high crystallisation temperatures, whereas β -spherulites are produced in a very inactive melt. β -cylindrites can be traced under an adequate mechanical load in the melt. The development of trans-crystalline structures is usually stimulated by the presence of additives (β -nucleants). A biaxially oriented β -iPP sample can be formed by epitaxial crystallisation occurring at the surface of a nucleating agent. The seemingly single crystallite rods also fall under SMSs of the β -phase. A spheriform cluster of primary crystallite structures with spherical symmetry distinguish the β -spherulites. Crystallisation taking place in PP in the molten state and under a high rate of super-cooling induce these spherulitic structures. β -spherulites have negative radial and/or banded type of spherulites which are formed during the process of crystallisation. Negative banded β -spherulites are formed in their longitudinal direction and are composed of twisted lamellar crystals. The β -spherulites have a stronger negative birefringence than the α -spherulites [3,7-10].

The presence of an active β -nucleating agent in a specimen can create β -hedritic structures at high temperatures of isothermal crystallisation (130-140 °C). β -hedrites are known by their polygonal patterns composed of lamellar crystallites. Maturity of the developed structure and the dependence of view angle can make hedrites appear differently and can be seen as hexagonites, axialites, ovalites, or quasi-spherulites [9-11]. β -hedrites are usually formed when the partly crystallised specimen is frozen at early stages of crystallisation. β -hexagonites are the most spectacular structures of the β -hedrites. β -hexagonites are normally represented by multilayer clusters of lamellar crystalline structures situated flat-on. Axialites are rod-like crystals having a strong negative birefringence. At the later stage of crystallisation the oval shapes, called ovalites, develop from axialites. Quasi-spherulites are immature spherulites formed at the transition state between the hedritic and spherulitic structures. β -cylindrites are a type of SMS formed by the use of injection molding, around the neighbouring zones of sheared melt [7,9,12].

The development and growth of a β -phase reveals interesting features when it undergoes β - to α -transformation (β - α phase transition). This phenomenon occurs when α -nuclei evolve onto a growing β -crystal which eventually ends up being segmented α -spherulites. Then the newly formed phase is a β - α twisted structure having a core of β -crystals overgrown by α -crystals. From a kinetics perspective, the growth rate of the α -phase is higher than that of the β -phase. In essence, β - α recrystallisation is likely to be encouraged by α -recrystallisation from semi-molten β -crystals during secondary crystallisation below a critical temperature ($T_R \sim 100$ -105 °C) [1,7,9]. The beta-alpha transition is susceptible to both thermal history and annealing through a step-by-step temperature gradient. Annealing is strictly dependent on the period of exposure. Mechanical deformation also falls under the contributing factors controlling β - α transformation. The beta phase in this case shows good mechanical stability up to the yield point [2,3,10,13,14].

Despite its polymorphic character, iPP shows very poor impact behaviour at lower temperatures. Due to this performance, some of the industrial applications are limited. To overcome this problem, elastomeric particles are introduced or propylene monomers are copolymerised with other olefin monomers [15]. Commercially synthesised impact polypropylene is normally produced by a two-reactor sequential polymerisation. The first

reaction is the homopolymerisation of the propylene monomer, followed by the copolymerisation of ethylene-propylene monomers in the second reactor. The resulting polymer is known as a high impact polypropylene copolymer (IPC), where the constituents are ethylene-propylene rubber (EPR), ethylene-propylene segmented copolymers and ethylene-propylene random copolymers. EPR is usually a discontinuous rubber phase which is heterogeneously dispersed in the continuous phase. Despite its molecular complexity, IPC has promising properties and it can be readily processed. IPC has a very high impact resistance which depends on the amount of the EPR phase added. Since a nucleating agent can manipulate the crystalline phase of iPP, it is possible that a β -nucleant can enhance the impact resistance of IPC even further, since iPP forms the major part of IPC [15,16,17].

Numerous investigations have recently been dedicated to PP copolymers due to their good mechanical properties for industrial applications. The introduction of fillers or additives in copolymers results in beneficial properties. Adding a β -nucleant into an iPP binary system changes the morphology and properties of the blend [18]. The nature and content of an elastomeric phase, which has an α -nucleating effect in the copolymer, control the efficiency of nucleated PP based systems. The β -nucleator efficiency to nucleate PP is strongly dependent on the crystallisation temperature (T_c) of the second component. Suppose the T_c of the second component is higher than that of PP, then there will be an insignificant impact on the promotion of β -modification. However, if the T_c is lower than that of PP, the number of β -crystals will decline [19].

iPP primarily crystallises into the α -crystals (α -iPP) under classical crystallisation conditions, while the β -crystals uncommonly occur unless induced under special conditions. The α -crystals form a thermodynamically stable phase [3]. The development of the β -form in commercial iPP could be induced by either a crystallisation temperature gradient, or by crystallisation induced by external strain, or by the introduction of selective β -nucleating agents. However, the particle distribution, size, as well as the dissolution of β -nucleant in iPP can influence the formation of the resulting β -form. Amongst all the possible methods used to form hexagonal crystals, the addition of a highly selective β -nucleating agent in iPP gives high β -contents [3,6,10]. However, not every nucleating agent is feasible for facilitating β -crystallisation, since some promote α -crystallization. Several β -nucleators are proven to have a fairly small ability in boosting β -crystal formation, since they promote both α - and β -crystal

formation. This will normally result in a nucleated semicrystalline iPP with a fairly small amount of β -crystals [1,3,20].

β -nucleating agents can be categorised into two classes: unsupported and bi-component β -nucleating agents. It was found that bi-component β -nucleants are more efficient than unsupported β -nucleants. When introducing a combination of different β -nucleants into iPP through *in situ* chemical reaction or mechanical blending, the β -nucleants react to form a substance that is more effective in initiating β -nucleation [4,10]. It was found in some cases that β -nucleation gave rise to more transparent materials, in which case the β -nucleating agents was referred to as clarifiers [20]. To accumulate a large β -crystal content in β -nucleated iPP specimens, some important prerequisites should be taken into account during processing. In particular, the processing should be between the upper and lower limits of the critical temperature of crystallisation ($T(\alpha\beta) - T(\beta\alpha)$), and in the presence of active and selective β -nucleants. To suppress the formation of α -crystals, a feasible flow and relaxation time should be chosen. The incorporation of α -nucleants or polymers with a high α -promoting activity into nucleated β -iPP, must also be avoided. However, in the event where the iPP internal lattice structure has a better match with that of the polymeric nucleating agent, the nucleation activity of the iPP matrix will be favoured [4,8,9,18]. The preparation of β -iPP blends is fairly simple if the second polymer component is an amorphous polymer, especially if the second polymer component remains in the molten state during crystallisation [21]. This ensures that the second polymer component does not inhibit the formation of β -crystals even if it has an active α -nucleating ability.

Several processing methods are considered to be significant when introducing β - and/or α -nucleants in iPP or iPP-based copolymers. Every processing method has its own unique impact on the resulting β -content. The most widely used methods for processing binary/ternary polymer-nucleant systems are extrusion, as well as compression- and injection-molding. Compression molding is frequently pinpointed as a suitable processing approach leading to a considerable amount of β -content, in comparison with the other two methods [22]. However, injection moulding is a better technique when it comes to the preparation of specifically shaped samples for certain analyses like mechanical testing.

β -modified polymers normally have improved properties compared to α -modified polymers as a result of their meta-stability. However, such properties are strongly dependent on the

way the β -nucleant is incorporated and on its critical concentration. The combination of the rubber phase and β -nucleants supports better formation of β -crystals. The nature and concentration of the elastomer subsequently affect the development of β -crystals. When there are rubber particles and β -crystals, the fracture resistance is strongly improved (increase in elongation at break or toughness). When only the fracture resistance is improved, the stiffness may reduce too much, and therefore, the treatment should be such that there is a functional balance between stiffness and toughness to broaden the range of applications [10,18,23].

1.2. Objectives of the study

The purpose of the current work is to stimulate the β -crystallisation of an IPC and to confirm the presence of these crystals through a number of techniques. The efficiency and selectivity of different β -nucleating agents in various ratios (1:2, 1:3, 1:0) were investigated. Calcium stearate, as well as pimelic and adipic acid, were introduced into IPC as unsupported and supported β -nucleating agents in order to initiate β -crystallisation of the polymer. The crystallisation kinetics was also investigated on some of the nucleated samples and pure IPC. IPC was also fractionated by temperature rising elution fractionation (TREF) and the fractions were treated with a 1:2 ratio of pimelic acid and calcium stearate. All the samples were analysed by X-ray diffraction (XRD), differential scanning calorimetry (DSC), thermogravimetric analysis (TGA), tensile testing, dynamic mechanical analysis (DMA), scanning electron microscopy (SEM), and impact testing in order to confirm the morphology of the different samples, and to establish the influence of different degrees of β -nucleation on the thermal and mechanical properties of IPC.

1.3 Thesis outline

The thesis layout is as follows:

- 📖 Chapter 1: General introduction
- 📖 Chapter 2: Literature review
- 📖 Chapter 3: Materials and methods
- 📖 Chapter 4: Results and discussion
- 📖 Chapter 5: Conclusions

1.4 References

1. A. Menyhard, J. Varga, G. Molnar. Comparison of different β -nucleators for isotactic polypropylene, characterization by DSC and temperature-modulated DSC (TMDSC) measurements. *Journal of Thermal Analysis and Calorimetry* 2006; 83:625-630.
DOI: 10.1007/s10973-005-7498-6
2. X. Li, H. Wu, T. Huang, Y. Shi, Y. Wang, F. Xiang, Z. Zhou. β/α transformation of β -polypropylene during tensile deformation: Effect of crystalline morphology. *Colloid and Polymer Science* 2010; 288:1539-1549.
DOI: 10.1007/s00396-010-2275-x
3. W. Xiao, P. Wu, J. Feng, R. Yao. Influence of a novel β -nucleating agent on the structure, morphology, and nonisothermal crystallization behaviour of isotactic polypropylene. *Journal of Applied Polymer Science* 2009; 111:1076-1085.
DOI: 10.1002/app.29139
4. J.X. Li, W.L. Cheung. Pimelic acid-based nucleating agents for hexagonal crystalline polypropylene. *Journal of Vinyl and Additive Technology* 1997; 3:151-156.
DOI: 10.1002/vnl.10182
5. R. Krache, R. Benavente, J.M. Lopez-Majada, J.M. Perena, M.L. Cerrada, E. Perez. Competition between α , β , and γ polymorphs in a β -nucleated metallocenic isotactic polypropylene. *Macromolecules* 2007; 40:6871-6878.
DOI: 10.1021/ma0710636
6. P. Zhang, X. Liu, Y. Li. Influence of β -nucleating agent on the mechanics and crystallization characteristics of polypropylene. *Materials Science and Engineering* 2006; 434:310-313.
DOI: 10.1016/j.msea.2006.07.049
7. Z. Horvath, I.E. Sajo, K. Stoll, A. Menyhard, J. Varga. The effect of molecular mass on the polymorphism and crystalline structure of isotactic polypropylene. *eXPRESS Polymer Letters* 2010; 2:101-114.
DOI: 10.3144/expresspolymlett.2010.15
8. D. Alcazar, J. Ruan, A. Thierry, B. Lotz. Structural matching between the polymeric nucleating agent isotactic poly(vinylcyclohexane) and isotactic polypropylene. *Macromolecules* 2006; 39:2832-2840.
DOI: 10.1021/ma052651r

9. J. Varga, G.W. Ehrenstein. High-temperature hedritic crystallization of the β -modification of isotactic polypropylene. *Colloid and Polymer Science* 1997; 275:511-519.
DOI: 10.1007/s003960050113
10. M. Dong, Z. Guo, Z. Su, J. Yu. The effects of crystallization condition on the microstructure and thermal stability of isotactic polypropylene nucleated by β -form nucleating agent. *Journal of Applied Polymer Science* 2011; 119:1374-1382.
DOI: 10.1002/app.32487
11. J. Varga, K. Stoll, A. Menyhard, Z. Horvath. Crystallization of isotactic polypropylene in the presence of a β -nucleating agent based on a trisamide of trimesic acid. *Journal of Applied Polymer Science* 2011; 121:1469-1480.
DOI: 10.1002/app.33685
12. G. Zheng, S. Li, X. Zhang, C. Liu, K. Dai, J. Chen, Q. Li, X. Peng, C. Shen. Negative effect of stretching on the development of β -phase in β -nucleated isotactic polypropylene. *Polymer International* 2011; 60:1016-1023.
DOI: 10.1002/pi.3033
13. J. Kotek, I. Kelnar, J. Baldrian, M. Raab. Tensile behaviour of isotactic polypropylene modified by specific nucleation and active fillers. *European Polymer Journal* 2004; 40:679-684.
DOI: 10.1016/j.eurpolymj.2003.12.004
14. H. Bai, Y. Wang, Z. Zhang, L. Hau, Y. Li, L. Lui, Z. Zhou, Y. Men. Influence of annealing on microstructure and mechanical properties of isotactic polypropylene with β -phase nucleating agent. *Macromolecules* 2009; 42:6647-6655.
DOI: 10.1021/ma9001269
15. J. Xu, Z. Fu, Z. Fan, L. Fang. Temperature rising elution fractionation of PP/PE alloy and thermal behaviour of the fractions. *European Polymer Journal* 2002; 38:1739-1743.
DOI: 10.1016/s0014-3057(02)00058-7
16. H. Mahdavi, M.E. Nook. Structure and morphology of a commercial high-impact polypropylene in-reactor alloy synthesized using a spherical Ziegler-Natta catalyst. *Polymer International* 2010; 59:1701-1708.
DOI: 10.1002/pi.2907

17. C. Grein, C.J.G. Plummer, H.-H. Kausch, Y. Germain, Ph. Beguelin. Influence of β nucleation on the mechanical properties of isotactic polypropylene and rubber modified isotactic polypropylene. *Polymer* 2002; 43:3279-3293.
DOI: 10.1016/S0032-3861(02)00135-0
18. N. Fanegas, M.A. Gomez, C. Marco, I. Jimenez, G. Ellis. Influence of a nucleating agent on the crystallization behaviour of isotactic polypropylene and elastomer blends. *Polymer* 2007; 48:5324-5331.
DOI: 10.1016/j.polymer.2007.07.004
19. Z. Yang, Z. Zhang, Y. Tao, K. Mai. Effects of polyamide 6 on the crystallization and melting behaviour of β -nucleated polypropylene. *European Polymer Journal* 2008; 44:3754-3763.
DOI: 10.1016/j.eurpolymj.2008.08.010
20. M. Blomenhofer, S. Ganzleben, D. Hanft, H.W. Schmidt, M. Kristiansen, P. Smith, K. Stoll, D. Mader, K. Hoffmann. Designer nucleating agents for polypropylene. *Macromolecules* 2005; 38:3688-3695.
DOI: 10.1021/ma0473317
21. A. Menyhard, J. Varga. The effect of compatibilizers on the crystallization, melting and polymorphic composition of β -nucleated isotactic polypropylene and polyamide 6 blends. *European Polymer Journal* 2006; 42:3257-3268.
DOI: 10.1016/j.eurpolymj.2006.09.003
22. R.-Y. Bao, W. Yang, X.-G. Tang, B.-H. Xie, M.-B. Yang. Hierarchical distribution of β -phase in compression- and injection-molded, polypropylene-based TPV. *Journal of Macromolecular Science, Part B: Physics* 2011; 50:62-74.
DOI: 10.1080/00222341003609518
23. J. Varga, A. Menyhard. Effect of solubility and nucleating duality of N,N-dicyclohexyl-2,6-naphthalenedicarboxamide on the supermolecular structure of isotactic polypropylene. *Macromolecules* 2007; 40:2422-2431.
DOI: 10.1021/ma062815j

CHAPTER 2

LITERATURE REVIEW

2.1 Introduction

2.1.1 Classification of nucleating agents, production, and utilities

Nucleating agents are compounded or non-compounded materials (organic or inorganic substances) which create spatial active sites for crystals to nucleate within the polymer domain. Nucleating agents are normally added to the polymers in quite low quantities. The type and extent of nucleation influence a wide range of polymer properties such as mechanical properties and stability to heat distortion. Good transparency and the reduction of crystal density can also be observed for certain nucleated specimens. Due to their structural configuration and the spatial arrangement of the atoms, some of the nucleating agents usually possess a fairly compact chemical architecture, giving rise to different polymer properties. Nucleating agents cause polymorphic materials to have a large amount of beta or alpha crystals, or they could enforce both crystalline phases (dual activity). Nucleated polymorphic materials show a γ -crystalline phase when treated under a very high pressure during processing. Matching of the crystal lattice structures of the nucleant and the polymorphic polymer helps to improve the nucleation activity [1-5].

Nucleating agents are usually classified as mono- or bi-component nucleants. The α - and β -nucleating agents are constituted of different arrangements of various compounds such as polydicarboxylic acids, commercially available diaromatic amides, aryl derivatives (sorbitol derivatives), and rare earth nucleating agents (WBG). Polydicarboxylic acids compounded with metallic salts of calcium, sodium, zinc, and iron form dicarboxylate salts [2,6-9]. If two nucleating agents are compounded together to form one individual nucleating agent, it is referred to as a bi-component nucleant. Bi-component nucleants are claimed to have high selectivity and efficiency in improving β -crystals. Since α -crystals form the core phase of polymorphic materials which cannot be completely suppressed, dual nucleation will always be seen. Polymers, particularly isotactic polypropylene (iPP), nucleated with a β -nucleant, have excellent properties which can be used in toughened plastic materials, microporous membranes, microporous fibres, thermoformed articles, and pressurised pipe systems [1,2,9].

2.2 β -nucleated isotactic polypropylene (β -NA-iPP)

2.2.1 Preparation and morphology

Isotactic polypropylene (iPP) is considered as one of the most interesting semicrystalline polymers due to its polymorphic characteristics. Its polymorphism is typically established within the crystalline phase, as this domain is intrinsically composed of somewhat active (robust) and inactive (idle) crystalline forms. In spite of its poor toughness, iPP is the best candidate for β -crystals stimulation because they can be easily activated, under specially appropriate conditions, for example when a selective and efficient beta nucleating agent (β -NA) is added to iPP. It was observed that nucleating agents can change the iPP morphological structure in quite different fashions [4,5,8,10-14]. β -NA can further increase α -crystal formation, or promote β -crystal formation, or enforce disproportionate amounts of α - and β forms. β -nucleated iPP is mostly prepared by extrusion, but sometimes also by injection or compression molding, or by the use of these methods in series. The preparation methods play a crucial role in the inducement of β -modification. Processing methods can bring about significant changes in the iPP crystalline morphology. Very fascinating crystalline features were observed by a number of researchers. Several publications reported that β -crystals could be seen in a situation where there is an excellent nucleation in iPP and a complete dissolution of β -NA. On the other hand, α -nucleating agents (α -NA) cause iPP to have high stiffness and better transparency [3,7,15,16].

Different nucleating agents have been used in iPP to investigate the changes in morphology. Mohmeyer *et al.* [16] investigated the morphological changes in NA-iPP by using different symmetric and asymmetric nucleating agents (dicyclohexyl-substituted 1,4-phenylene-bisamides and cyclohexyl/n-alkyl-substituted 1,4-phenylene-bisamide) with various alkyl chain lengths. The extruded samples were pelletized and processed by injection moulding. The symmetric compounds showed significantly better inducement of β -polymorphism than the asymmetric ones. However, all the additives caused the formation of three-dimensional fibrillar-dendritic structures in the iPP melt, that were observed through optical light microscopy. The mono-alkylated (asymmetric) compounds caused a dramatic decrease in haziness when compared with the symmetric compounds. This was explained to be caused by the presence of β -polymorphs in iPP and by the partial dissolution of the nucleating agent in

the iPP melt. Haziness is normally controlled by either the complete dissolution of the nucleating agent or the formation of β -crystals.

Nucleating agents of different configurations can also change the morphological parameters of iPP, clarity, crystal size, and haziness [15,17]. Menyhard's group [18] investigated the effect of nucleating agents on the iPP crystal structure, and three different nucleating agents were used. Visual studies showed that iPP, nucleated with poly(vinylcyclohexane) (PVCH), developed a large supermolecular structure even when prepared by injection-moulding (injection- and compression-moulding were employed). On the other hand, 1,2,3,4-bis(3,4-dimethyl-benzidilene), a sorbitol derivative nucleant, caused the formation of a microcrystalline pattern in iPP which resulted in an improvement of its optical properties. A classical heterogeneous nucleating agent gave rise to a microspherulitic structure in iPP.

2.2.2 Thermal properties

Semicrystalline polymers such as iPP have homogeneous nucleation and very low crystallisation rates in the absence of additives. However, the presence of catalyst residues (impurities) could cause iPP to show heterogeneous nucleation behaviour. The crystallisation rate of iPP from the molten state depends on the nucleation rate, and on the development of spherulites. The addition of nucleating agents in semicrystalline iPP helps to increase the nucleation rate. The competitive nucleation mechanism of β -nucleation and self α -nucleation during crystallisation would lead to a dual effect of spherulites development [8,11,19,20]. The concentration of nucleants in iPP was investigated by a number of research groups and it was found that it has a considerable impact on the crystallisation rate. Nucleating agents having a high α -nucleating activity such as calcium glutarate and aluminium pimelate induce nucleation and growth of well-developed α -spherulites similar to those found in pure iPP. However, nucleating agents with good activity of β -nucleation, like calcium pimelate and titanium oxide pimelate cause the formation of well-developed β -spherulites at slightly higher temperatures [6,7,9,20,21].

The α -polymorph is thermally the most stable phase, followed by the γ -polymorph, while the β -polymorph is the least stable phase of β -nucleated iPP [5,12]. A number of researchers investigated the crystallisation behaviour of nucleated iPP with different types and contents of NAs [6,10,20]. Xu and co-workers [7] investigated the use of various contents of β -

nucleating agent in iPP. The β -nucleating agent was a complex compound of lanthanum stearate and stearic acid, which was incorporated in iPP in different contents ranging from 0 to 0.4 wt%. Non-isothermal crystallisation kinetics studies were performed on the respective β -nucleated iPP samples, and the results showed that the crystallisation peak temperature of β -nucleated iPP increased relative to that of virgin iPP. The crystallisation activation energy increased at lower β -nucleating agent contents, while the crystallisation rate was reduced inconsistently, because it was dependent on the amounts of α - and β -polymorphs present in iPP. Xiao *et al.* [8] investigated the effect of the different cooling rates on iPP nucleated with a novel rare-earth containing β -nucleating agent (WBG). iPP was nucleated with different contents (0.025 – 0.15 wt%) of WBG, and 0.08 wt% was found as a critical concentration for their system. The authors found that the decreasing of the cooling rates at the critical concentration of WBG increases the amount of β -crystals in iPP. The crystallisation peak temperature (T_c) shifted to higher values with decreasing cooling rates. This was attributed to the rapid crystallisation rate of WBG (0.08 wt%) nucleated iPP when compared to pure iPP.

Duo [22] used a bi-component nucleator composed of different ratios of pimelic acid (PA) and calcium stearate (Cast) to establish the influence of isothermal crystallisation temperature on the nucleation of iPP. The samples were isothermally crystallised at 120 °C for 30 minutes. The results showed that the amount of β -crystals increased with an increase in calcium stearate concentration. Samples constituting 0.15 % PA and 0.5 % Cast were also exposed for 30 minutes to crystallisation temperatures ranging from 100 to 140 °C. The amount of β -crystals increased with increasing crystallisation temperature up to 130 °C, but significantly decreased at 140 °C. Varga *et al.* [23] made the same observations when using 10 to 100 ppm tris-2,3-dimethyl-hexylamide of trimesic acid as a β -nucleating agent in iPP. They obtained large amounts of the β -polymorph in the 110-125 °C range. They explained the observation as being due to the lower crystallisation rates and shorter crystallisation times at the higher temperatures of crystallisation (>130 °C).

Romankiewicz *et al.* [24] structurally characterised iPP doped with different contents of 1,3:2,4-bis(3,4-dimethylbenzylideno) sorbitol and N,N'-dicyclohexyl-2,6-naphthaleno dicarboxy amide as α - and β -nucleant, respectively. They observed that the crystallisation temperature in the presence of both nucleants increased with an increase in nucleant content. However, the β -nucleant was more efficient at lower contents, which was confirmed by a

noticeable increase in T_c when compared with the α -nucleant at the same content. The presence of both nucleants accelerated the crystallisation, as was demonstrated by the crystallisation half-life which reduced from 120 to 105 s.

2.2.3 Mechanical properties

It is well known that iPP have extremely low impact properties at lower temperatures. However, iPP have important spherulitic features in its crystalline phase which can improve the mechanical properties when they are activated. In essence, β -crystals in iPP bring about an excellent toughness and durability when compared to α - and γ -crystals. A number of investigations were done on the mechanical properties of β -nucleated iPP [9,17,25-29]. These researchers deduced that β -crystals cause iPP to have improved elongation at break, higher toughness, and an excellent impact strength. However, the improved toughness comes in most cases at the expense of other properties such as stiffness, heat resistance, and shear strength. The α -polymorph causes iPP to have increased stiffness and, as a result, a combination of α - and β -nucleants should give rise to a good balance between toughness and stiffness. Several published investigations showed that the β -nucleant content can reach a saturation point in an iPP matrix, above which no further improvements in mechanical properties can be observed. This is, however, strongly dependent on the type of β -nucleant employed in the system [1,3,7,8,15,30-32].

β -nucleating agents change the spherulite sizes, resulting in changed mechanical properties. Liu *et al.* [15] investigated the effect of 1,3,2,4-di(p-hydroxyl) benzyldiene sorbitol content (0.1-0.5 wt%) on the mechanical properties of iPP. They observed that the impact strength reached a maximum value when the concentration of nucleating agent was 0.1 wt%. This was ascribed to an increased number of spherulites which resulted in a good spherulite homogeneity. However, when the content was greater than 0.1 wt%, the impact strength reduced gradually because of a rare molecular flexibility caused by an increase in crystallinity. The elongation at break and tensile strength reached maximum values at 0.2 wt% nucleating agent. When the concentration of β -nucleant was increased to 0.3 wt% and more, the homogeneity of the spherulites was poor, leading to a sharp decrease in Young's modulus, elongation at break and impact strength. Luo's group [33] made similar observations where WGB (in the range of 0.025-1 wt%) was added to iPP. They observed a rapid increase in impact strength when the WGB content was less than 0.1 wt%. It was

suggested that WBG dissolved completely below 0.1 wt% and iPP produced a large amount of β -crystals due to a good β -nucleation. In the range of 0.1-0.5 wt%, the amount of β -crystals increased even further and formed a large number of tie molecules which increased the impact strength, but decreased the elongation at break. At a concentration of 1 wt% the WBG dissolved only partially and some of its particles remained in the solid state during processing. This caused iPP to form small and irregular β -crystallites, which weakened the connectivity of inter-crystallites, and elongation at break and impact strength were sharply decreased.

Zhao and Xin [32] used (1,3:2,4-bis(3,4-dimethylbenzylidene) (3988), sodium 2,2'-methylene-bis(4,6-di-tert-butylphenyl) phosphate (NA11), N,N'-dicyclohexylterephthalamide (DCHT) and heptane dicarboxylate (HPN-68)) as nucleating agents to control the mechanical properties of iPP. They added the α - and β -nucleants individually, and combined in various ratios, to iPP. The 3988, NA11, and HPN-68 were found to promote α -nucleation, whereas DCHT promoted β -nucleation of the polymer. The impact strength of the DCHT-nucleated iPP increased, while the flexural modulus decreased. However, the α -NAs showed contradictory behaviour. The iPP nucleated with mixed DCHT/3988 showed mechanical properties close to those of DCHT, while iPP nucleated with DCHT/HPN-68 showed properties similar to iPP nucleated with HPN-68. This was ascribed to the large difference in nucleation efficiency (NE) between the α -NAs (3988 and HPN-68) and the β -NA (DCHT). NA with large NE seemed to have controlled the resulting mechanical properties. When the iPP was doped with a DCHT/NA11 mixture, the tensile and impact strength, as well as flexural modulus, increased. This resulted from a competitive nucleation mechanism occurring between the compounds because of the small difference in NE [20]. The authors concluded that a balance between stiffness and toughness in iPP can be achieved by using suitable α/β compounded NAs, with small differences in NE and feasible ratios between α and β NAs.

2.3 β -nucleated isotactic polypropylene blends

2.3.1 Preparation and morphology

A fair amount of research has been done on the rubber modified NA-iPP morphology. Mechanical- and solution-blending were methods used to prepare rubber modified NA-iPP

blends. The dispersion, size and shape of the elastomeric phase, and its interaction with the iPP matrix, determined the morphology and properties of the blends. Among the most utilised elastomers are ethylene-propylene rubber (EPR), ethylene-propylene-diene terpolymer (EPDM), styrene-ethylene butylene-styrene triblock copolymer (SEBS), and metallocenic ethylene-octene copolymer (EO) [34-38]. The studies showed that when NA-iPP is blended with polymers having good α -crystal formation activity, like poly(vinylidene-fluoride) (PVDF) and polyamide (PA), the β -nucleation in iPP is disturbed. In addition, polymers such as polyamides tend to react with NAs having polar groups, encapsulating the NAs and restricting β -crystal formation. However, some investigations showed that a compatibilizer can bring about good dispersion of the discontinuous phase in iPP, and somehow increase the formation of β -crystals [39-42].

Fanegas and co-workers [35,36] investigated the influence of a nucleating agent on the morphology of iPP blended with SEBS and EO, respectively. The samples were prepared by melt mixing, and transmission electron microscopy (TEM) analysis showed that the particle sizes of the elastomeric particles in both binary systems decreased in the presence of 0.1 wt% methylene-bis(4,6-di-tert-butylphenyl) nucleating agent. However, SEBS showed a narrower distribution of the elastomeric domain size than EO. Polarised optical microscopy observations indicated that the same nucleating agent can dramatically increase the content of crystalline nuclei in both the nucleated iPP/elastomer blends when compared with the non-nucleated binary blends at different predetermined crystallisation temperatures.

Menyhard and Varga [42] investigated the use of maleic anhydride compatibilizer in an NA-iPP/PA6 blend. β -crystals were hardly formed in the uncompatibilized β -nucleated blends because of the selective encapsulation of the β -nucleating agent by PA6. Due to the poor interaction between iPP and PA6, the iPP crystalline phase could not induce trigonal (β -form) formation because of phase separation. When maleic anhydride grafted iPP (MAPP) was blended with the iPP homopolymer and PA6, the resulting reaction between the succinic anhydride groups of the compatibilizer and the amine end groups of PA resulted in a strong interfacial adhesion in the ternary blend. Consequently, the PA6 droplets decreased in size and β -spherulites within the crystalline phase of iPP were observed. Yang and Mai [43] investigated the influence of maleic anhydride grafted poly(ethylene-co-vinyl acetate) (EVA-g-MA) on the morphology of a ternary blend of NA-iPP and PA6. The SEM images revealed a discernible phase separation for the uncompatibilized β -nucleated 80/20 w/w iPP/PA6

blend, and a poor distribution of PA6 in the iPP continuous phase. The authors suggested that this resulted from the poor interaction between the individual components because of a polarity difference. The encapsulation of the β -nucleating agent by PA fractions left iPP with virtually no NA for nucleation. The introduction of EVA-g-MA in these blends improved the formation of the β -polymorph, because the compatibilizer reduced the PA6 crystal size and the resultant encapsulation of NA, and increased the dispersion of the NA and PA6 in iPP. As a result, the blend showed an increase in β -crystal content.

Shangguan *et al.* [34] investigated preparative methods where non-nucleated iPP was blended with EPR using melt and solution mixing methods. The influence of annealing on the blends at 200 °C for different times (5-720 min) was also investigated. The DSC curves of 85/15 w/w iPP/EPR, isothermally crystallised by quenching to 125 °C, showed that the β -polymorph was induced in the melt-mixed matrices, which was not observed for the solution mixed blends. Phase contrast microscopy showed similar images, which indicated that the different preparative methods did not seriously affect the morphologies.

2.3.2 Thermal properties

In a number of papers it was shown that the second party in iPP blends might have a negative or positive impact on the β -nucleation of iPP [35,39,43-46]. A second polymer component with strong α -crystallisation ability in iPP blends hampers the β -nucleation. Such materials can also increase the crystallinity of α -crystals in a β -nucleated iPP. It was reported that β -nucleants tend to be encapsulated within the polymer blended with iPP, thereby minimising the potential of β -NA to nucleate iPP. However, the amount of β -crystals can be increased by using compatibilizers, which brings about a better dispersion of the discontinuous phase in iPP. Compatibilization does not significantly affect the crystallisation temperature of β -nucleated iPP, but can improve the β -nucleation. Several studies showed that the crystallisation temperature and β -nucleation are affected by the content and the nature of the second polymer component blended with NA-iPP. Polymers which are referred to as polymeric nucleating agents such as acrylonitrile-butadiene-styrene can cause β -nucleation in iPP if there is as a perfect match of their crystal lattice structures [35,40-43,47,48].

Yang and co-workers [43] investigated the crystallisation and melting behaviour of β -nucleated iPP/PA6 blends, compatibilized with different contents of maleic anhydride grafted polyethylene-vinyl acetate (EVA-g-MA). It was observed that the T_c increased in both the β -iPP/EVA-g-MA and β -iPP/PA6/EVA-g-MA blends with an increase in the EVA-g-MA content. The amount of β -crystals was, however, considerably higher in the β -iPP/PA6/EVA-g-MA blend and almost unchanged in the β -iPP/EVA-g-MA blend. They suggested that the EVA-g-MA inhibited the crystallisation of β -iPP due to polar interaction between the NA (nano- CaCO_3) and the backbone of EVA-g-MA. This resulted in decreasing T_c and nucleation for iPP. In their other work [40] they showed that 10 wt% of PA6 increased the T_c of non-nucleated iPP. The matrix was, however, rich in the α -polymorph because of the strong ability of α -formation possessed by PA6. DSC results indicated that the addition of PA6 into a β -nucleated iPP decreased the T_c of iPP. The introduction of compatibilizer, PP-g-MA, promoted the dispersion of PA6 through β -iPP, and this resulted in a decreasing domain size and led the matrix to be rich in the β -polymorph.

Yang *et al.* [49] also investigated the crystallisation and melting characteristics caused by different compatibilizers in a β -nucleated iPP/PA6 blend. The compatibilizers were PP-g-MA, EVA-g-MA, POE-g-MA (maleic anhydride grafted poly(ethylene octane)), and PP-g-GMA (glycidyl methacrylate grafted polypropylene). The MA-grafted compatibilizers had a strong compatibilization effect on the blend when compared with the GMA-grafted one, which had a lower polarity. This was observed from DSC curves where the T_c of the β -nucleated iPP/PA6 shifted to lower temperatures after addition of the MA-grafted compatibilizers. The GMA-grafted compatibilizer had a marginal influence on the T_c of the β -nucleated iPP/PA6. XRD results showed the large amount of the β -polymorph for the MA-grafted compatibilizers, while the β -polymorph content was much lower when the GMA-grafted compatibilizer was used. This was attributed to the better dispersion of the β -nucleating agent caused by MA, which resulted in an iPP matrix rich with β -crystals.

Shu *et al.* [47] studied the effect of different polymeric nucleating agents (acrylonitrile-butadiene-styrene (ABS), styrene-butadiene (K-resin), styrene-acrylonitrile (SAN)) on the formation of the β -polymorph in iPP. From the analysis carried out by DSC, the iPP/K-resin and iPP/SAN blends showed a single melting peak at around 165 °C, which was attributed to the α -phase. However, the iPP/ABS blend showed two distinct peaks at about 152 and 168

°C, which were ascribed to the melting peaks of the β - and α -phases, respectively. It was deduced that ABS has a strong ability to induce the β -form of iPP due to its special molecular structure comprising polybutadiene (PB) and SAN blocks.

2.3.3 Mechanical properties

Several investigations were carried out on the mechanical properties of nucleated iPP-based polymer blends. It is well-known that the combination of β -nucleating agents and rubber particles generate a super-proportional route to improve the impact resistance of semicrystalline iPP. This resulted in an undesirable impact strength which sometimes tends to leave iPP with unnecessarily low stiffness. Some researchers tried to find a functional balance between the stiffness and impact strength in iPP/elastomer blends by introducing a nucleating agent in the system [36-38,44]. However, the use of semicrystalline polymers with a strong ability for α -formation negatively affected the nucleation mechanism of iPP. When an α -promoting polymer is blended with β -nucleated iPP and there is an apparent phase separation, there is less energy dissipation for impact strength. β -crystals have a stronger ability to absorb energy than α -crystals. Compatibilization helps in improving the homogeneity of the discontinuous phase and the amount of β -polymorph will somehow be increased, which leads to samples with high energy absorption during deformation [40-43,44,50].

Jang *et al.* [44] investigated the changes in Izod impact strength and flexural modulus caused by EPR content in a β -nucleated and un-nucleated iPP/EPR blend. They observed that the impact strength and flexural modulus increased with an increase in EPR content for both the nucleated and un-nucleated blends. Comparatively, the impact strength and flexural modulus were much higher for the β -nucleated iPP/EPR blends than for the un-nucleated ones. They suggested that the β -nucleant (sodium benzoate) generated many nuclei and microcrystals between the neighbouring spherulites during their growth. As a result, interpenetrating polymer network (IPN) structures could easily be formed which improved certain mechanical properties. The β -crystals caused high-energy dissipation due to the formation of many entanglements caused by microfibrils.

Grein and Gahleimer [38] used NA11 and calcium pimelate as α - and β -nucleants in two iPP/EPR blends which were denoted by PP-1.9 and PP-4.2. The PP-1.9 and PP-4.2 blends

contained rubbery phases with intrinsic viscosity values of 1.9 dl/g and 4.2 dl/g, respectively. The fracture resistance of the β -PP-4.2 blend was roughly close to that of the non-nucleated PP-4.2, whilst it was lower in α -PP-4.2, because of a large inter-particle distance between the rubbery particles. It was suggested that the stress transfer from the rubbery phase to the matrix and the ductility of the β -phase were not so effective. On the other hand, the impact resistance of the nucleated α - and β -PP-1.9 improved because of the lower packing density of the microstructure, the favourable lamellar arrangement and the higher β -phase mobility. It was concluded that NA11 can bring about a good balance between toughness and stiffness in the PP-1.9 grade.

Zhang *et al.* [50] investigated the β to α transformation in both β -iPP and β -iPP/PA6 blends, caused by tensile deformation of different cross-head speeds. They observed that the β -nucleated iPP/PA6 blend did not exhibit a β to α transformation at the various strains tested, whereas the β -iPP did. This was attributed to the decrease in elongation at break observed in the blend. The presence of PA6 in the β -iPP/PA6 blend suppressed the formation of β -crystals and led to a decrease in the elongation at break. It was concluded that the β -phase is mechanically more stable than the α -phase.

2.4 References

1. J. Kotek, M. Raab, J. Baldrain, W. Grellmann. The effect of specific β -nucleation on morphology and mechanical behaviour of isotactic polypropylene. *Journal of Applied Polymer Science* 2002; 85:1174-1185.
DOI: 10.1002/app.10701
2. Q. Dou, Q.-L. Lu, H.-D. Li. Effect of metallic salts of malonic acid on the formation of β crystalline form in isotactic polypropylene. *Journal of Macromolecular Science, Part B: Physics* 2008; 47:900-912.
DOI: 10.1080/0022234082216053
3. Q. Dou, Q.-L. Lu. Effect of calcium malonate on the formation of β crystalline form in isotactic poly(propylene). *Polymers for Advanced Technologies* 2008; 19:1522-1527.
DOI: 10.1002/pat.1160

4. W. Lin, C.T. Bellehumeur. Morphology and coalescence of ethylene copolymers: Influence of thermal treatments and sorbitol nucleating agents. *Journal of Applied Polymer Science* 2006; 102:5443-5455.
DOI: 10.1002/app.25081
5. G. Yang, X. Li, J. Chen, J. Yang, T. Huang, X. Liu, Y. Wang. Crystallization behavior of isotactic polypropylene induced by competition action of β nucleating agent and high pressure. *Colloid and Polymer Science* 2012; 290:531-540.
DOI: 10.1007/s00396-011-2573-y
6. Z. Zhang, C. Wang, Z. Junping, K. Mai. β -nucleation of pimelic acid supported on metal oxides in isotactic polypropylene. *Polymers International* 2012; 61:818-824.
DOI: 10.1002/pi.4148
7. L. Xu, X. Zhang, K. Xu, S. Lin, M. Chen. Variation of non-isothermal crystallization behavior of isotactic polypropylene with varying β -nucleating agent content. *Polymer International* 2010; 59:1441-1450.
DOI: 10.1002/pi.2891
8. W. Xiao, P. Wu, J. Feng, R. Yao. Influence of a novel β -nucleating agent on the structure, morphology, and nonisothermal crystallization behaviour of isotactic polypropylene. *Journal of Applied Polymer Science* 2009; 111:1076-1085.
DOI: 10.1002/app.29139
9. Q. Dou. Effect of metallic salts of pimelic acid and crystallization temperatures on the formation of β crystalline form in isotactic poly(propylene). *Journal of Macromolecular Science, Part B: Physics* 2007; 46:1063-1080.
DOI: 10.1080/00222340701581334
10. Z. Wei, W. Zhang, G. Chen, J. Liang, S. Yang, P. Wang, L. Liu. Crystallization and melting behaviour with individual and compound nucleating agents. *Journal of Thermal Analysis and Calorimetry* 2010; 102:775-783.
DOI: 10.1007/s10973-010-0725-9
11. H. Bai, Y. Wang, Q. Zhang, L. Lui, Z. Zhou. A comparative study of polypropylene nucleated by individual and compounding nucleating agents. I. Melting and isothermal crystallization. *Journal of Applied Polymer Science* 2009; 111:1624-1637.
DOI: 10.1002/app.29153
12. A. Zeng, Y. Zheng, S. Qiu, Y. Guo, B. Li. Mechanical properties and crystallization behaviour of polypropylene with cyclodextrin derivative as β -nucleating agent. *Colloid and Polymer Science* 2011; 289:1157-1166.

- DOI: 10.1007/s00396-011-2441-9
13. Y. Cao, J. Feng, P. Wu. DSC and morphological studies on the crystallization behaviour of β -nucleated isotactic polypropylene composites filled with Kelvar fibers. *Journal of Thermal Analysis and Calorimetry* 2011; 103:339-345.
DOI: 10.1007/s10973-010-0948-9
 14. D.W. van der Meer, B. Pukanszky, G.J. Vancso. On the dependence of impact behavior on the crystalline morphology in polypropylenes. *Journal of Macromolecular Science* 2002; 41:1105-1119.
DOI: 10.1081/MB-120013087
 15. T. Liu, H. Meng, T. Liu, X. Sheng, X. Zhang. Effect of 1,3-2,4-di(p-hydroxyl) benzylidene sorbitol on mechanical properties of isotactic polypropylene. *Polymer-Plastics Technology and Engineering* 2011; 50:1165-1169.
DOI: 10.1080/03602559.2011.574669
 16. N. Mohmeyer, H.-W. Schmidt, P.M. Kristiansen, V. Altstadt. Influence of chemical structure and solubility of bisamide additives on the nucleation of isotactic polypropylene and the improvement of its charge storage properties. *Macromolecules* 2006; 39:5760-5767.
DOI: 10.1021/ma060340q
 17. F. Luo, C. Geng, K. Wang, H. Deng, F. Chen, Q. Fu, B. Na. New understanding in tuning toughness of β -polypropylene: The role of β -nucleated crystalline morphology. *Macromolecules* 2009; 42:9325-9331.
DOI: 10.1021/ma901651f
 18. A. Menyhard, M. Gahleitner, J. Varga, K. Bernreitner, P. Jaaskelainen, H. Oysæd, B. Pukanszky. The influence of nucleus density on optical properties in nucleated isotactic polypropylene. *European Polymer Journal* 2009; 45:3138-3148.
DOI: 10.1016/j.eurpolymj.2009.08.006.
 19. L. Chvatalova, J. Navratilova, R. Cermak, M. Raab, M. Obadal. Joint effects of molecular structure and processing history on specific nucleation of isotactic polypropylene. *Macromolecules* 2009; 42:7413-7417.
DOI: 10.1021/ma9005878
 20. H. Bai, Y. Wang, L. Lui, J. Zhang, L. Han. Nonisothermal crystallization behaviors of polypropylene with α/β nucleating. *Journal of Polymer Science: Part B: Polymer Physics* 2008; 46:1853-1867.
DOI: 10.1002/polb.21520

21. Q. Dou. Effect of calcium salts of glutaric acid and pimelic acid on the formation of β crystalline form in isotactic polypropylene. *Polymer-Plastics Technology and Engineering* 2008; 47:851-857.
DOI: 10.1080/03602550802188938
22. Q. Dou. Effect of the composition ratio of pimelic acid/calcium stearate bicomponent nucleator and crystallization temperature on the production of β crystal form in isotactic polypropylene. *Journal of Applied Polymer Science* 2008; 107:958-965.
DOI: 10.1002/app.26404
23. J. Varga, K. Stoll, A. Menyhard, Z. Horvath. Crystallization of isotactic polypropylene in the presence of a β -nucleating agent based on a trisamide of trimesic acid. *Journal of Applied Polymer Science* 2011; 121:1469-1480.
DOI: 10.1002/app.33685
24. A. Romankiewicz, T. Sterzynski, W. Brostow. Structural characterization of α - and β -nucleated isotactic polypropylene. *Polymer International* 2004; 53:2086-2091.
DOI: 10.1002/pi.1632
25. Y.-H. Chen, G.-J. Zhong, Y. Wang, Z.-M. Li, L. Li. Unusual tuning of mechanical properties of isotactic polypropylene using counteraction of shear flow and β -nucleating agent on β -form nucleation. *Macromolecules* 2009; 42:4343-4348.
DOI: 10.1021/ma900411f
26. G. Zheng, S. Li, X. Zhang, C. Liu, K. Dai, J. Chen, Q. Li, X. Peng, C. Shen. Negative effect on the development of β -phase in β -nucleated isotactic polypropylene. *Polymer International* 2011; 60:1016-1023.
DOI: 10.1002/pi.3033
27. Y.-F. Zhang, Y. Chang, X. Li, D. Xie. Nucleation effects of a novel nucleating agent bicyclic[2,2,1]heptane di-carboxylate in isotactic polypropylene. *Journal of Macromolecular Science* 2011; 50:266-274.
DOI: 10.1080/00222341003648995
28. X. Li, H. Wu, T. Huang, Y. Shi, Y. Wang, F. Xiang, Z. Zhou. β/α transformation of β -polypropylene during tensile deformation: Effect of crystalline morphology. *Colloid and Polymer Science* 2010; 288:1539-1549.
DOI: 10.1007/s00396-010-2275-x
29. A. Menyhard, J. Varga, G. Molnar. Comparison of different β -nucleators for isotactic polypropylene, characterisation by DSC and temperature-modulated DSC (TMDSC) measurements. *Journal of Thermal Analysis and Calorimetry* 2006; 83:625-630.

- DOI: 10.1007/s10973-005-7498-6
30. M. Raab, J. Scudla, J. Kolarik. The effect of specific nucleation on tensile mechanical behaviour of isotactic polypropylene. *European Polymer Journal* 2004; 40:1317-1323.
DOI: 10.1016/j.eurpolm.2004.02.027
 31. L. Balzano, G. Portale, G.W.M. Peters, S. Rastogi. Thermoreversible DMDBS phase separation in iPP: The effects of flow on the morphology. *Macromolecules* 2008; 41:5350-5355.
DOI: 10.1021/ma7024607
 32. S. Zhao, Z. Xin. Nucleation characteristics of the α/β compounded nucleating agents and their influence on crystallization behaviour and mechanical properties of isotactic polypropylene. *Journal of Polymer Science: Part B: Polymer Physics* 2010; 48:653-665.
DOI: 10.1002/poib.21935
 33. F. Luo, K. Wang, N. Ning, C. Geng, H. Deng, F. Chen, Q. Fu, Y. Qian, D. Zheng. Dependence of mechanical properties on β -form content and crystalline morphology for β -nucleated isotactic polypropylene. *Polymers for Advanced Technologies* 2011; 22:2044-2054.
DOI: 10.1002/pat.1718
 34. Y. Shangguan, L. Zhao, L. Tao, Q. Zheng. Formation of β -iPP in isotactic polypropylene/ethylene-propylene rubber blends: Effects of preparation method, composition, and thermal condition. *Journal of Polymer Science: Part B: Polymer Physics* 2007; 45:1704-1712.
DOI: 10.1002/polb.21199
 35. N. Fanegas, M.A. Gomez, C. Macro, I. Jimenez, G. Ellis. Influence of a nucleating agent on the crystallization behaviour of isotactic polypropylene and elastomer blends. *Polymer* 2007; 48:5324-5331.
DOI: 10.1016/j.polymer.2007.07.004
 36. N. Fanegas, M.A. Gomez, I. Jimenez, C. Macro, J.M. Garcia-Martinez, G. Ellis. Optimizing the balance between impact strength and stiffness in polypropylene/elastomer blends by incorporation of a nucleating agent. *Polymer Engineering and Science* 2008; 48:80-87.
DOI: 10.1002/pen.20886

37. C. Grein, C.J.G. Plummer, H.-H. Kausch, Y. Germain, Ph. Beguelin. Influence of β nucleation on the mechanical properties of isotactic polypropylene and rubber modified isotactic polypropylene. *Polymer* 2002; 43:3279-3293.
DOI: 10.1016/S0032-3861(02)00135-0
38. C. Grein, M. Gahleitner. On the influence of nucleation on the toughness of iPP/EPR blends with different rubber molecular architectures. *eXPRESS Polymer Letters* 2006; 2:392-397.
DOI: 10.3144/expresspolymlett.2008.47
39. A. Menyhard, J. Varga, A. Liber, G. Belina. Polymer blends based on the β -modification of polypropylene. *European Polymer Journal* 2005; 41:669-677.
DOI: 10.1016/j.eurpolymj.2004.10.036
40. Z. Yang, Z. Zhang, Y. Tao, K. Mai. Effects of polyamide 6 on the crystallization and melting behavior of β -nucleated polypropylene. *European Polymer Journal* 2008; 44:3754-3763.
DOI: 10.1016/j.eurpolymj.2008.08.010
41. R. Masirek, E. Piorkowska. Nucleation of crystallization in isotactic polypropylene and polyoxymethylene with poly(tetrafluoroethylene) particles. *European Polymer Journal* 2010; 46:1436-1445.
DOI: 10.1016/j.eurpolymj.2010.04.021
42. A. Menyhard, J. Varga. The effect of compatibilizers on the crystallization, melting and polymorphic composition of β -nucleated isotactic polypropylene and polyamide 6 blends. *European Polymer Journal* 2006; 42:3257-3268.
DOI: 10.1016/j.eurpolymj.2006.09.003
43. Z. Yang, K. Mai. Crystallization and melting behavior of β -nucleated isotactic polypropylene/polyamide 6 blends with maleic anhydride grafted polyethylene-vinyl acetate as a compatibilizer. *Thermochimica Acta* 2010; 511:152-158.
DOI: 10.1016/j.tca.2010.08.007
44. G.-S. Jang, N.-J. Jo, W.-J. Cho, C.-S. Ha. Isothermal crystallization behavior and properties of polypropylene/EPR blends nucleated with sodium benzoate. *Journal of Applied Polymer Science* 2002; 83:201-211.
DOI: 10.1002/app.10068
45. R.-Y. Bao, W. Yang, X.-G. Tang, B.-H. Xie, M.-B. Yang. Hierarchical distribution of β -phase in compression- and injection-molded, polypropylene-based TPV. *Journal of Macromolecular Science, Part B: Physics* 2011; 50:62-74.

- DOI: 10.1080/00222341003609518
46. J. Varga, A. Menyhard. Crystallization, melting and structure of polypropylene/poly(vinylidene-fluoride) blends. *Journal of Thermal Analysis and Calorimetry* 2003; 73:735-743.
DOI: 10.1023/A:1025870111612
47. Q. Shu, X. Zou, W. Dai, Z. Fu. Formation of β -iPP in isotactic polypropylene/acrylonitrile-butadiene-styrene blends: Effect of resin type, phase composition, and thermal condition. *Journal of Macromolecular Science, Part B: Physics* 2012; 51:756-766.
DOI: 10.1080/00222348.2011.609797
48. D. Alcazar, J. Ruan, A. Thierry, B. Lotz. Structural matching between the polymeric nucleating agent isotactic poly(vinylcyclohexane) and isotactic polypropylene. *Macromolecules* 2006; 39:2832-2840.
DOI: 10.1021/ma052651r
49. Z. Yang, Z. Zhang, Y. Tao, K. Mai. Preparation, crystallization behavior, and melting characteristics of β -nucleated isotactic polypropylene blends with polyamide 6. *Journal of Applied Polymer Science* 2009; 112:1-8.
DOI: 10.1002/app.29362
50. R.H. Zhang, D. Shi, S.C. Tjong, R.K.Y. Li. Study on the β to α transformation of polypropylene crystals in compatibilized blend of polypropylene/polyamide-6. *Journal of Polymer Science: Part B: Polymer Physics* 2007; 45:2674-2681.
DOI: 10.1002/poib.21287

CHAPTER 3

MATERIALS AND METHODS

3.1 Materials

3.1.1 Impact polypropylene copolymer (IPC)

Commercial IPC grade (trade name CMR648) with a melt flow rate (MFR) of 8.5 g / 10 min (230 °C / 2.16 kg) was purchased from Sasol Polymers, South Africa. It has an ethylene content ranging between 10 and 13%, a melting temperature of 163 °C and a density of 0.904 g cm⁻³.

3.1.2 Pimelic acid

Pimelic acid (C₇H₁₂O₄) was supplied by Sigma-Aldrich, South Africa. It has a melting temperature of 106 °C and a density of 1.28 g cm⁻³.

3.1.3 Adipic acid

Adipic acid (C₆H₁₀O₄) was supplied by Sigma-Aldrich, South Africa. It has a melting temperature of 152 °C and a density of 1.36 g cm⁻³.

3.1.4 Calcium stearate

Calcium stearate (C₃₆H₇₀CaO₄) was supplied by Sigma-Aldrich, South Africa. It has a melting temperature of 149–155 °C and a density of 1.08 g cm⁻³.

3.1.5 Acetone

Acetone (CH₃COCH₃) with the density of 0.79 g cm⁻³ was supplied by Laboratory Consumables & Chemical Supplies, South Africa. It was used to dissolve the individual and compounded nucleants.

3.1.6 Irganox 1010 and Irgafos 168 (antioxidant)

The antioxidant was supplied by Sasol *via* the University of Stellenbosch, South Africa. It was dissolved together with the nucleants to prevent thermo-degradation of IPC during processing at high temperatures.

3.2 Preparation of IPC nucleated samples

3.2.1 Dissolution of nucleating agents

Individual and compounded nucleating agents, together with 0.03 wt% of antioxidant, were completely dissolved in a sufficiently large volume of acetone at room temperature. The total weight percentage of nucleant was kept constant at 0.6 wt%. In the case of the bi-component nucleant the respective nucleants were calculated in such a way that their combined weight percentage was 0.6 wt%. The mass ratios of the mono- and bi-component nucleating agents are shown in Table 3.1. The pimelic and adipic acids, and the calcium stearate, are respectively denoted by Pim, Adi and Cast throughout the writing of this work.

Table 3.1 Mass ratios of the respective nucleating agents and the total mass of the IPC matrix in the blends

IPC (g)	Pimelic acid (g)	Adipic acid (g)	Calcium stearate (g)	Ratio
99.4	0.2		0.4	1:2
99.4		0.2	0.4	1:2
99.4	0.15		0.45	1:3
99.4		0.15	0.45	1:3
99.4	0.6			1:0
99.4		0.6		1:0
99.4			0.6	0:1

3.2.2 Blending of nucleating agents and IPC

The completely dissolved nucleants (0.6 wt%) together with 1.5 wt% antioxidant were transferred into a beaker containing 99.4 g IPC pellets. The solution covered all the pellets in

a beaker. Each composition (shown in Table 3.1) was left in a fume-hood overnight to ensure the complete evaporation of acetone. The dried compositions were extruded by using a Brabender Plastograph single screw-extruder at 60 rpm screw speed. The temperature profile of the four controllable thermocouples was set to be 150, 175, 175 and 200 °C from the hopper to the die. The extruded samples were cooled and pelletized. Pristine IPC with antioxidant but free from nucleating agent was also prepared using the same processing method. The granules were then placed between two pressure release hot stages at 200 °C for 5 minutes to ensure the complete melting of the granules. The molten samples were pressed at 200 °C under 50 kPa for 5 minutes to form 15 x 15 cm² square sheets. After removal from the hot press the sheets were left at room temperature for 24 hours. The films were then placed between the two cold plates of the hot press. The temperature was then gradually increased to 200 °C and the films were re-pressed for 10 minutes. The hydraulic pressure was then decreased to zero while the film was left between the hot plates. The hot press was then switched off to allow the temperature to decrease until it was at ambient temperature. The samples were then removed and stored for further analysis.

3.3 Preparation of TREF fractions

3.3.1 Temperature rising elution fractionation (TREF)

TREF can be defined as an analytical technique used to fractionate semicrystalline polymers on the basis of chain crystallisabilities. It involves two consecutive steps: crystallisation and elution. The sample has to be completely dissolved in a suitable solvent at high temperature and then transferred into the TREF column containing sea sand. Temperature inside the column is gradually decreased using a low cooling rate. During the crystallisation step the polymer chains crystallise into an orderly onion-like structure, with an increasing crystallisability. During the elution step, solvent flows in through the column coil and the temperature is increased. Solvent, containing dissolved layers of different crystallinity, is flushed out, low crystallinity fractions first. The fractions are collected over well defined temperature ranges as the elution temperature increases (Figure 3.1) [1,2].

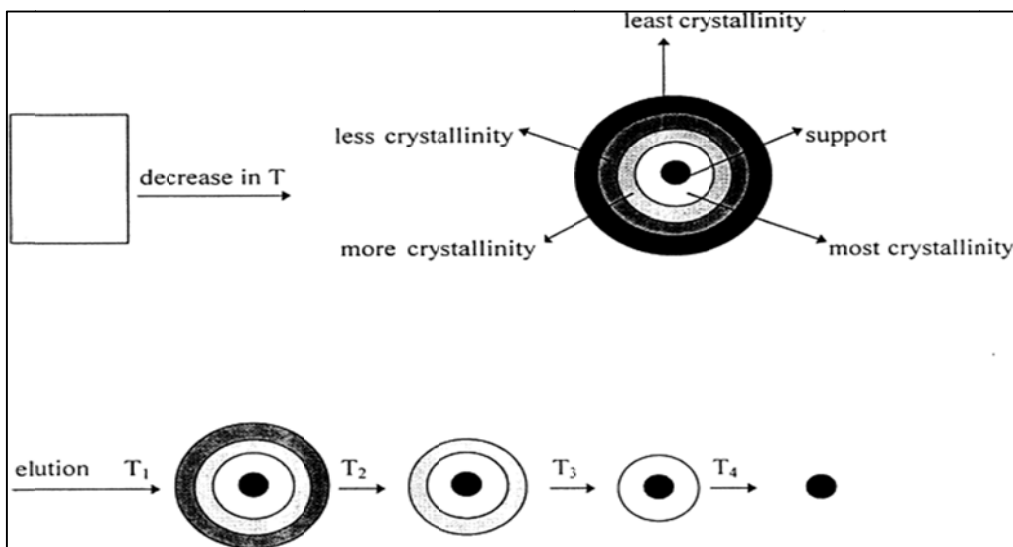


Figure 3.1 Schematic representation of separation mechanism of TREF [2]

TREF was used in this work to fractionate IPC according to chain crystallisability, and the fractions of higher isotacticity were considered. The TREF fractions were prepared by dissolving 3 g of IPC pellets and 0.06 g of an antioxidant in 300 cm³ of xylene at 135 °C. The solution was then introduced into a column containing preheated sea sand to avoid an unexpected re-crystallisation of the sample. The whole composition was cooled down and the elution temperature was subsequently increased starting below 25 to 140 °C. Fractions in the temperature ranges 71-80, 81-90, 91-100, 101-110, 111-120, and 121-140 °C, respectively denoted by 80C, 90C, 100C, 110C, 120C, and 140C, were reserved for further use in this work.

3.3.2 Blending of nucleating agents and TREF fractions

The bi-component nucleating agent was dissolved using the same method described above. However, the only nucleating agent used was 1:2 Pim-Cast because of its efficiency in producing the β -polymorph. The TREF fractions were covered with an acetone solution containing 0.6 wt% Pim-Cast (1:2) and 1.5 wt% of an antioxidant. All the compositions were left in a fume hood overnight to allow the acetone to evaporate. The dried fractions were then placed between the hot plates at 175 °C and pressed for 5 minutes.

3.4 Sample analysis

3.4.1 Differential scanning calorimetry (DSC)

DSC is a technique in which sample phase changes are recorded as a function of temperature. It measures the difference in heat flow rate into a sample subjected to a controlled temperature programme, and a reference subjected to the same temperature programme, as function of temperature. There are two basic DSC techniques: heat flux and power compensation. Heat flux DSC measures directly the temperature difference and transfers it to heat flow. The power-compensation DSC measures directly the heat flow needed to keep the sample and reference temperatures the same. However, both DSC techniques share a common performance, observing thermal events with no change in the mass of the sample. DSCs are normally used to examine solid phase and glass transitions, crystallisation, melting, and decomposition in polymers [3,4].

A Perkin Elmer Pyris-1 DSC was used in this work to quantitatively determine the amount of β -polymorph formed in nucleated IPC and in the TREF fractions. The DSC was calibrated using the melting temperatures of indium and zinc, and the melting enthalpy of indium. The analyses were done under flowing nitrogen atmosphere (20 ml min^{-1}). Samples with masses between 5 and 10 mg were sealed in aluminium pans. The samples were heated from 25 to $220 \text{ }^\circ\text{C}$ and held for 5 minutes to erase the thermal and mechanical history [5,6], cooled from 220 to $25 \text{ }^\circ\text{C}$, and re-heated from 25 to $200 \text{ }^\circ\text{C}$ at $10 \text{ }^\circ\text{C min}^{-1}$. Each composition was analysed three times to confirm reproducibility. Non-isothermal crystallisation kinetics were investigated for pure IPC, IPC/Pim-Cast (1:2), and IPC/Pim-Cast (1:3) by DSC, where the sample was heated from 25 to $220 \text{ }^\circ\text{C}$ at a heating rate of $10 \text{ }^\circ\text{C min}^{-1}$, and then cooled from 220 to $25 \text{ }^\circ\text{C}$ using different cooling rates ($2.5, 5, 10, 20,$ and $40 \text{ }^\circ\text{C min}^{-1}$). The Kissinger and Avrami-Ozawa methods were used to determine the crystallization kinetics of the different crystalline phases [7,8]. Since the α - and β -crystals co-crystallise during the cooling process, the crystallisation kinetics were evaluated for the combined crystallisation.

3.4.2 Thermogravimetric analysis (TGA)

TGA can be explained as a technique used to measure the mass change of the samples when subjected to a controlled temperature. A sample is placed in a furnace and the mass change is recorded by a thermobalance. TGA analyzes the samples' decomposition temperature and thermal stability through mass changes as a function of temperature in the scanning or isothermal modes. The sample can also be analyzed under reactive or non-reactive (inert) atmospheres, depending on the objective of the investigation [3].

A Perkin Elmer TGA-7 was used to determine whether the nucleating agent and β -nucleation have improved the thermal stability of the samples. Samples with masses in the range of 5–10 mg were placed in a platinum pan. The samples were heated from 25 to 600 °C at a heating rate of 10 °C min⁻¹ under nitrogen purge (flow rate 20 ml min⁻¹).

3.4.3 Dynamic mechanical analysis (DMA)

This technique is normally used to examine the molecular relaxations of polymeric materials and determines mechanical or flow properties as a function of temperature and frequency. The DMA imposes a sinusoidal stress on the sample and the resulting stress response is monitored. In most of the commercial DMA techniques the strain is normally a controlled input, and the stress response is investigated [3,9].

The DMA was used in the present work to evaluate the shift in glass transition temperature (T_g) of the nucleated IPC. The influence of β -nucleation on the loss and storage modulus was also investigated. The settings used to perform the analysis on DMA are as follows:

Frequency	1 Hz
Amplitude	20 μ m
Temperature range	-50 to 50 °C
Temperature program mode	Ramp
Measurement mode	Bending (dual cantilever)
Heating rate	3 °C min ⁻¹
Preloading force	0.02 N

Sample length	52 mm
Sample width	12 mm
Sample thickness	1.8 mm

3.4.4 Tensile testing

Most of the tensile testing instruments are vertically placed techniques having two discrete clamps which impose an effective force to deform the sample biaxially. The applied force is recorded as a function of clamp separation. The samples are usually in the form of dumbbells to facilitate the deformation between the clamps and reduce possible slipping on the clamped portions of the material. The load-elongation results are converted into a stress-strain curve [9].

The prime purpose of using tensile testing in this work was to investigate the influence of β -nucleation on the tensile parameters of the different compositions. The tensile analysis of the samples was performed by a Hounsfield H5KS universal testing machine. The dumbbell shaped samples had a Gauge length of 20 mm, a thickness of 2 mm and a width of range between 5 mm. The cross-head speed used to test the samples was 10 mm min⁻¹ at a controlled ambient temperature of 24 °C. Five samples of each composition were tested and average values with standard deviations are presented.

3.4.5 Impact testing

The conventional methods normally employed to examine the impact properties of polymers are Charpy and Izod. Impactors are able to register the energy lost by a pendulum or falling mass when it strikes the sample. This is the energy needed for the sample to fracture. Both methods can use either notched or un-notched samples. However, notching of the samples for impact testing is very helpful, especially when a sample is too rubbery, as the notch serves as a crack initiator [10].

A Ceast Impactor II was used to investigate the impact properties of the nucleated IPC, in order to establish whether β -nucleation gives rise to improved impact properties. Rectangular shaped samples with a width of 10 mm, a thickness of 3 mm and a length of 83 mm were V-

notched (2 mm deep) edgewise. The pendulum-like hammer was situated at an angle of 50° from the release spot and the samples were tested at an ambient temperature of 24 °C. Five samples of each composition were tested and the average and standard deviation values are presented.

3.4.6 Scanning electron microscopy (SEM)

SEM is an electron microscopy technique used to examine the microscopic structure of the samples by scanning the surface of the material. SEM uses an electron beam to scan the specimens on the surface and is capable of creating a three-dimensional images because of its large depth of field. It uses an acceleration voltage in the range of 1-40 kV to activate the electron beam which is scattered on the sample's surface [3].

A Tescan Vega 3 scanning electron microscope was used to investigate the surface structures of IPC and nucleated IPC. The distribution of the rubber spheres within the PP matrix was also investigated. All the specimens were etched for 24 hours with xylene solvent at ambient temperature. The samples were then sputter-coated with gold for 40 seconds prior to SEM analysis and the gold layer was 330 nm thick. The acceleration voltage used to scan the samples was 10 kV.

3.4.7 Fourier transform infrared (FTIR) spectroscopy

Infrared (IR) spectroscopy analyses the molecular vibrations of chemical bonds in materials. In a conventional IR spectrophotometer, the IR beam is directed through the sample chamber and measured against the reference beam at each wavelength over the entire spectral region. The molecules then absorb the IR radiation at certain wavenumbers corresponding to the absorption energy, which is the energy that initiates the transitions between the vibrational states of the bonds in the molecules. IR can be employed to identify compounds and ascertain sample composition, as well as the interaction of new bonds formed in polymer blends or composites [11,12].

A Perkin Elmer Spectrum 100 infrared spectrometer was used to investigate whether an *in situ* chemical reaction occurred between the nucleating agents at room temperature. It was

particularly used to identify new bonds in the bi-component nucleants. The chemical interaction between the IPC and the nucleants were also investigated by FTIR. The samples were analysed in an attenuated total reflectance (ATR) detector over a 400-4000 cm^{-1} wavenumber range at a resolution of 8 cm^{-1} .

3.4.8 Wide angel X-ray diffraction (WAXD)

X-ray diffractometry is a technique in which the crystal pattern of atomic and molecular structures can be determined. Principally, it generates a beam of X-rays which is diffracted by crystalline structures into particular directions. The measured intensities and angels of the diffracted beams can be used to form a picture of the crystalline structure of the investigated sample [3].

A Bruker AXS D8 advanced diffractometer with filtered Cu-K_α radiation, and a PSD Vantec-1 gas detector with up to 1600 channels, was used to analyse the samples. The samples were scanned at 2θ angles between 10 ° and 50 °, with a step size of 0.014 °.

3.5 References

1. S. Anantawaraskul, J.B.P. Soares, P.M. Wood-Adams. Fractionation of semicrystalline polymers by crystallization analysis fractionation and temperature rising elution fractionation. *Advanced Polymer Science* 2005: 182:1-54.
DOI: 10.1007/b135559
2. J. Xu, L. Feng. Application of temperature rising elution fractionation in polyolefins. *European Polymer Journal* 2000; 36:867-878.
DOI: 10.1016/S0014-3057(99)00143-3
3. Y. Leng. *Materials characterization: Introduction to Microscopic and Spectroscopic Methods*. John Wiley and Sons, Singapore (2008).
4. J.D. Menczel, L. Judovits, R.B. Prime, H.E. Bair, M. Reading, S. Sweir. Differential scanning calorimetry (DSC). In: J.D. Menczel, R.B. Prime (Eds). *Thermal Analysis of Polymers: Fundamentals and Applications*. John Wiley and Sons, Inc., Hoboken (2009).

5. A. Menyhard, J. Varga, G. Molnar. Comparison of different β -nucleators for isotactic polypropylene, characterisation by DSC and temperature-modulated DSC (TMDSC) measurements. *Journal of Thermal Analysis and Calorimetry* 2006; 83:625-630.
DOI: 10.1007/S10973-005-7498-6
6. Y.-F. Zhang, Y. Chang, X. Li, D. Xie. Nucleation effects of a novel nucleating agent bicyclic[2,2,1]heptane di-carboxylate in isotactic polypropylene. *Journal of Macromolecular Science, Part B: Physics* 2011; 50:266-274.
DOI: 10.1080/00222341003648995
7. L. Xui, X. Zhang, K. Xu, S. Lin, M. Chen. Variation of non-isothermal crystallization behavior of isotactic polypropylene with varying β -nucleating agent content. *Polymer International* 2010; 59:1441-1450.
DOI: 10.1002/pi.2891
8. J. Wang, Q. Dou. Non-isothermal crystallization kinetics and melting behaviors of isotactic polypropylene/*N,N,N'*'-tris-tert.butyl-1,2,5-benze-tricarboxamide. *Journal of Macromolecular Science, Part B: Physics* 2008; 47:629-642.
DOI: 10.1080/00222340802118283
9. R.P. Chartoff, J.D. Menczel, S.H. Dillman. Dynamic mechanical analysis (DMA). In: J. D. Menczel, R. B. Prime (Eds). *Thermal Analysis of Polymers: Fundamentals and Applications*. John Wiley and Sons, Inc., Hoboken (2009).
10. A. Rudin. *The Elements of Polymer Science and Engineering*, 2nd Ed.: An Introductory Text and Reference for Engineers and Chemists. Academic Press, San Diego (1999).
11. B.J. Hunt, M.I. James. *Polymer Characterisation*. Blackie Academic and Professional: Chapman and Hall, New York (1993).
12. D. Lin-Vlen, N.B. Colthup, W.G. Fateley, J.G. Grasselli. *The Handbook of Infrared and Raman Characteristic Frequencies of Organic Molecules*. Academic Press, Inc., San Diego (1991).

CHAPTER 4

RESULTS AND DISCUSSION

4.1 Differential scanning calorimetry (DSC)

4.1.1 Unfractionated IPC

The nucleation efficiency (NE) of the individual α and β nucleating agents is shown in Figure 4.1. NE is dependent on both the molecular or crystal structure and the concentration and particle size of the nucleating agents. To get a clear insight in the efficiency of NAs, the NE was estimated using the method developed by Fillon *et al.* [1]:

$$\text{NE (\%)} = \frac{T_{\text{cNA}} - T_{\text{c1}}}{T_{\text{c2max}} - T_{\text{c1}}} \quad (4.1)$$

where T_{cNA} , T_{c1} , and T_{c2max} are the crystallisation peak temperatures of the nucleated, non-nucleated, and self-nucleated polymer, respectively. Fillon *et al.* approximated T_{c2max} by heating the sample to a temperature of 40 °C above the melting temperature at a heating rate of 10 °C min⁻¹. It was then held there for ten minutes to erase all previous thermal history. The sample was then cooled to a temperature $T_1 = 50$ °C at a cooling rate of 10 °C min⁻¹. Thus, the crystallisation will take place at the lower limit of the crystallisation range (T_{c1}). The polymer was heated again until it was partially molten (melting temperature range). The secondary crystallisation was followed by a subsequent cooling of the partially molten sample and the crystallisation peak temperature is T_{c2} ($T_{\text{c2}} > T_{\text{c1}}$). The maximum crystallisation peak temperature (T_{c2}) is denoted T_{c2max} ($T_{\text{c2max}} \sim 140$ °C). The values of non-nucleated (T_{c1}) and nucleated (T_{cNA}) crystallisation temperatures are shown in Table 4.1. T_{c1} is the crystallisation temperature of the pristine IPC whereas T_{cNA} is that of the nucleated samples.

It can be clearly seen that pimelic acid (Pim) and its combination with calcium stearate (CaSt) have the highest nucleation efficiency of about 35%. This can be attributed to the perfect matching of the dimensional lattice between the c-axis of IPC and the corresponding distance in the crystal face of Pim [2].

Table 4.1 Crystallisation peak temperatures (T_c), and melting peak temperatures of the β - and α - polymorphs ($T_{\beta 1}$ and $T_{\alpha 1}$), in IPC

Sample	$T_c / ^\circ\text{C}$	$T_{\beta 1} / ^\circ\text{C}$	$T_{\alpha 1} / ^\circ\text{C}$
Pristine IPC	120.1 ± 0.1		165.1 ± 0.8
IPC/Pim	127.2 ± 0.6	155.1 ± 0.4	166.8 ± 1.0
IPC/Pim-CaSt (1:2)	127.1 ± 0.3	155.3 ± 0.4	167.2 ± 1.0
IPC/Pim-CaSt (1:3)	127.0 ± 1.3	155.3 ± 1.7	167.3 ± 2.0
IPC/CaSt	120.9 ± 0.0	151.6 ± 0.2	165.7 ± 0.4
IPC/Adi	121.0 ± 0.1	152.6 ± 0.9	166.4 ± 0.4
IPC/Adi-CaSt (1:2)	122.2 ± 1.4	153.0 ± 1.5	166.5 ± 1.5
IPC/Adi-CaSt (1:3)	120.2 ± 1.1	150.7 ± 0.5	164.7 ± 0.5

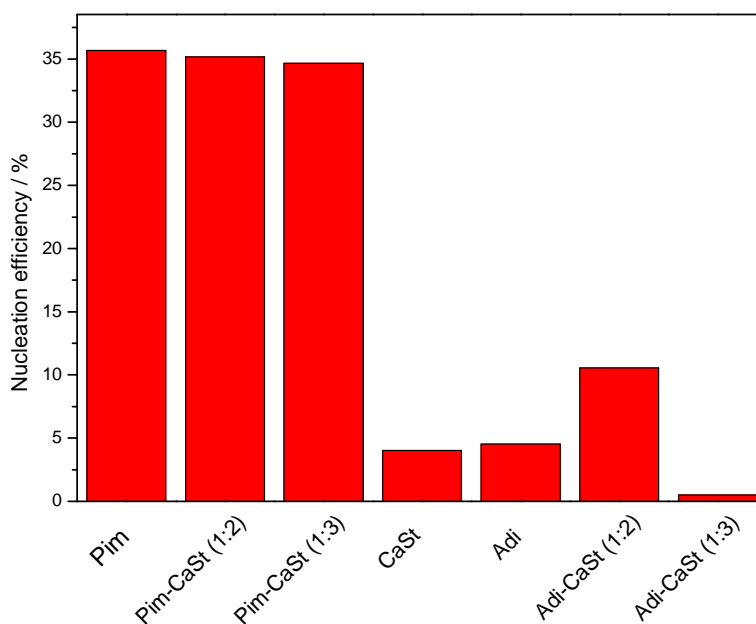


Figure 4.1 The nucleation efficiency of IPC nucleated with individual and compounded nucleating agents

Calcium stearate (CaSt) and adipic acid (Adi), on the other hand, have low NE values of about 5%. Pim and its combination with CaSt cause an increase in T_c of iPP, while Adi, CaSt and their combination have very little effect on T_c . The high NE value for IPC-Pim suggests that the nucleation efficiency of Pim will not be significantly affected when compounded

with CaSt. As can be seen in Figure 4.1, there is only a slight decrease in NE when Pim is compounded with CaSt. It is clear that the calcium pimelate, which probably forms when Pim is compounded with CaSt, is equally efficient as nucleating agent. Adi and CaSt have low NE values, but the calcium adipate, formed when compounding Adi and CaSt in a 1:2 mass ratio, has an observably better NE. When compounded in a 1:3 mass ratio, the product has a much lower NE than both Adi and CaSt. It is not clear why there is such a big difference in nucleation efficiencies of the two Adi-CaSt combinations. One reason may be experimental errors in the determination of the crystallisation peak temperatures. As can be seen from Table 4.1, the standard deviation on the T_c value for IPC/Adi-CaSt (1:2) is quite big. Another reason may be that for the Adi-CaSt (1:2) not all the Adi has reacted with CaSt (the molar ratio is about 2:1) and that the combination of the unreacted Adi and the calcium adipate is a more effective nucleating agent than Adi-CaSt (1:3), which will contain less unreacted Adi.

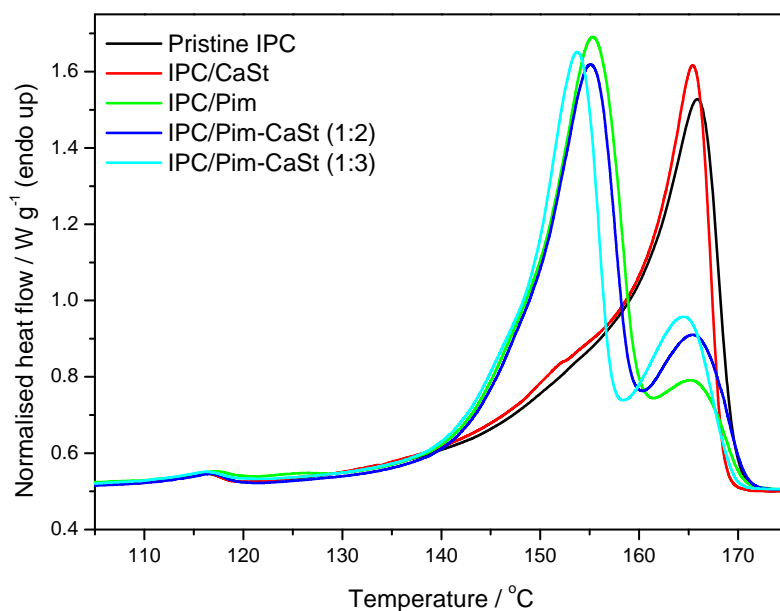


Figure 4.2 DSC heating curves of IPC nucleated with individual (Pim, CaSt) and compounded nucleants

The first heating curves of all the IPC samples nucleated with the individual and compounded nucleating agents are shown in Figures 4.2 and 4.3. Both figures show three distinctive peaks where the small peak at about 115 °C is attributed to the melting peak of the crystallisable polyethylene (PE) segments present in IPC. This peak can be seen in both the pure and

nucleated samples. It is clear that the addition of nucleants did not change the melting profile of these segments. There is also a peak at about 155 °C in Figure 4.2, which is ascribed to the melting of the β -crystals. This peak can also be seen around 150 °C in Figure 4.3. Another melting peak is observed around 165 °C and it is attributed to the melting of the α -crystals [3].

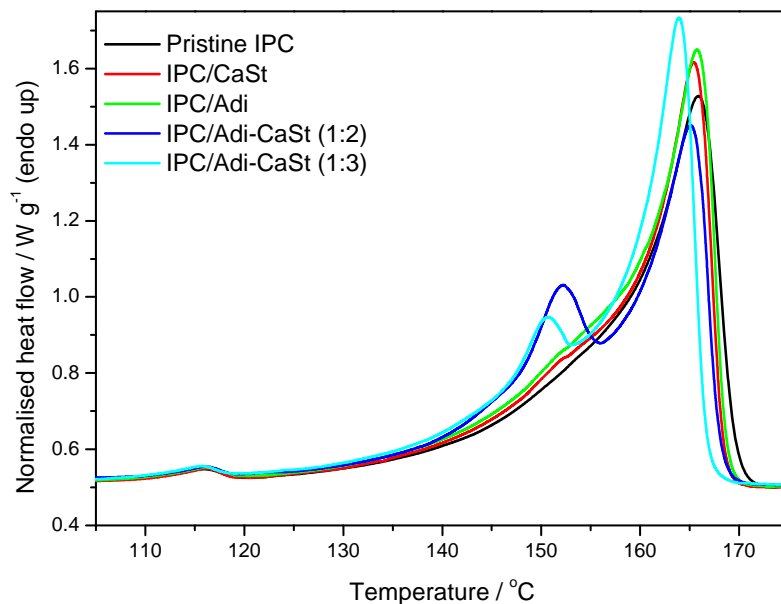


Figure 4.3 DSC heating curves of IPC nucleated with individual (Adi, CaSt) and compounded nucleants

It is worth noting that all the investigated NAs induced β -crystals in IPC, even though their efficiency differed. In Figure 4.2 the β -crystal melting peak is only pronounced in IPC/Pim, IPC/Pim-CaSt (1:2), and IPC/Pim-CaSt (1:3), while in IPC/CaSt it is almost negligibly small. Figure 4.3 shows that the β -crystal melting peak is more resolved but still small for the IPC/Adi-CaSt (1:2) and IPC/Adi-CaSt (1:3) samples. Pim alone is therefore a very efficient and selective β -nucleant. The compounding of Pim and CaSt could not further improve the effectiveness of β -nucleation in IPC, and the presence of CaSt also did not significantly improve the poor nucleating efficiency of Adi.

An increase in the Adi-CaSt ratio increases the melting enthalpy of the α -crystals (Table 4.2). The calcium adipate seems to have a dual activity to enhance both α - and β -crystal formation,

but it has a lower efficiency to induce β -crystal formation. The β -crystal peak is, however, much better resolved and more intense than those of IPC-Adi and IPC-CaSt, although not nearly as strong as in the case of Pim and Pim-CaSt. As the amount of CaSt increases in Adi-CaSt, the intensity of the β -crystal peak decreases slightly while that of the α -crystal increases. This confirms that the presence of primarily calcium adipate has a stronger ability for α -crystal formation. It can be seen from Table 4.1 that the melting peak temperatures of the α - and β -phases are very similar within experimental error for all the samples. The small differences observed may be related to crystal sizes and size distributions, which will be due to differences in effectiveness of crystal growth.

The DSC cooling curves of the virgin and nucleated samples are shown in Figures 4.4 and 4.5. The melting enthalpies of the α - and β -crystals, the β -crystal fractions, and the total crystallinities are tabulated in Table 4.2. The β -contents for all the samples were calculated using Equation 4.2.

$$K_{\text{DSC}}(\%) = \frac{X_{\beta}}{X_{\beta} + X_{\alpha}} \quad (4.2)$$

where X_{β} and X_{α} are the crystallinity values of the β - and α -crystals, respectively. The combined crystallinity of the α - and β -phases was calculated using Equation 4.3, after resolving the slightly overlapping melting peaks.

$$X(\%) = \frac{\Delta H_m}{\Delta H_m^{\circ}} \times w_{\text{IPC}} \quad (4.3)$$

where $(\Delta H_m \times w_{\text{IPC}})$ is the normalised melting enthalpy and ΔH_m° is the melting enthalpy of the pure crystalline PP. The ΔH_m° values for the β - and α -crystals were taken as 168.5 J g^{-1} and 177 J g^{-1} , respectively [4]. The total crystallinity, X_{DSC} , is the sum of the α - and β -crystallinities in each case.

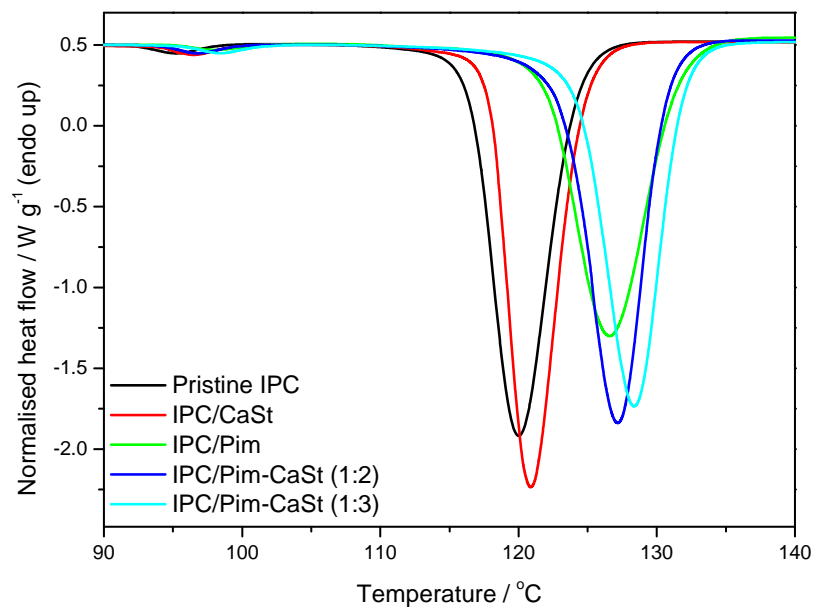


Figure 4.4 DSC cooling curves of IPC nucleated with individual (Pim, CaSt) and compounded nucleants

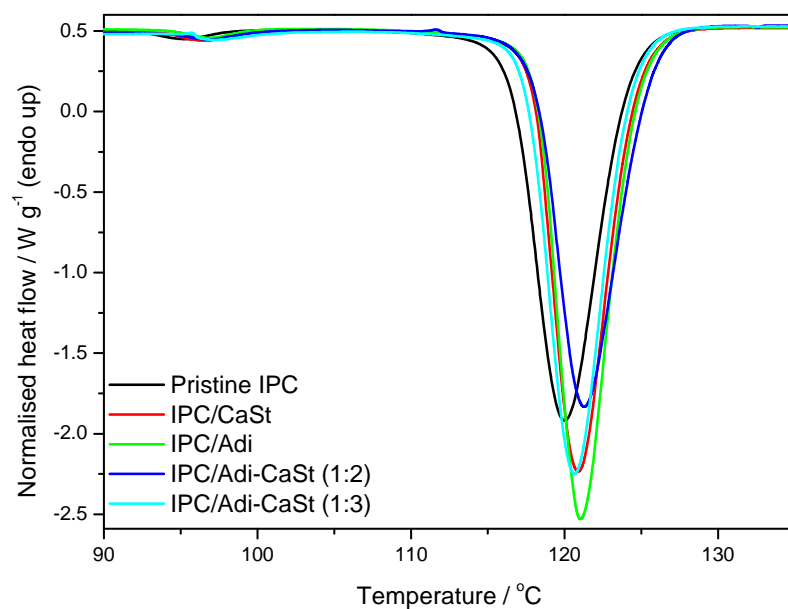


Figure 4.5 DSC cooling curves of IPC nucleated with individual (Adi, CaSt) and compounded nucleants

Table 4.2 Summary of the DSC melting and crystallisation results of the investigated samples

Sample	$\Delta H_{m,\beta} / \text{J g}^{-1}$	$\Delta H_{m,\alpha} / \text{J g}^{-1}$	$K_{\text{DSC}} / \%$	$X_{\text{DSC}} / \%$
Pristine IPC		77.2 ± 0.1		43.6
IPC/Pim	60.8 ± 1.7	10.8 ± 1.4	85.5 ± 1.9	30.6
IPC/Pim-CaSt (1:2)	65.4 ± 1.9	8.7 ± 1.6	88.8 ± 2.1	43.7
IPC/Pim-CaSt (1:3)	65.3 ± 0.5	9.8 ± 1.1	87.5 ± 1.1	44.3
IPC/CaSt	0.4 ± 0.0	61.4 ± 1.5	0.6 ± 0.0	34.9
IPC/Adi	3.0 ± 0.0	60.3 ± 0.0	10.0 ± 0.0	17.9
IPC/Adi-CaSt (1:2)	11.6 ± 0.0	58.9 ± 1.2	17.1 ± 0.3	40.2
IPC/Adi-CaSt (1:3)	5.0 ± 0.4	70.4 ± 1.6	6.9 ± 0.7	42.7

$\Delta H_{m,\beta}$ and $\Delta H_{m,\alpha}$ are the melting enthalpies of the β - and α -crystals; K_{DSC} and X_{DSC} are the calculated amount of β -content and total crystallinity.

Figures 4.4 and 4.5 show two crystallisation peaks for all the investigated samples. The first peak appearing around 95 °C is ascribed to the crystallisation of the PE segments in IPC. The crystallisation peak at higher temperatures is ascribed to the crystallisation of both the α - and β -crystals. The presence of different nucleating agents gives rise to crystallisation at different temperatures. The presence of CaSt alone in IPC slightly increases T_c , whereas Pim and Pim-CaSt significantly increase this value. This can be explained by the good nucleation activity of Pim. There is very little difference between the T_c values of IPC and its samples nucleated with Adi, CaSt and Adi-CaSt. This is in line with the already discussed low nucleating efficiency of these NAs.

4.1.2 Fractionated IPC

The DSC heating curves of the non-nucleated and nucleated TREF crystallised fractions are shown in Figures 4.6 and 4.7. To prepare the nucleated fractions, the different fractions were doped with a Pim-CaSt (1:2) compounded nucleant because it was found to be the most effective in β -crystal formation. 80C and its nucleated counterpart show peaks around 105 and 130 °C, which are attributed to the melting temperatures of low molar mass polyethylene

(PE) and polypropylene (PP) segments. The 90C and nucleated 90C show the melting peaks of the higher molar mass fractions of PE and PP around 110 and 145 °C. The melting temperatures of the 100C and 100C/Pim-CaSt (1:2) have shifted to 118 and 158 °C for the PE and PP segments. However, the nucleated 100C shows the melting of β -crystals at a temperature slightly above 150 °C. Generally, the addition of the bi-component nucleant did not really induce the formation of β -crystals in the lower temperature fractions. This can be explained by the lack of isotacticity in these PP fractions.

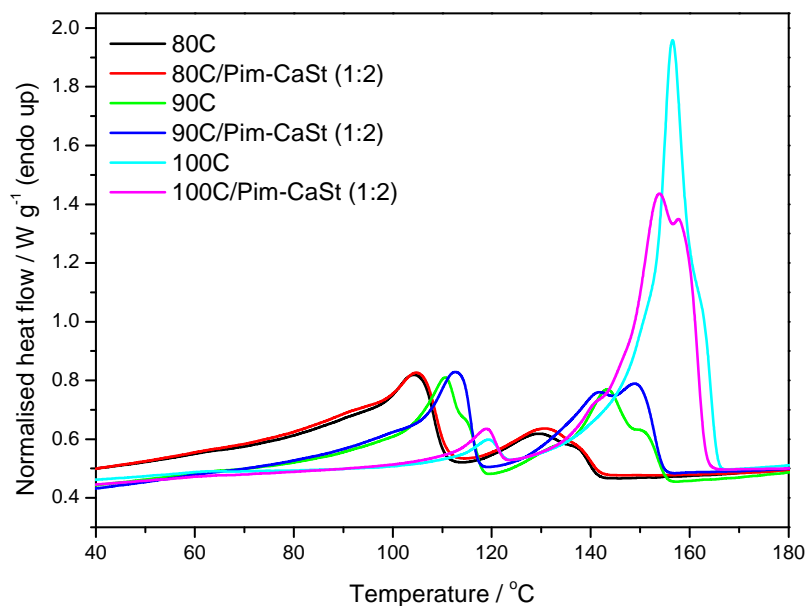


Figure 4.6 DSC heating curves of nucleated and non-nucleated 80C, 90C, and 100C fractions

It was found that the fractionation of IPC through temperature gradient TREF elutes fractions of increasing isotacticity with increasing elution temperature. Figure 4.7 shows the DSC heating curves of the fractions eluted at higher temperatures, without and with nucleation treatment. The amounts of PE are clearly very low, as can be seen from the small peak at about 120 °C. All the non-nucleated fractions have large amounts of PP segments melting between 155 and 170 °C. The nucleated 110C and 120C fractions clearly formed β -crystals, which is not observed for the nucleated 140C fraction. The latter fraction probably has lower isotacticity than the other two fractions. Fan *et al.* [5] reported that fractions eluted at lower and higher fractionation temperatures exhibit higher molar masses than those eluted at

intermediate temperatures. It should be noted that the nucleated 110C and 120C fractions have crystal imperfections, as they show an $\alpha_1 \rightarrow \alpha_2$ transformation. This can be associated with the melting of the less thermally stable α_1 -crystal (α_1) and re-organisation into the more thermally stable crystal (α_2) (melting-recrystallisation phenomenon). The cooling curves of all the investigated fractions can be seen in Appendix A.

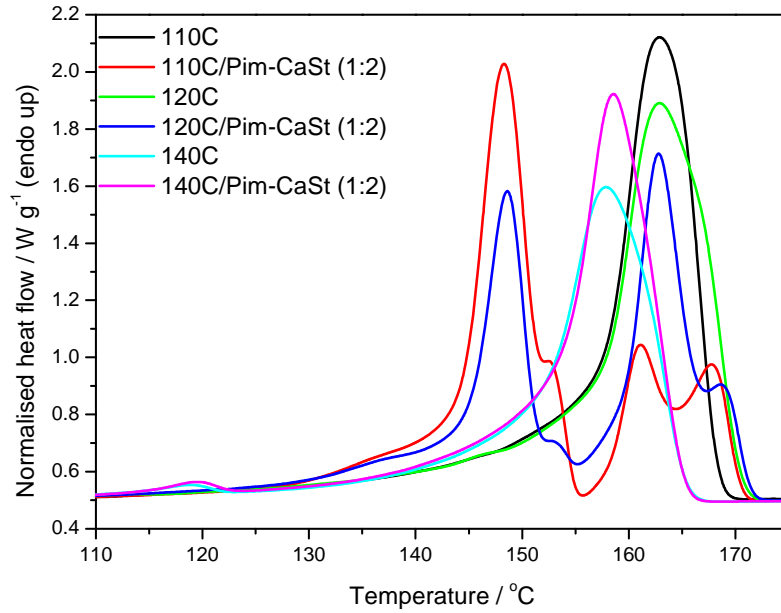


Figure 4.7 DSC heating curves of nucleated and non-nucleated 110C, 120C, and 140C fractions

4.1.3 Nonisothermal crystallisation behaviour

The nonisothermal crystallisation kinetics was evaluated by using the Ozawa and Avrami-Ozawa equations [6-8]. The crystallisation activation energy values of virgin IPC and IPC/Pim-CaSt (1:2) were determined through Kissinger's method. Equation 4.9 is the well-known Avrami equation for isothermal kinetics analysis. The general form of Avrami equation is:

$$X_t = 1 - \exp(-Z_t t^n) \quad (4.4)$$

where X_t is the relative crystallinity at time t , n is the Avrami parameter which depends on the nucleation mechanism, and Z_t is a constant which describes the nucleation and growth parameters. At constant temperature Equation 4.4 can be modified to give Equation 4.5.

$$\ln(-\ln(1 - X_t)) = \ln Z_t + n \ln t \quad (4.5)$$

Ozawa considered the effect of cooling rate and the Avrami equation was adapted to Equation 4.6.

$$X_t = 1 - \exp\left(-\frac{K(T)}{\varphi^m}\right) \quad (4.6)$$

where X_t is the relative crystallinity at time t , m is the Ozawa parameter which also depends on the nucleation mechanism, and $K(T)$ is the crystallisation rate constant. Equation 4.6 can be re-arranged into Equation 4.7.

$$\ln(-\ln(1 - X_t)) = \ln K(T) - m \ln \varphi \quad (4.7)$$

The relationship between the temperature and crystallisation time can be described by Equation 4.8.

$$t = \frac{T_0 - T}{\varphi} \quad (4.8)$$

where T is the temperature at time t , T_0 is the temperature at the start of the crystallisation process. Since the degree of crystallinity is related to the cooling rate φ and the crystallisation time t , combination of Equations 4.5 and 4.7 gives Equation 4.9.

$$\ln Z_t + n \ln t = \ln K(T) - m \ln \varphi \quad (4.9)$$

which may be rearranged to give Equation 4.10.

$$\ln \varphi = \ln F(T) - a \ln t \quad (4.10)$$

where $F(T) = \{K(T)/Z_t\}^{1/m}$ refers to the cooling rate value, which has to be chosen at unit crystallisation time when the measured system amounts to a certain degree of crystallinity. According to Liu *et al.* [6] $F(T)$ has a definite physical and practical meaning, but it is not clear from the rest of their discussion exactly what this meaning is. The parameter a is the ratio of the Avrami exponent n to the Ozawa exponent m ($a = n/m$). All the kinetics graphs are shown in Appendix B.

The cooling curves of the investigated pristine and nucleated IPC samples are presented in Figures 4.8 and 4.9. The samples were cooled from the molten state at different cooling rates (2.5 to 40 °C min⁻¹). It is evident that T_c decreases with an increase in cooling rate. This is in line with the results reported in previous studies [6,7], and it is because crystallisation is a kinetic time-dependent process. The pristine IPC has lower T_c values than the nucleated IPC sample (Figure 4.10). The presence of compounded NAs, because of their nucleation effect, causes the IPC crystallisation to start at higher temperatures.

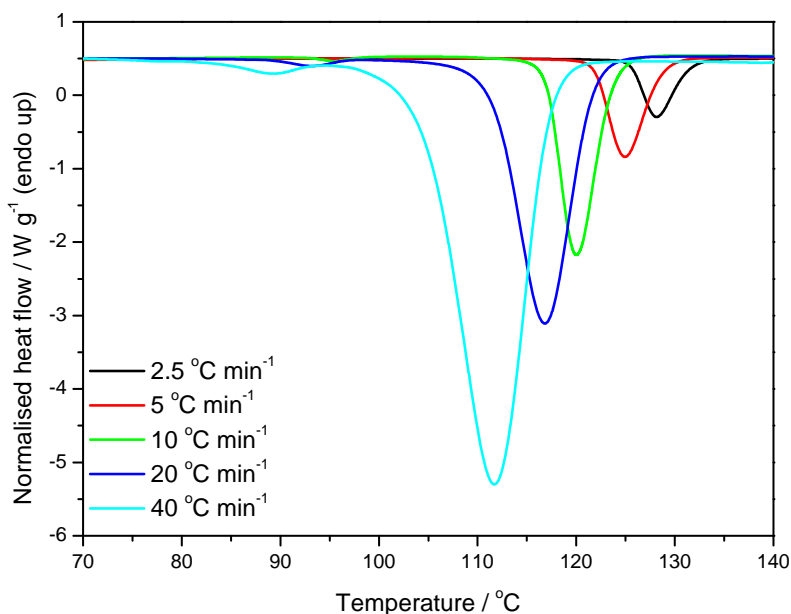


Figure 4.8 DSC cooling curves of the pristine IPC during non-isothermal crystallisation at different cooling rates

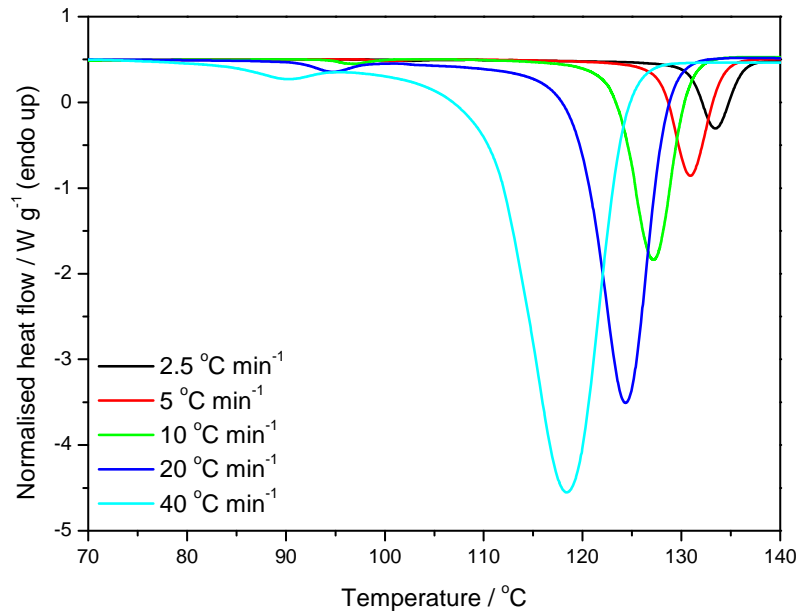


Figure 4.9 DSC cooling curves of IPC nucleated with a bi-component Pim-CaSt (1:2) nucleant during non-isothermal crystallisation at different cooling rates

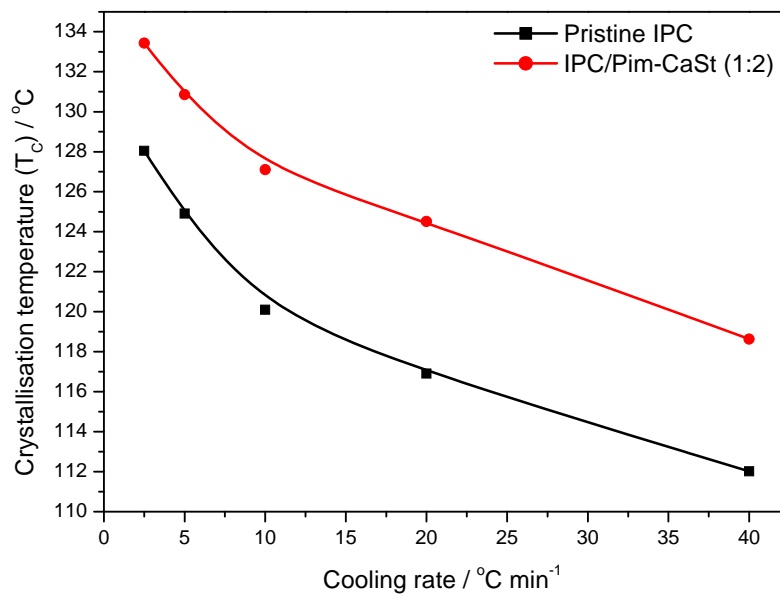


Figure 4.10 Crystallisation peak temperatures of pure and nucleated IPC at different cooling rates

The relative crystallinity for each investigated sample is shown as a function of crystallisation temperature by Equation 4.11. Figures 4.11 and 4.12 show the degree of crystallinity as a function of crystallisation time for different cooling rates.

$$X_t = \frac{\int_{T_o}^T (dH_c/dT)dT}{\int_{T_o}^{T_\infty} (dH_c/dT)dT} \quad (4.11)$$

where T_o and T_∞ are the onset and end of crystallisation temperatures, and dH_c/dT is the rate of heat evolution at temperature T . All the curves show a sigmoidal shape, and the crystallisation times decrease with increasing cooling rate. The crystallisation half-life was determined from the sigmoidal curves as the time at 50% relative crystallinity and are tabulated in Table 4.3 for the different cooling rates. The crystallisation half-lives of the pristine IPC and IPC/Pim-CaSt (1:2) are virtually the same at the same cooling rates. It seems as if the NA did not significantly influence the crystallisation rate of the IPC, although the crystallisation in this case started at higher temperatures. Other authors found that the crystallisation half-life slightly decreased in nucleated samples when compared to that of the pure material at the same cooling rate [7]. The Ozawa parameters (m) of the samples were obtained from the slope of the linear Ozawa plots according to Equation 4.7, and are tabulated in Table 4.4. The average values of 2.8 and 3.0 indicate that the crystallisation mode is a three-dimensional growth with athermal nucleation mechanism [8]. It seems as if the nucleation mechanism did not change with the addition of Pim-CaSt (1:2).

Table 4.3 Crystallisation half-life ($t_{1/2}$) at different cooling rates for neat and nucleated IPC

Pristine IPC					
Cooling rate / °C min⁻¹	2.5	5	10	20	40
$t_{1/2}$ / min	2.2	1.4	0.8	0.4	0.3
IPC/Pim-CaSt (1:2)					
Cooling rate / °C min⁻¹	2.5	5	10	20	40
$t_{1/2}$ / min	2.2	1.2	0.8	0.4	0.2

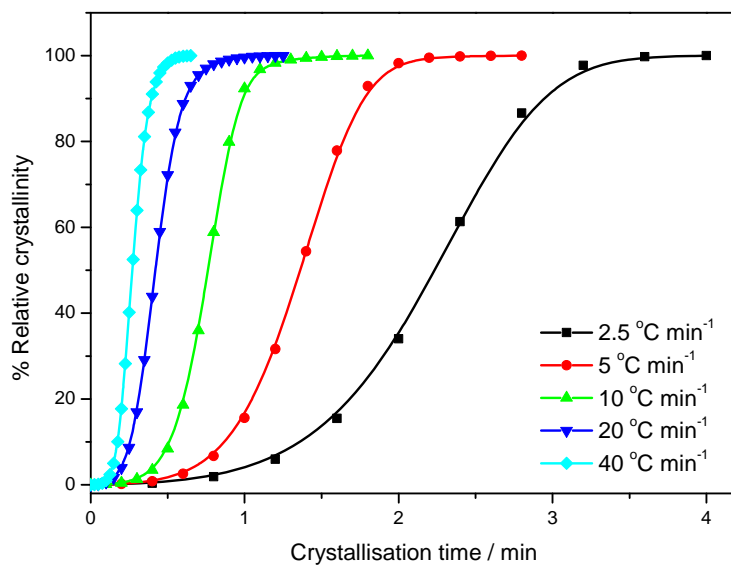


Figure 4.11 Relative degree of crystallinity versus crystallisation time for pristine IPC

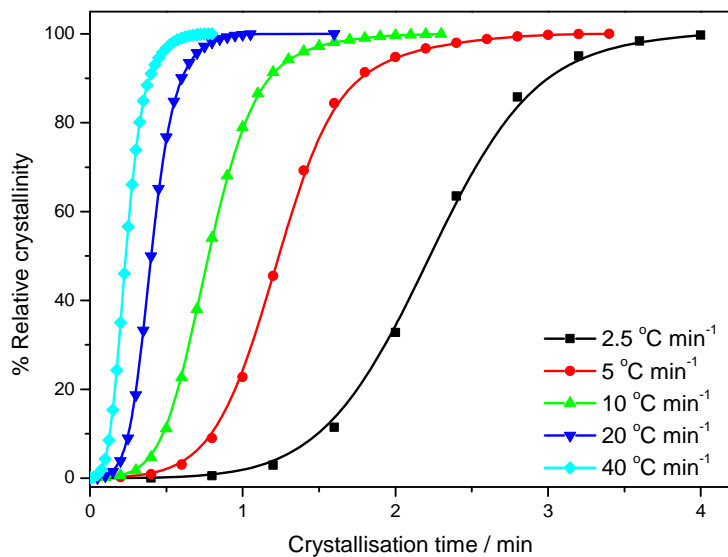


Figure 4.12 Relative degree of crystallinity versus crystallisation time for IPC/Pim-CaSt (1:2)

Table 4.4 Nonisothermal crystallisation kinetics parameters determined by the Ozawa-Avrami and Kissinger methods

	a	m	$\Delta E / \text{kJ mol}^{-1}$
Pristine IPC	1.3	2.8	230
IPC/Pim-CaSt (1:2)	1.2	3.0	255

Table 4.4 summarises the crystallisation parameters obtained from the Avrami-Ozawa and Kissinger kinetic analyses. a ($= n/m$) was estimated from the slope of the Avrami-Ozawa linear plots (shown in Appendix B), where n and m are the Avrami and Ozawa exponents. The crystallisation activation energy (ΔE) is slightly lower for the pristine IPC, which confirms that the α -crystallisation is the thermodynamically preferred process.

4.2 Wide angle x-ray diffraction

The β -content in the nucleated samples was calculated using the Turner Jones equation [4] (Equation 4.4).

$$K_{\text{XRD}} = \frac{A_{\beta(300)}}{A_{\beta(300)} + A_{\alpha(110)} + A_{\alpha(040)} + A_{\alpha(130)}} \quad (4.12)$$

where $A_{\beta(300)}$ is the area under the (300) reflection peak, and $A_{\alpha(110)}$, $A_{\alpha(040)}$, and $A_{\alpha(130)}$ are the areas under the (110), (040), and (130) reflection peaks, respectively. The peaks are at 16.1° for $A_{\beta(300)}$, and 14.1° , 16.9° , and 18.8° for the $A_{\alpha(110)}$, $A_{\alpha(040)}$, and $A_{\alpha(130)}$ on the spectrum. The total crystallinity of all the samples was calculated by using Equation 4.8.

$$X_{\text{XRD}} = \frac{\Sigma A_{\text{cryst}}}{\Sigma A_{\text{cryst}} + \Sigma A_{\text{amorp}}} \quad (4.13)$$

where A_{cryst} and A_{amorp} are the fitted areas of the crystal and amorphous domains, respectively.

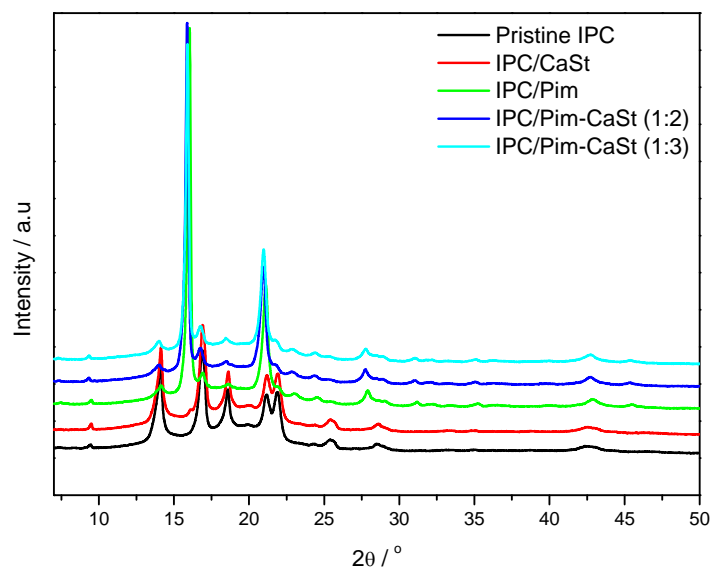


Figure 4.13 XRD spectra of nucleated and non-nucleated IPC with individual (Pim, CaSt) and compounded nucleants

The XRD spectra of all the samples are shown in Figures 4.13 and 4.14. The peaks that are more prominent for the α - and β -polymorphs are used in Equation 4.7. Generally, the formation of β -crystals is seen in all the nucleated samples. Since Pim has a good nucleation efficiency, the strong α -peaks of the lattice coordinates (040) and (130) decreased considerably. Even where the Pim is compounded with CaSt at various ratios there is also a decrease in the intensity of these peaks. When Adi is compounded with CaSt in a 1:2 ratio the development of the β -crystal peak can be seen, which shows that calcium adipate is a more efficient nucleating agent than the individual nucleants.

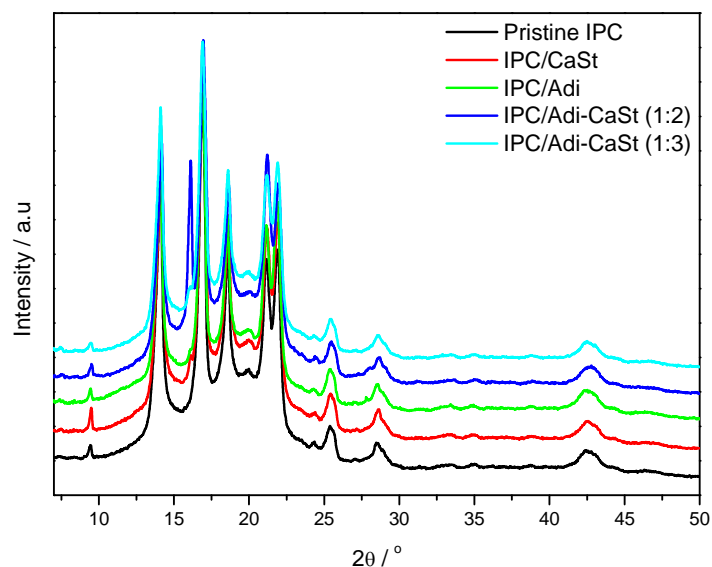


Figure 4.14 XRD spectra of nucleated and non-nucleated IPC with individual (Adi, CaSt) and compounded nucleants

Table 4.3 summarises the XRD peak areas and the calculated crystallinities and β -contents. It can be seen that the β -contents of the Pim and Pim-CaSt nucleated samples are virtually the same, and the values are in line with the values obtained from the DSC melting peaks (Table 4.2). Adding CaSt, as well as an increase in the amount of CaSt, obviously does not have a significant impact on the formation of β -crystals. This can be attributed to the high NE of Pim. The total crystallinity for pristine IPC, determined from XRD, is slightly lower than that determined from the DSC melting peaks, but the total crystallinities for the nucleated samples are much higher. The reason for this is probably that the crystals, formed as a result of nucleation in the presence of Pim, are thermally labile and that ‘de-crystallisation’ takes place during the heating process in the DSC. For the Adi and Adi-CaSt samples both the β -content and crystallinities correlate well with those determined from the DSC curves.

Table 4.5 Summary of the XRD crystalline phase parameters of the investigated samples

Sample	A_{α} (110) ~ 14.1°	A_{α} (040) ~ 16.9°	A_{α} (130) ~ 18.8°	A_{β} (300) ~ 16.1°	K_{XRD} / %	X_{XRD} / %
Pristine IPC	11588	10873	4175			32
IPC/Pim	1455	716	957	27254	90	70
IPC/Pim-CaSt (1:2)	1393	984	719	25323	89	80
IPC/Pim-CaSt (1:3)	1103	1165	672	24078	89	78
IPC/CaSt	11690	11734	4438			16
IPC/Adi	10052	9469	4021			21
IPC/Adi-CaSt (1:2)	8078	8360	3962	2742	12	27
IPC/Adi-CaSt (1:3)	10330	10038	4149			29

A_{α} (110), A_{α} (040), A_{α} (130) and A_{β} (300) are peak areas of the alpha and beta crystals at reflection lattice planes of (110), (040), (130), and (300), respectively. K_{XRD} and X_{XRD} are the amount of β -crystals and the total crystallinity calculated using XRD.

4.3 Fourier transform infrared (FTIR) spectroscopy

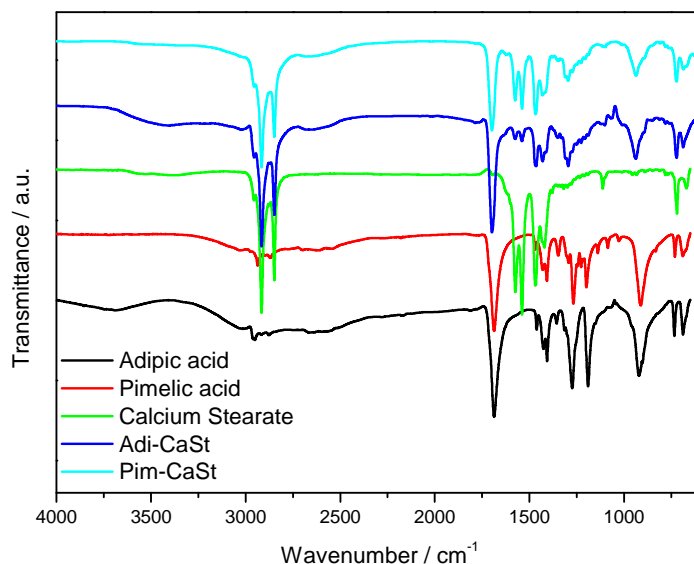


Figure 4.15 FTIR spectra of individual and compounded nucleating agents

Figure 4.15 shows the FTIR spectra of the individual and compounded nucleating agents dissolved in acetone at room temperature, and dried overnight. Both the dicarboxylic acids have fairly strong peaks in the range of 1145-1358 cm^{-1} that are associated with the secondary alcohol groups. CaSt shows the very strong peaks of the carboxylate salts (anions) in the 1506-1666 cm^{-1} range. The secondary alcohol in diacids (hydroxyl functional groups) and carboxylate anions in CaSt are reactive functional groups. In both mixtures there is the development of one peak in the range of 1200-1320 cm^{-1} which is attributed to as an anhydride cyclic ring. Two peaks reflecting the carboxyl groups (C=O) on the anhydride ring (β -diketone) are also observed in the range 1513-1613 cm^{-1} . The mixture of Pim and CaSt have more intense peaks of C=O than the mixture of Adi and CaSt. This can be associated with the seven carbons in Pim and six carbons in Adi. The newly formed anhydride rings will differ by one carbon atom. It seems as if both diacids formed calcium adipate and calcium pimelate when compounded with CaSt at room temperature.

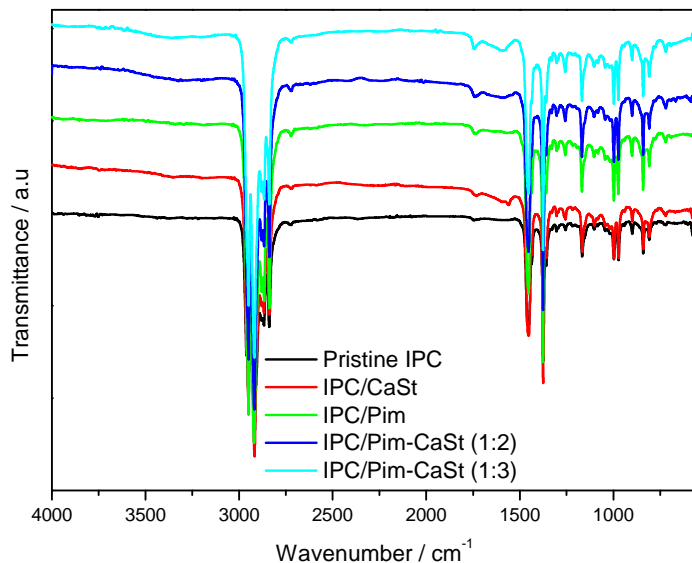


Figure 4.16 FTIR spectra of IPC samples prepared in the absence and presence of individual and compounded Pim and CaSt

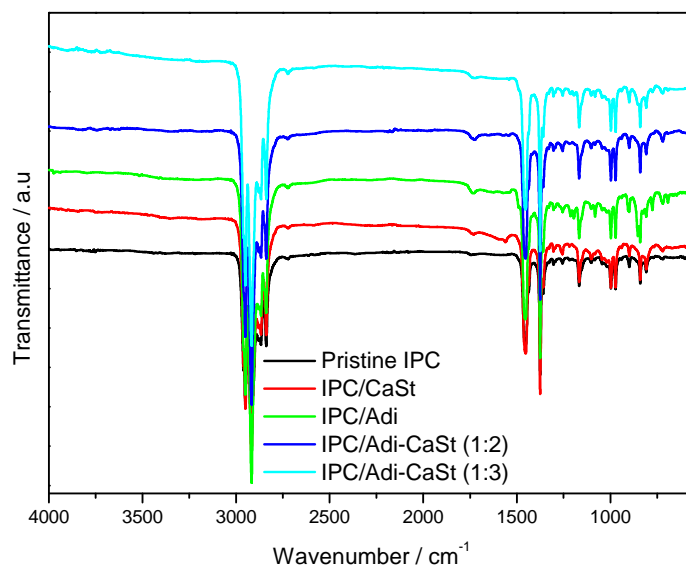


Figure 4.17 FTIR spectra of IPC samples prepared in the absence and presence of individual and compounded Adi and CaSt

The FTIR spectra of IPC and the nucleated samples are presented in Figures 4.16 and 4.17. There is a peak in the range of $1511-1847\text{ cm}^{-1}$ for all the nucleated samples, which is not observed in the pristine IPC. This peak can be ascribed to the carbonyl groups present in nucleating agents. The nucleated samples show another peak in the $670-750\text{ cm}^{-1}$ range which is assigned to the methyl rocking $-(\text{CH}_2)_n-$ vibration, which suggests the presence of the hydrocarbon chains of the acids and CaSt on the surface of IPC. The IPC matrix has a hydrophobic character, while all the nucleating agents have both hydrophobic and hydrophilic characters. Thus the IPC chains interact better with the non-polar part of the NAs. This phenomenon drives the IPC chains to create stable β -nuclei [9]. The nucleating agents create certain spatial sites for IPC nucleation, even though there is a barely observed chemical interaction between them. It is also clear that the system employed in the current work does not change the chemical structure of IPC.

4.4 Scanning electron microscopy (SEM)

The SEM images of all the unetched samples are shown in Figures 4.18 and 4.19. The pictures all look very similar, and it is not possible to distinguish between the different phases in the copolymer at this magnification.

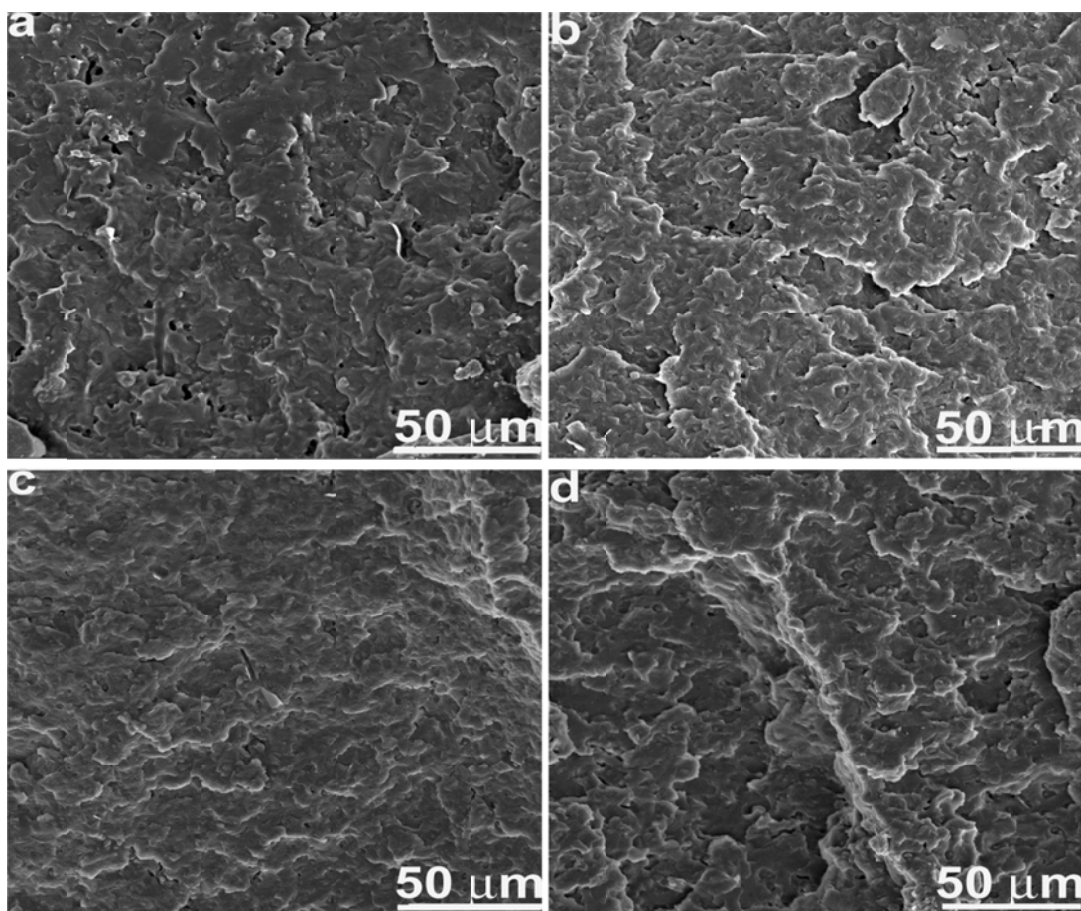


Figure 4.18 SEM micrographs of unetched (a) pristine IPC, (b) IPC/Pim, (c) IPC/Pim-CaSt (1:2), and (d) IPC/Pim-CaSt (1:3)

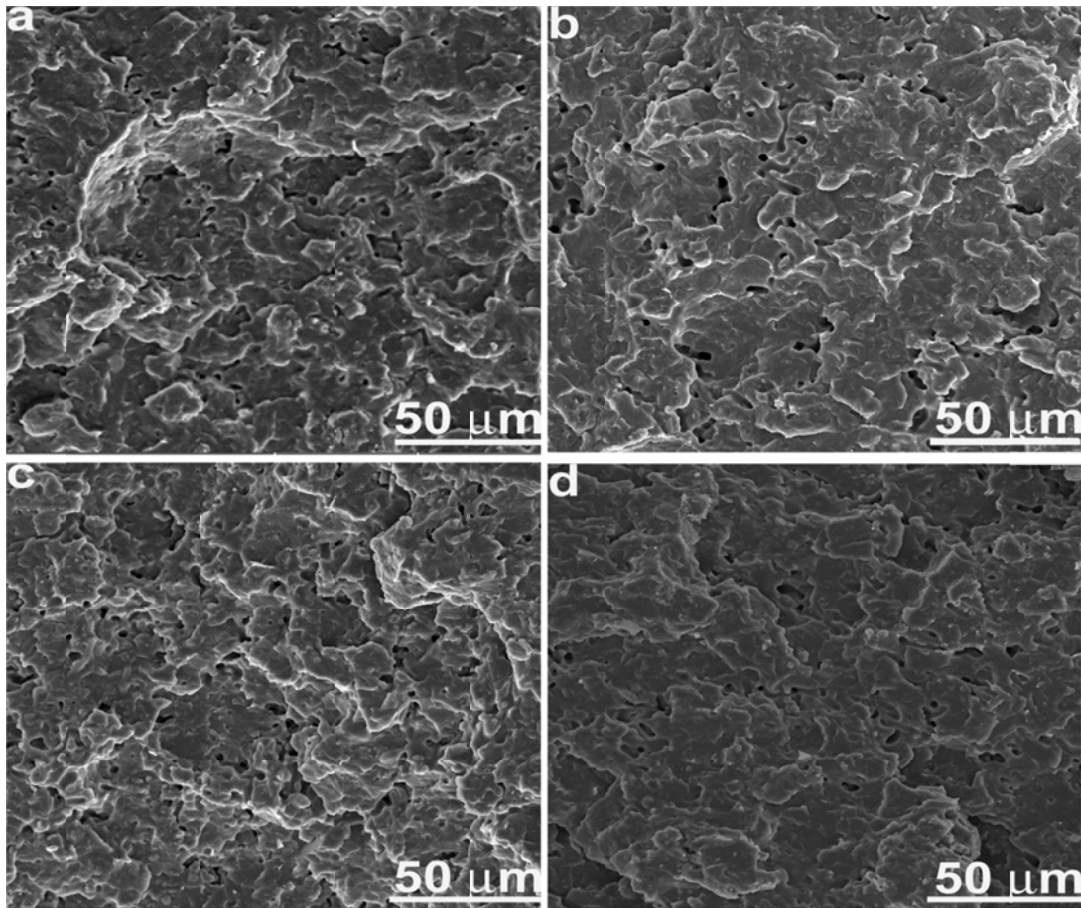


Figure 4.19 SEM micrographs of unetched (a) IPC/CaSt, (b) IPC/Adi, (c) IPC/Adi-CaSt (1:2), and (d) IPC/Adi-CaSt (1:3)

In order to see if β -nucleation had any influence on the size and distribution of the EPR (ethylene-propylene rubber) rubbery phase in IPC, the samples were etched with xylene. The SEM pictures of the etched samples are shown in Figure 4.20. Again the pictures of the pristine IPC and the nucleated samples look very similar, which is an indication that the size and distribution of the rubbery EPR phase was not significantly influenced by the β -nucleation process. Any changes in mechanical properties will, therefore, be the result of the formation of β -crystals in the IPC, and not that of changes in the size and distribution of the rubbery EPR phase.

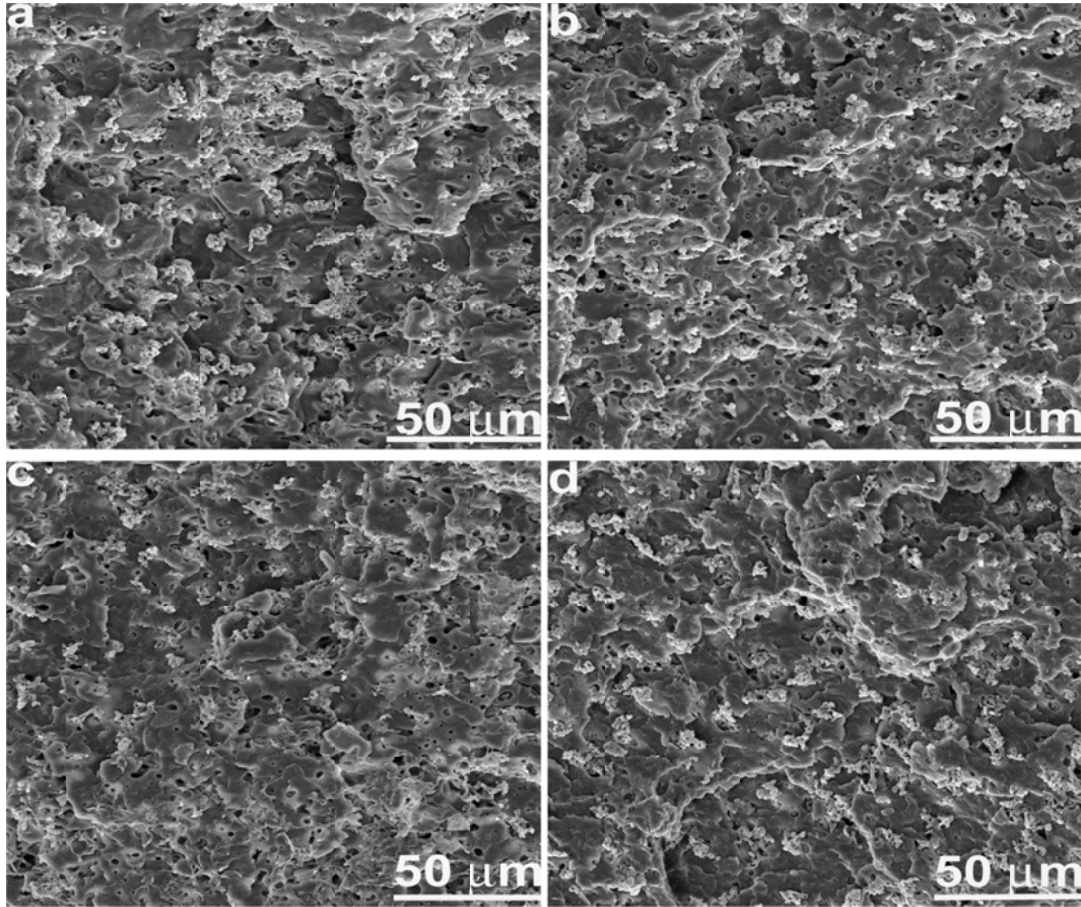


Figure 4.20 SEM micrographs of etched (a) pristine IPC, (b) IPC/Adi, (c) IPC/Pim, and (d) IPC/CaSt

Higher magnification SEM pictures for some of the etched samples are shown in Figure 4.21. All these pictures clearly show two different phases in the different samples, that are probably the rubbery EPR phase and the continuous PP phase. It is clear that the xylene etching did not completely remove the rubbery EPR phase, which is still visible in all the pictures. These pictures also confirm that β -nucleation did not change the size and dispersion of this rubbery phase.

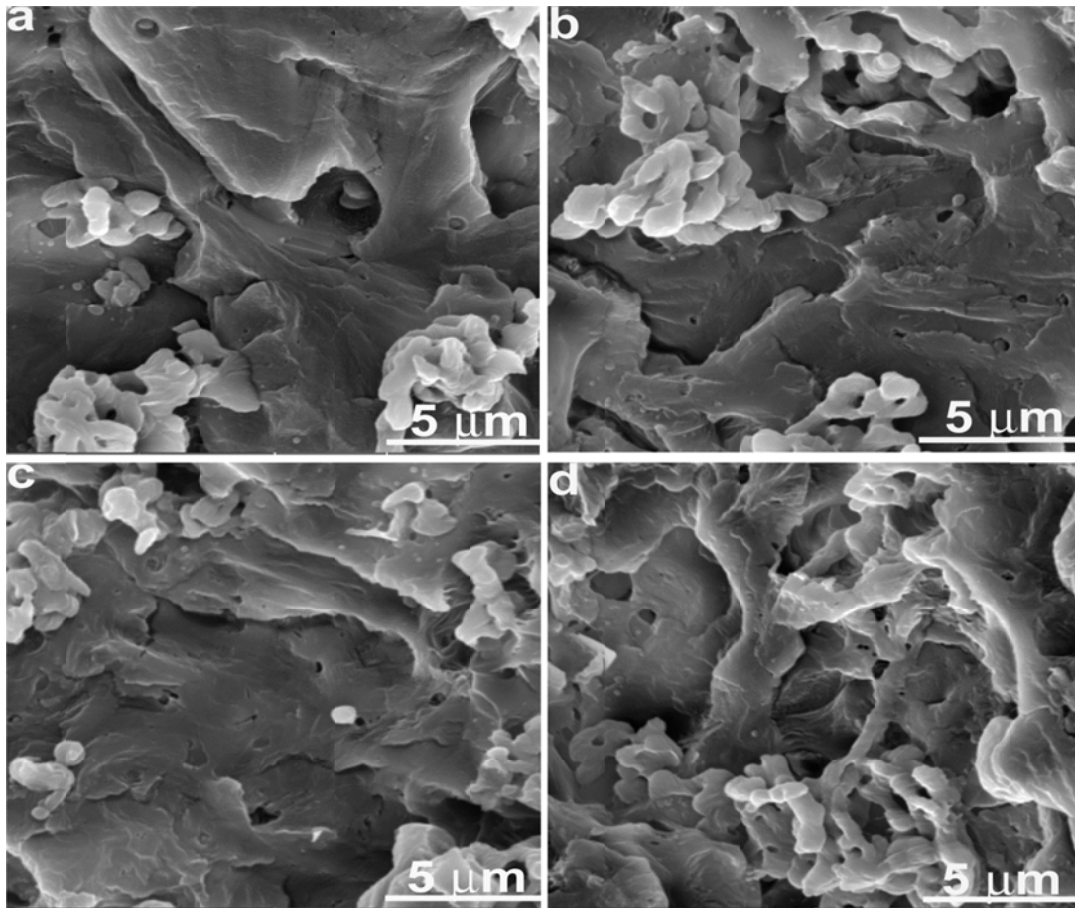


Figure 4.21 SEM micrographs of etched (a) pristine IPC, (b) IPC/Pim, (c) IPC/Pim-CaSt (1:2), and (d) IPC/Pim-CaSt (1:3) samples

4.5 Thermogravimetric analysis (TGA)

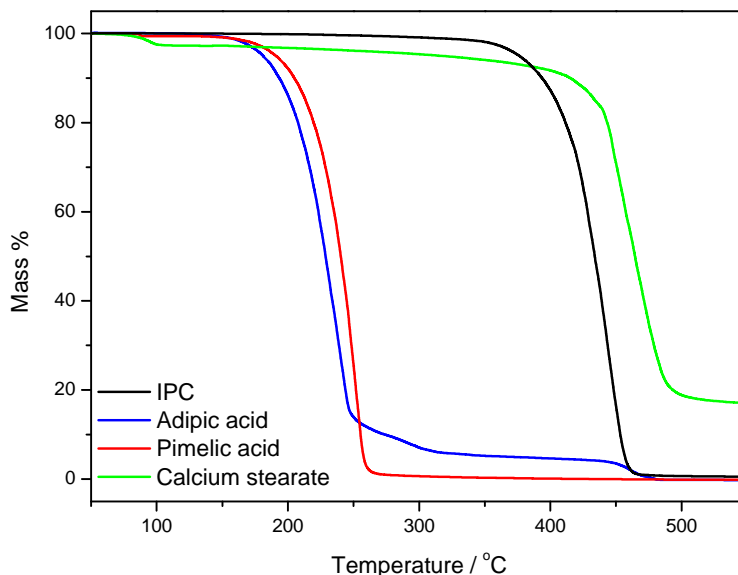


Figure 4.22 TGA curves of IPC and the individual nucleating agents

Figure 4.22 presents the TGA curves of the individual nucleating agents and the pristine IPC. CaSt shows two degradation steps at about 100 and 450 °C. These could be attributed to the evaporation of water and the degradation of the calcium stearate. It does not decompose completely as it forms calcium carbonate which is thermally stable up to 600 °C. CaSt is obviously more thermally stable than the other materials. Adi shows three decomposition steps around 200, 250 and 450 °C. These steps may be ascribed to the formation of volatile products such as alkenes, alkyls, CO₂, H₂, and CO, because carboxylic acids evolve several compounds when exposed to high temperatures [10]. Pim shows only one degradation step, that may be associated with the cleavage of the hydrocarbon chain of this compound. IPC has a higher thermal stability than the dicarboxylic acids, but lower than that of CaSt.

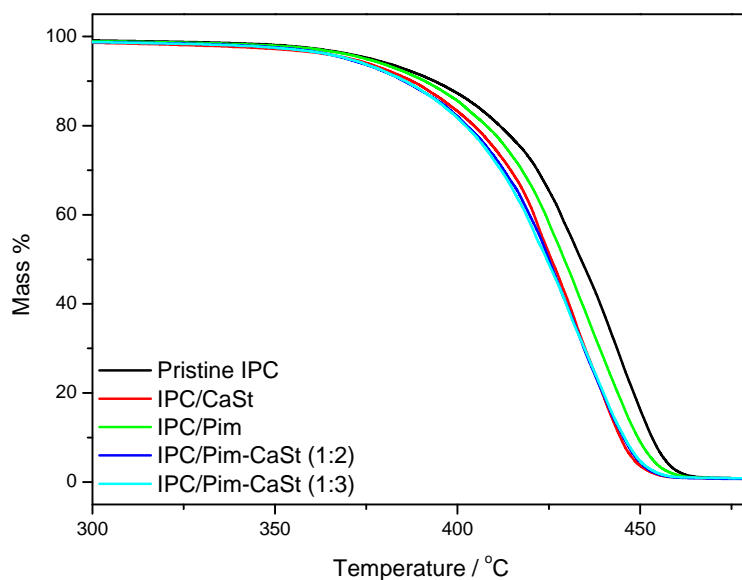


Figure 4.23 TGA curves of pristine IPC and IPC nucleated with individual (Pim, CaSt) and compounded nucleants

The TGA curves of pure IPC and the nucleated samples are shown in Figures 4.23 and 4.24, and Table 4.6 summarizes the degradation temperatures at 30 and 70% mass loss. All the samples show only one degradation step, and they decompose completely. The presence of nucleating agents slightly decreases the thermal stability of IPC. Kim and Barteau [10] investigated the catalytic decomposition mechanism of several carboxylic acids on TiO_2 . They found that carboxylic acids can form free radicals, which may attack polymer chains and initiate degradation at lower temperatures. This could be one of the reasons for the general lower thermal stabilities of the nucleated samples. Heating of CaSt yields calcium carbonate and possibly diacids [11]. These diacids can also form free radicals when heated, which will contribute to the decreasing thermal stability of IPC.

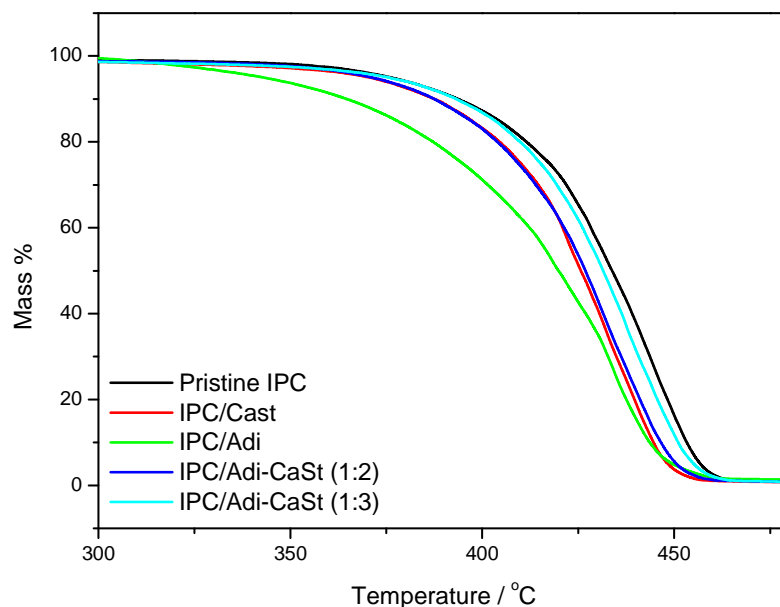


Figure 4.24 TGA curves of pristine IPC and IPC nucleated with individual (Adi, CaSt) and compounded nucleants

Table 4.6 TGA results of all the samples

Sample	T _{30%} / °C	T _{70%} / °C
Pristine IPC	421.8	443.5
IPC/Pim	417.6	438.3
IPC/Pim-CaSt (1:2)	411.6	434.4
IPC/Pim-CaSt (1:3)	411.6	434.4
IPC/CaSt	414.4	435.7
IPC/Adi	401.0	432.7
IPC/Adi-CaSt (1:2)	413.2	435.7
IPC/Adi-CaSt (1:3)	419.6	440.1

4.6 Tensile and impact properties

The tensile properties and the impact strength of all the investigated samples are shown in Figures 4.24 to 4.26, and the numerical values are summarised in Table 4.7. All the stress-strain curves are shown in Appendix C.

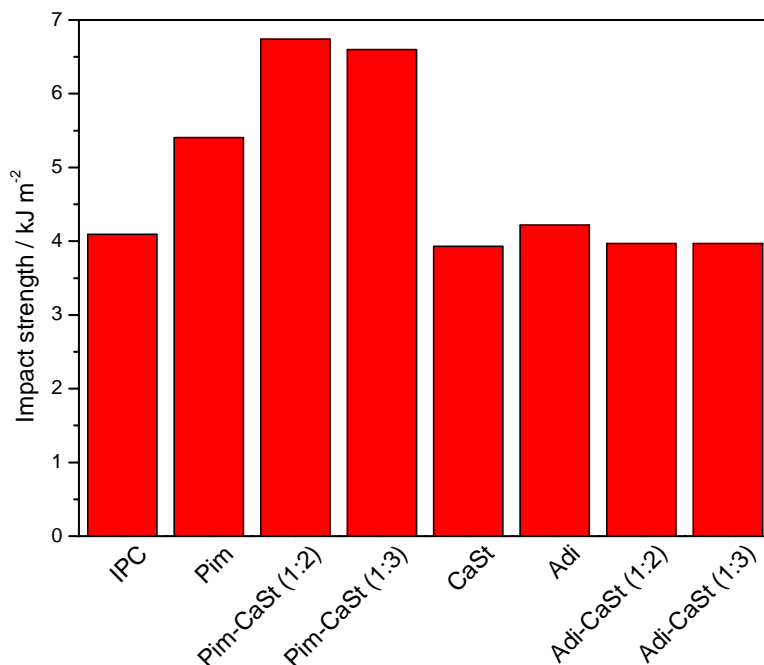


Figure 4.25 Charpy impact strength of pristine IPC and all the nucleated IPC samples

The presence of Pim and Pim-CaSt significantly increased the impact resistance of IPC, as can be seen in Figure 4.25. The improvement in impact resistance can be associated with the formation of β -crystals, which was not or only slightly observed for the samples prepared in the presence of Adi, CaSt and Adi-CaSt. The latter samples show impact strength values that are almost the same as that of pristine IPC. It has been shown that the β -phase provides more mechanical strength to a polymer than the more prominent α -phase [4,12]. Pim and Pim-CaSt nucleated samples have virtually the same amount of β -crystals, even though their impact properties differ. Luo *et al.* [13] found that impact properties depend on the size of the spherulites and the number of tie molecules. These factors determine how much energy will be dissipated by the matrix during impact.

Table 4.7 Summary of tensile and impact results for pristine IPC and the nucleated samples

Sample	σ_b / MPa	σ_y / MPa	ϵ_b / %	ϵ_y / %	E / MPa	Impact strength / kJ m^{-2}
Pristine IPC	17.1 ± 0.7	18.0 ± 0.5	17.1 ± 0.7	16.2 ± 3.2	703 ± 16	4.1 ± 0.5
IPC/Pim	15.4 ± 0.5	15.1 ± 0.7	50.1 ± 6.5	46.4 ± 6.5	645 ± 12	5.4 ± 0.6
IPC/Pim-CaSt (1:2)	15.0 ± 0.5	14.8 ± 0.6	55.2 ± 13.4	52.2 ± 14.8	644 ± 20	6.7 ± 0.4
IPC/Pim-CaSt (1:3)	15.5 ± 0.3	15.4 ± 0.3	60.0 ± 2.2	57.0 ± 3.0	642 ± 22	6.6 ± 0.2
IPC/CaSt	17.5 ± 0.9	17.4 ± 0.9	48.4 ± 3.2	45.4 ± 5.7	680 ± 35	4.0 ± 0.2
IPC/Adi	16.6 ± 0.3	16.3 ± 0.3	30.7 ± 4.2	27.9 ± 4.0	654 ± 22	4.2 ± 0.3
IPC/Adi-CaSt (1:2)	16.1 ± 0.2	15.9 ± 0.2	40.9 ± 3.9	37.3 ± 4.0	635 ± 8	4.0 ± 0.4
IPC/Adi-CaSt (1:3)	17.3 ± 1.0	16.7 ± 0.4	39.5 ± 1.5	34.1 ± 1.6	648 ± 8	4.0 ± 0.2

ϵ_y , σ_y , ϵ_b , σ_b , and E are the elongation at yield, yield stress, elongation at break, stress at break, and Young's modulus of elasticity

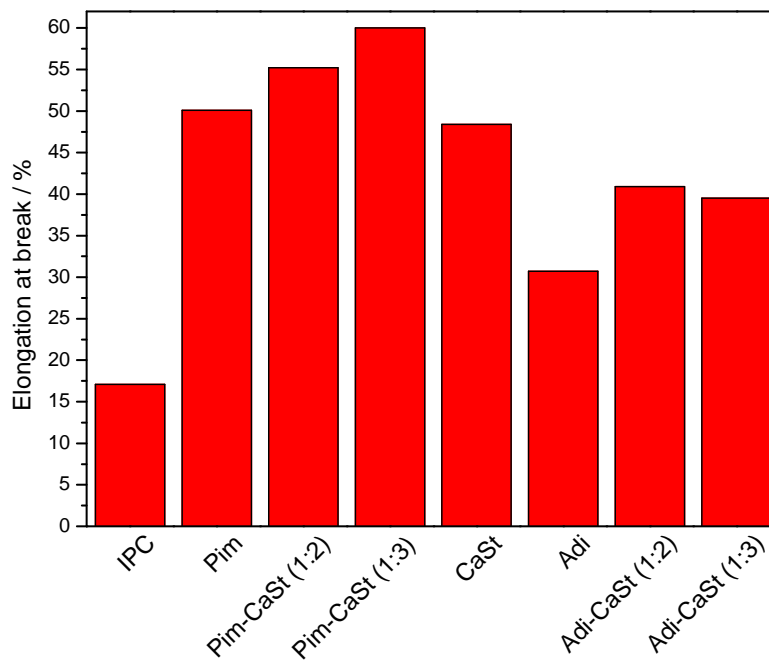


Figure 4.26 Elongation at break of pristine IPC and all the nucleated IPC samples

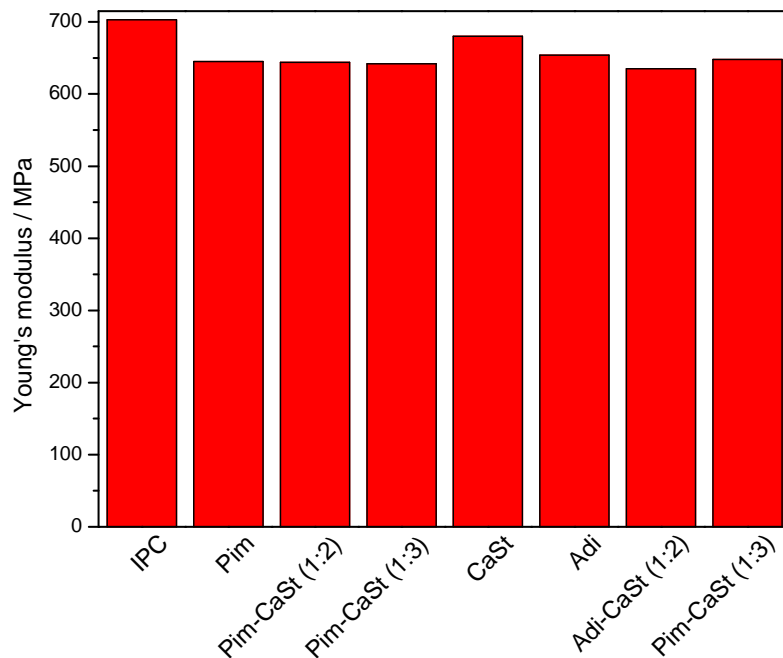


Figure 4.27 Young's modulus of pristine IPC and all the nucleated IPC samples

Figures 4.26 and 4.27 show the elongation at break and Young's modulus of all the investigated samples. All the samples show higher elongation at break values than pristine IPC, and the values for the samples nucleated with Pim-CaSt are the highest (Figure 4.26). The elongation at yield show similar increases (Table 4.7). This can be associated with the toughening effect brought by β -nucleation. Grein and co-workers [14] suggested that under mechanical loading, β -iPP can have enhanced ductility, which results from the β - to α -phase transformation. Additionally, β -crystals apparently have more tie molecules than α -crystals, leading to a stronger boundary strength between the spherulites [13]. Young's modulus, yield stress and stress at break changed very little for the nucleated samples (Table 4.7). It was reported previously that the nucleated samples show a significant decrease in Young's modulus and tensile strength [2,15]. This was associated with the β -nucleated resins having a stronger ability to initiate plastic flow during stress, a lower packing density leading to a weaker cohesive force of the β -phase, and a favourable β -lamellar arrangement with no cross-hatching structures. In our case, however, the IPC did not show a considerable loss of stiffness or strength after treatment with the nucleating agents.

4.7 Dynamic mechanical analysis (DMA)

The dynamic mechanical behaviour of all the samples is shown in Figures 4.28 to 4.31. The $\tan \delta$ curves show only one peak around 10 to 20 °C for all the samples (Figures 4.28 and 4.29). This peak is ascribed to the glass transition or β -relaxation of the PP amorphous domains. The Pim and Pim-CaSt nucleated samples show a slight shift of this peak to higher temperatures. Labour and others [15,16] suggested that when the T_g shifts to high temperatures in β -iPP, it is a reflection of slight immobilization of the chains in the amorphous phase in the vicinity of the β -lamellae. On the other hand, the Adi and Adi-CaSt nucleated samples show almost no shift of the β -relaxation peak. This is in line with the previous results that indicated a very small extent of β -nucleation for these samples.

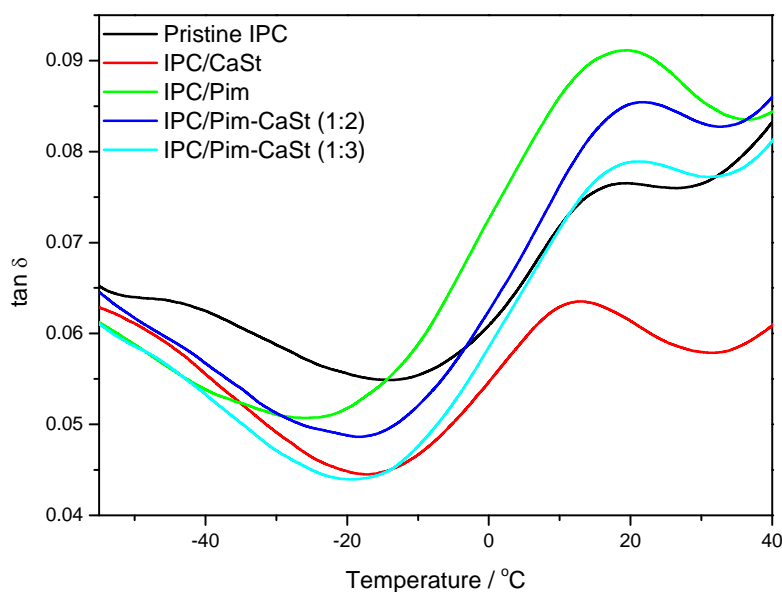


Figure 4.28 DMA $\tan \delta$ curves for pure IPC and the nucleated (Pim, CaSt) samples

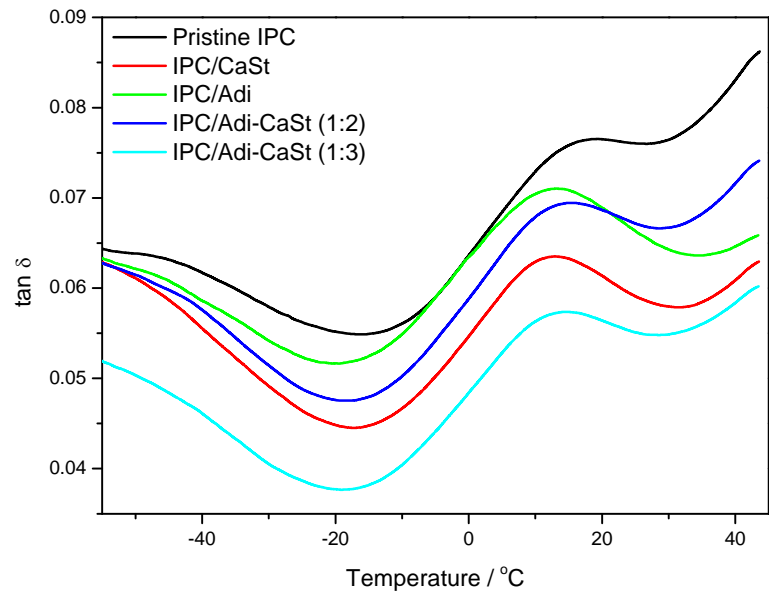


Figure 4.29 DMA $\tan \delta$ curves for pure IPC and the nucleated (Adi, CaSt) samples

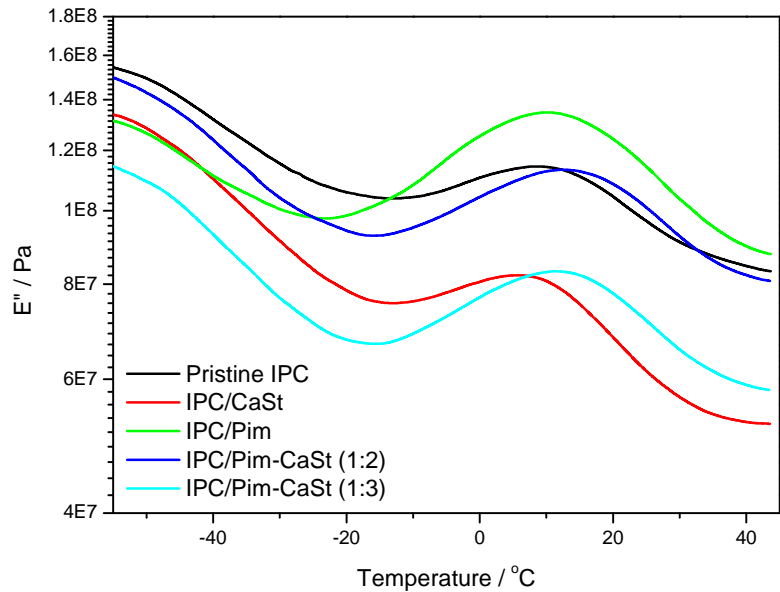


Figure 4.30 DMA loss modulus curves for pure IPC and the nucleated (Pim, CaSt) samples

The loss modulus curves for all the samples are presented in Figures 4.30 and 4.31. These curves clearly confirm the shift of the β -relaxation peak. The β -nucleated samples also seem to have more intense β -relaxation peaks. Luo *et al.* [17] investigated the toughness of a β -IPC by an approximation of the peak intensity. They pointed out that the higher the peak intensity of the β -relaxation, the larger the toughness of the β -nucleated IPC. This observation was confirmed in our analysis of the tensile- and impact properties of these samples, where the impact strength and elongation at yield significantly increased for the β -nucleated samples.

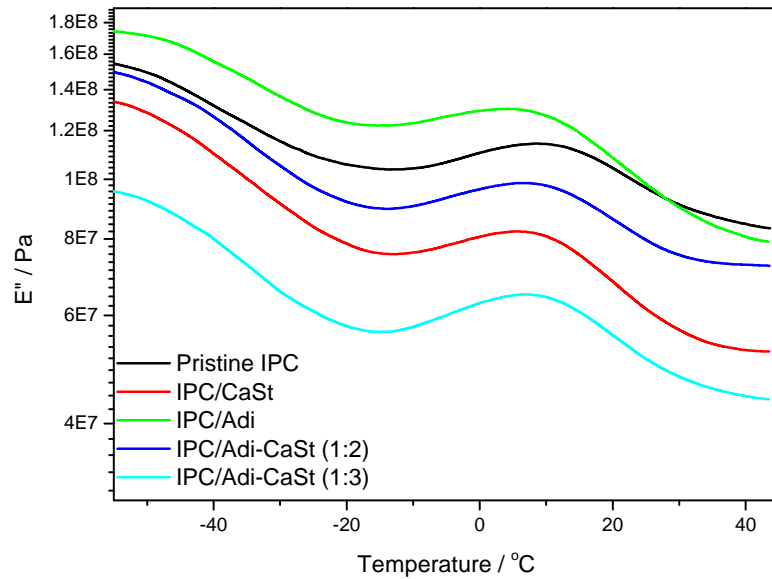


Figure 4.31 DMA loss modulus curves for pure IPC and the nucleated (Adi, CaSt) samples

4.8 References

1. B. Fillon, A. Thierry, B. Lotz, J.C. Wittmann. Efficiency scale for polymer nucleating agents. *Journal of Thermal Analysis* 1994; 42:721-731.
DOI: 10.1007/BF02546745
2. A. Zeng, Y. Zheng, S. Qui, Y. Guo, B. Li. Mechanical properties and crystallization behavior of polypropylene with cyclodextrin derivative as β -nucleating agent. *Colloid and Polymer Science* 2011; 289:1157-1166.
DOI: 10.1007/s00396-011-2441-9

3. Z. Wei, W. Zhang, G. Chen, J. Liang, S. Yang, P. Wang, L. Liu. Crystallization and melting behavior of isotactic polypropylene nucleated with individual and compound nucleating agents. *Journal of Thermal Analysis and Calorimetry* 2010; 102:775-783.
DOI: 10.1007/s10973-010-0725-9
4. F. Luo, K. Wang, N. Ning, C. Geng, H. Deng, F. Chen, Q. Fu, Y. Qian, D. Zheng. Dependence of mechanical properties on β -form content and crystalline morphology for β -nucleated isotactic polypropylene. *Polymer for Advanced Technologies* 2011; 22:2044-2054.
DOI: 10.1002/pat.1718
5. Y. Fan, C. Zhang, Y. Xue, X. Zhang, X. Ji, S. Bo. Microstructure of two polypropylene homopolymers with improved impact properties. *Polymer Journal* 2011; 52:557-563.
DOI: 10.1016/j.polymer.2010.12.009
6. T. Liu, Z. Mo, S. Wang, H. Zhang. Nonisothermal melt and cold crystallisation kinetics of poly(aryl ether ether ketone ketone). *Polymer Engineering and Science* 1997; 37:568-575.
DOI: 10.1002/pen.11700
7. L. Xu, X. Zhang, K. Xu, S. Lin, M. Chen. Variation of non-isothermal crystallization behavior of isotactic polypropylene with varying β -nucleating agent content. *Polymer International* 2010; 59:1441-1450.
DOI: 10.1002/pi.2891
8. X.L. Jiang, S.J. Luo, K. Sun, X.D. Chen. Effect of nucleating agents on crystallization kinetics of PET. *eXPRESS Polymer Letters* 2007; 1:245-251.
DOI: 10.3144/expresspolymlett.2007.37
9. X. Li, K. Hu, M. Ji, Y. Huang, G. Zhou. Calcium dicarboxylates nucleation of β -polypropylene. *Journal of Applied Polymer Science* 2002; 86:633-638.
DOI: 10.1002/app.10913
10. K.S. Kim, M.A. Barteau. Pathways for carboxylic acid decomposition on titania. *Langmuir* 1988; 4:945-953.
DOI: 10.1021/la00082a028
11. S. Gal, T. Meisel, L. Erdey. On the thermal analysis of aliphatic carboxylic acids and their salts. *Journal of Thermal Analysis* 1969; 1:159-170.
DOI: 10.1007/BF01909666

12. Q. Duo, Q.-L. Lu. Effect of calcium malonate on the formation of β crystalline form in isotactic polypropylene. *Polymers for Advanced Technologies* 2008; 19:1522-1527.
DOI: 10.1002/pat.1160
13. F. Luo, J. Wang, H. Bai, K. Wang, H. Deng, Q. Zhang, F. Chen, Q. Fu, B. Na. Synergistic toughening of polypropylene random copolymer at low temperature: β -modification and annealing. *Materials Science and Engineering A* 2011; 528:7052-7059.
DOI: 10.1016/j.msea.2011.05.030
14. C. Grein, C.J.G. Plummer, H.-H. Kausch, Y. Germain, Ph. Beguelin. Influence of β nucleation on the mechanical properties of isotactic polypropylene and rubber modified isotactic polypropylene. *Polymer* 2002; 43:3279-3293.
DOI: 10.1016/S0032-3861(02)00135-0
15. C. Grein. Toughness of neat, rubber modified and filled β -nucleated polypropylene: from fundamentals to application. *Advances in Polymer Science* 2005; 188:43-104.
DOI: 10.1007/b136972
16. T. Labour, C. Gauthier, R. Seguela, G. Vigier, Y. Bomal, G. Orange. Influence of the β crystalline phase on the mechanical properties of unfilled and CaCO_3 -filled polypropylene. I. Structural and mechanical characterisation. *Polymer* 2001; 42:7127-7135.
DOI: 10.1016/S0032-3861(01)00089-1
17. F. Luo, C. Xu, K. Wang, H. Deng, F. Chen, Q. Fu. Exploring temperature dependence of the toughening behavior of β -nucleated impact polypropylene copolymer. *Polymer* 2012; 53:1783-1790.
DOI: 10.1016/j.polymer.2012.02.024

CHAPTER 5

CONCLUSIONS

The aim of the current work was (i) to induce the highest possible β -crystal content in an impact polypropylene copolymer (IPC) by adding nucleating agents (NAs) and also by using a feasible preparation method, (ii) to establish the nucleation efficiency (NE) of the individual and bi-component nucleants, and (iii) to investigate the effect of β -nucleation on the thermal and mechanical properties of IPC. Another objective was to determine in which of the IPC TREF fractions the formation of β -crystals is dominant.

Nucleated IPC samples were prepared by extrusion followed by compression moulding under pre-investigated conditions that were found to induce the highest β -crystal content. When using pimelic acid based NAs, we managed to obtain samples with about 90% of β -crystals. However, calcium stearate and adipic acid based NAs had very low NE values, and correspondingly gave rise to very low or no β -crystal contents. Generally the combination of pimelic acid and adipic acid with calcium stearate did not significantly change the NEs of the respective acids, although the Adi-CaSt (1:2) combination seemed to have given slightly better results. Analysis of the TREF fractions showed that the 110C and 120C fractions had very high β -crystal contents, while the lower temperature and the 140C fractions did not show any β -crystal content. This observation was related to the isotactic PP content in the different fractions.

Investigation of the crystallinities of the different nucleated samples showed higher total crystallinity values for the Pim nucleated samples from the XRD measurements than from the DSC measurements. This was attributed to the fact that the crystals, formed as a result of nucleation in the presence of Pim, were thermally labile and that 'de-crystallisation' took place during the heating process in the DSC. The α - and β -crystallization were found to occur over the same temperature range, and non-isothermal crystallisation kinetics revealed the crystallisation to occur according to a three-dimensional growth with athermal nucleation mechanism. The treatment with NAs did not seem to change the crystallisation mechanism of

IPC, although it was found that α -crystallisation is the thermodynamically preferable process because of the low crystallisation activation energy of non-nucleated IPC.

None of the NAs chemically reacted with IPC, and the chemical structure of the polymer was thus intact during the treatment. Although there were different crystal structures in the nucleated IPC, it was not possible to visually distinguish between them through the use of electron microscopy. β -nucleation also did not seem to have changed the distribution of the soft EPR fractions in the IPC. The thermal stabilities of the β -nucleated samples slightly decreased, probably because of the catalytic effect of the NAs on the decomposition of the polymer. Elongation at yield and break increased, indicating the improved ductility of the nucleated IPC. The small changes in Young's modulus and yield stress suggest that the nucleated IPC did not lose its stiffness. The property that was most affected by β -nucleation was the impact resistance of the IPC. This value increased by more than 50% for the IPC/Pim-CaSt samples. The glass transition temperatures of the β -nucleated samples were obviously higher than those of the other samples.

To summarize, although the α -polymorph was not completely suppressed, even when using high NE NAs, most of the properties were positively influenced by the presence of β -crystals. Our study indicated that, although compounding of Pim with CaSt had a strong influence on some properties, β -nucleation by Pim alone would be sufficient to form a large concentration of β -crystals, which would have a positive impact on most of the properties. Adi and CaSt were, however, found to be fairly inefficient β -nucleating agents.

Recommendations for future work:

- ❖ The use of IPCs with different rubber contents and melt flow indices in order to investigate the effect of the rubbery phase content on the formation of β -crystals.
- ❖ It is also important to use other microscopic techniques to try and distinguish between the different crystalline phases.
- ❖ The total concentration of the nucleating agent should be evaluated to find the optimum concentration for the formation of the highest possible β -crystal content. Similarly the preparation method should be critically evaluated.

ACKNOWLEDGEMENTS

I would like pass my sincere gratitude to our Lord Jesus Christ for giving us an enormous strength and power to make the work of this project and the compilation of this thesis possible.

I would also like give great thanks to my supervisor and co-supervisor, **Prof. Adriaan S. Luyt and Prof. Albert J van Reenen**, for their support and helpful guidance which enriched my knowledge. During the rough time when I was preparing my samples they were very helpful. They also give me great support during my travelling periods to Stellenbosch, and Prof van Reenen always made me feel welcome. The thesis writing was well guided by Prof. Luyt and I just want thank him for grooming me and developing my writing skills.

Studying could not have been possible if the University of the Free State did not give me an opportunity to do my studies, and for this I am very grateful. I also need to give a big thanks to Prof Luyt's secretary, Mrs Marlize Jackson, for always being so friendly and welcoming.

I'd like to thank my parents (Mr and Mrs Joseph and Elisa Motsoeneng) for giving life, nurturing, raising me up, and also teaching me respect, responsibility, care and loving myself and other people around me.

Sense of gratitude to all my fellow polymer science research group and colleagues (Mr. Mfiso Mngomezulu, Mr. Tshwafo Motaung, Ms. Julia Puseletso Mofokeng, Mr. Thabang Hendrica Mokhothu, Mr. Teboho Mokhena, Mr. Sefadi, Ms. Motshabi Sibeko, Mr. Jonas Mochane, Mr. Tladi Mofokeng, Ms. Sheryl-Ann Clarke, Mr. Tsietsi Tsotetsi, Mrs Nomampondomise Molefe, Mrs Moipone Malimabe, and Mr Rantoa Moji), for being so helpful, giving support, interest and useful inputs.

All sense of gratitude to my brothers Felleng, Thapelo, Sabata and Gauta, and to my niece Mamokete Dhladhla.

I wish to greatly thank my best friends ÉI Deere Bendiòn de Sòzä Béninhø, Tladi Mofokeng, Jonas Mochane, and Teboho Mokhena for helping me to surmount the rough times, and for all the good ideas shared.

Appendix A

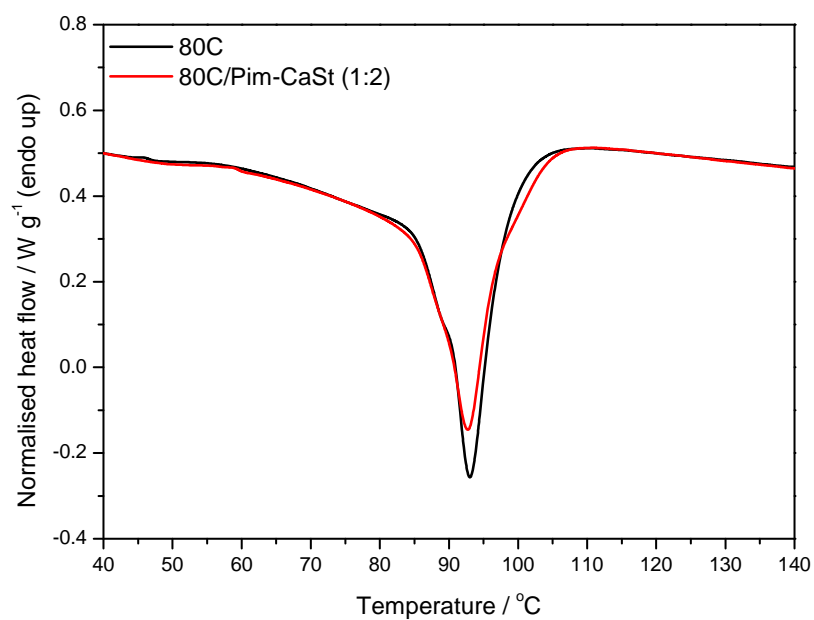


Figure A.1 DSC cooling curves of nucleated and non-nucleated 80C

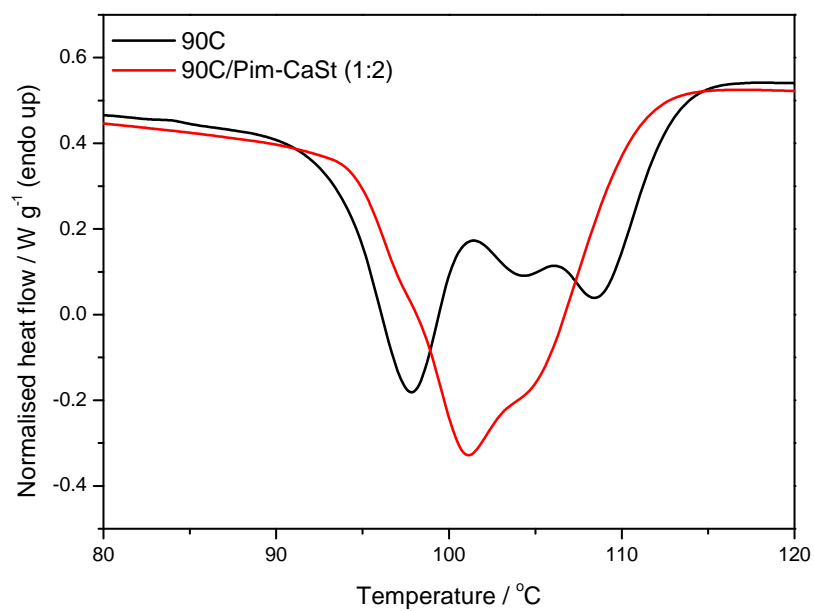


Figure A.2 DSC cooling curves of nucleated and non-nucleated 90C

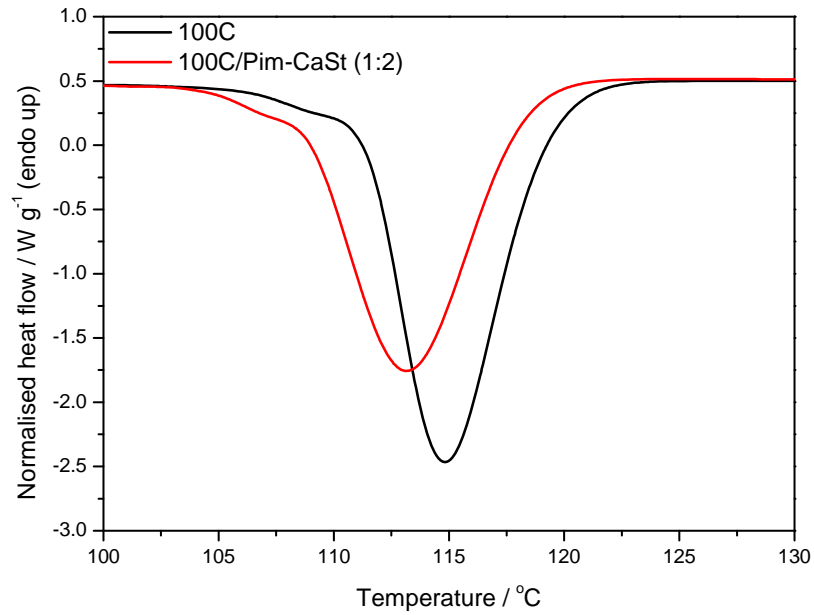


Figure A.3 DSC cooling curves of nucleated and non-nucleated 100C

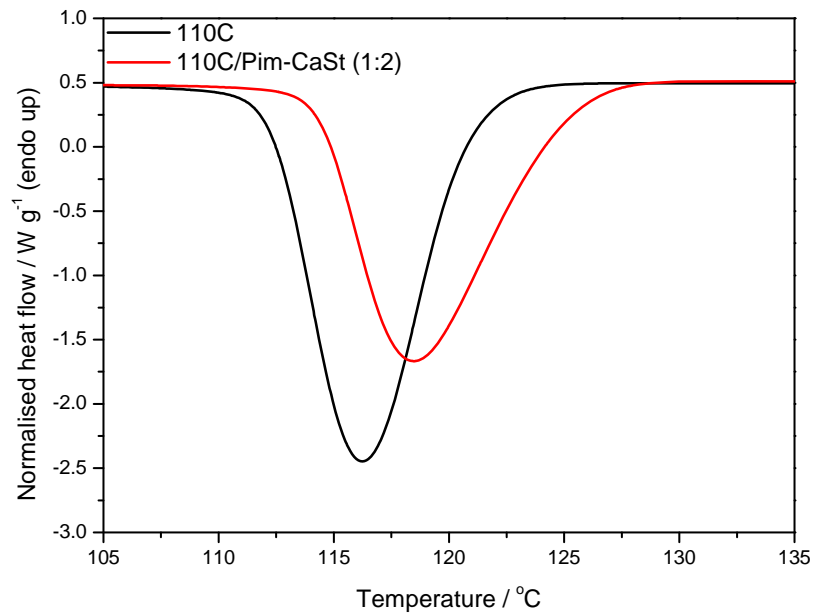


Figure A.4 DSC cooling curves of nucleated and non-nucleated 110C

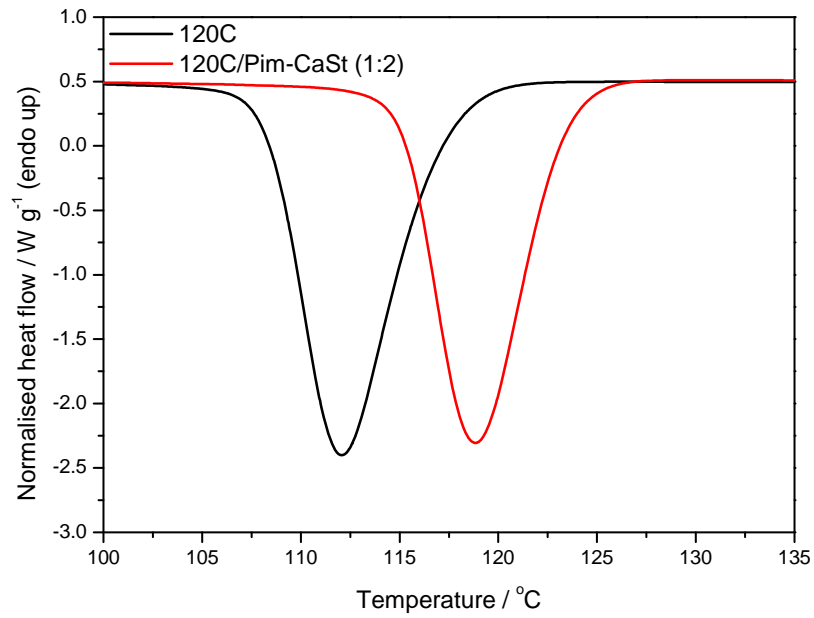


Figure A.5 DSC cooling curves of nucleated and non-nucleated 120C

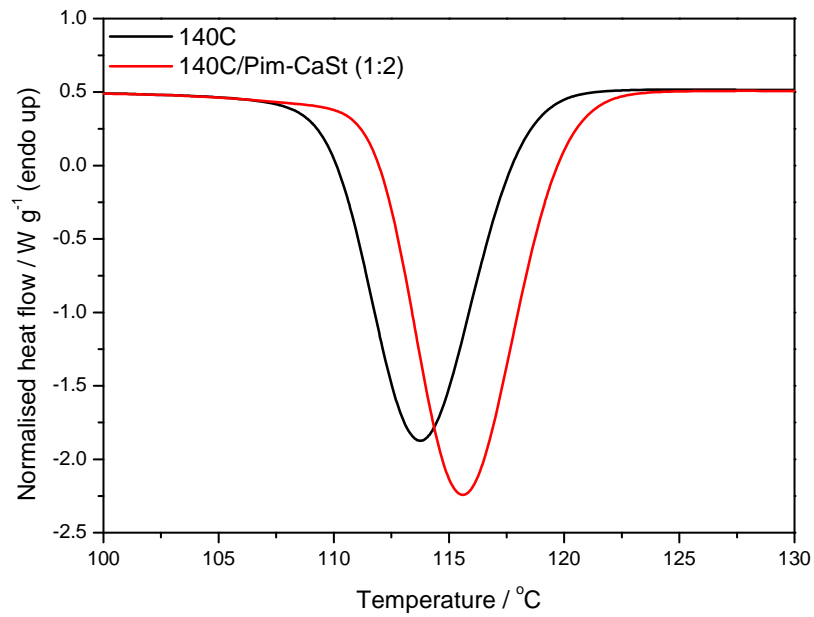


Figure A.6 DSC cooling curves of nucleated and non-nucleated 120C

Appendix B

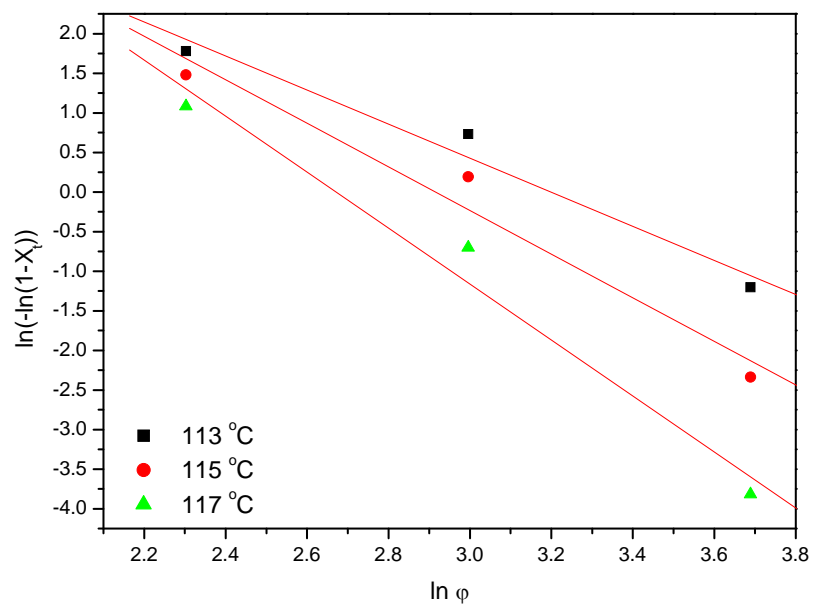


Figure B.1 $\ln(-\ln(1-X_t))$ versus $\ln \phi$ of pristine IPC

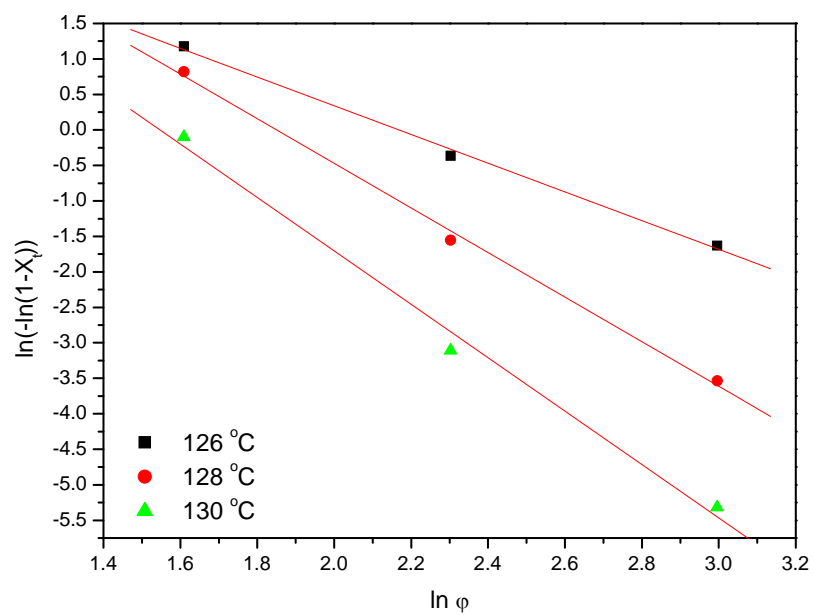


Figure B.2 $\ln(-\ln(1-X_t))$ versus $\ln \phi$ of IPC/Pim-CaSt (1:2)

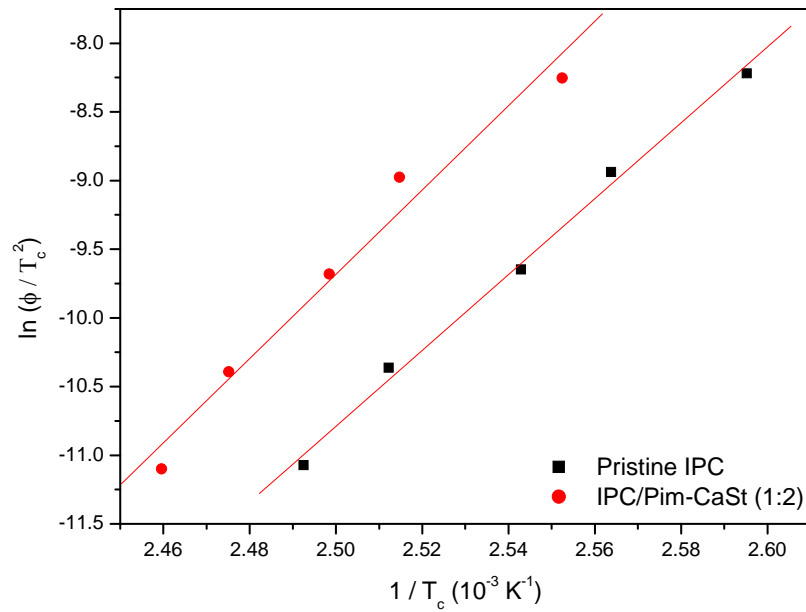


Figure B.3 Kissinger plot for determining nonisothermal crystallisation activation energies

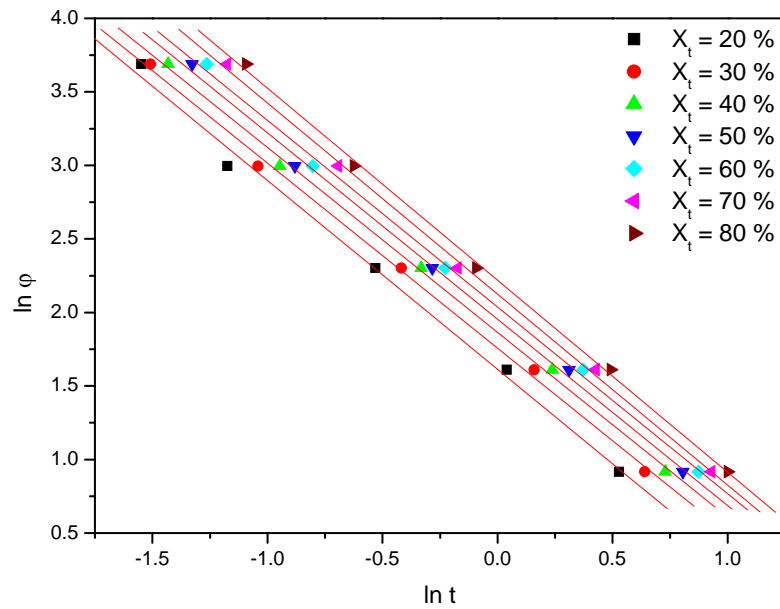


Figure B.4 Plot of $\ln \phi$ versus $\ln t$ of pristine IPC at various cooling rates

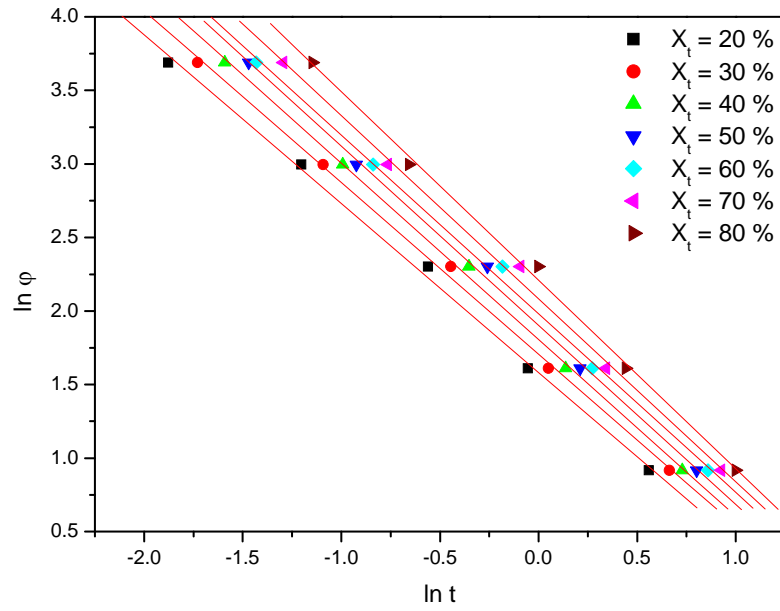


Figure B.5 Plot of $\ln \phi$ versus $\ln t$ of IPC/Pim-CaSt (1:2) at various cooling rates

Appendix C

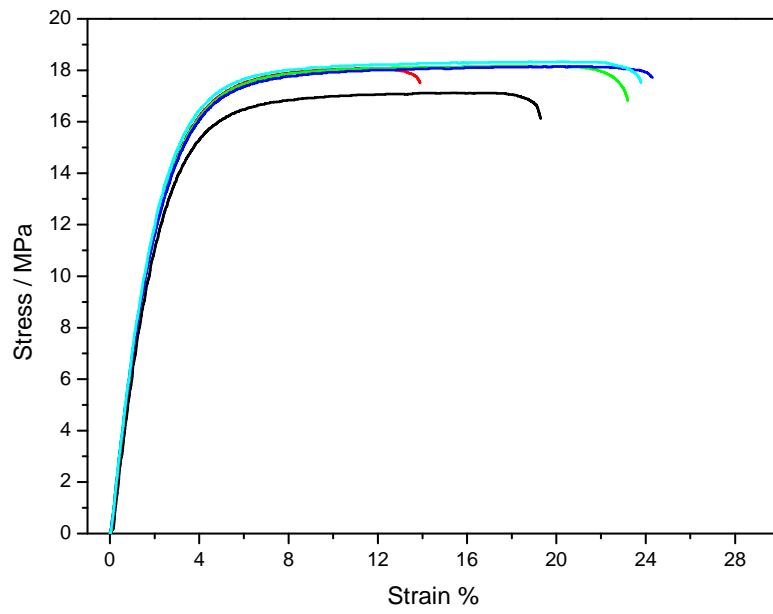


Figure C.1 Stress-strain curves of the pristine IPC

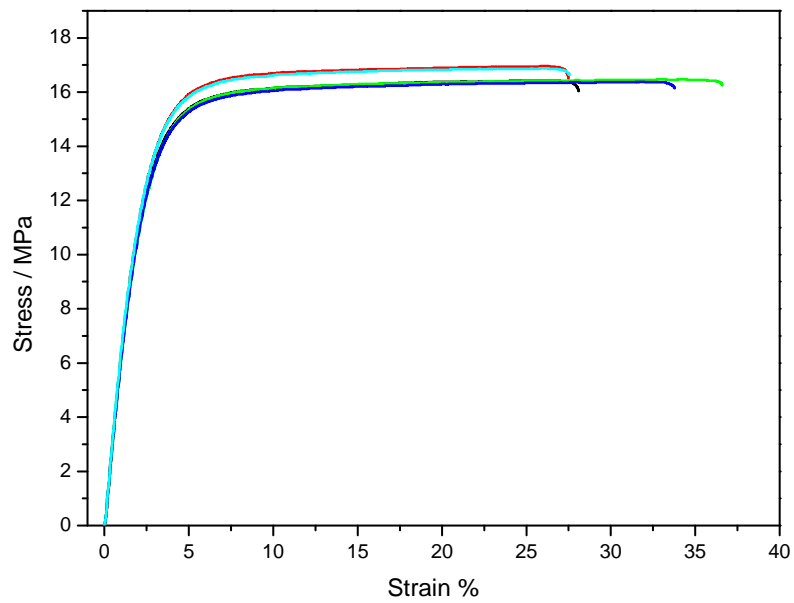


Figure C.2 Stress-strain curves of IPC/Adi

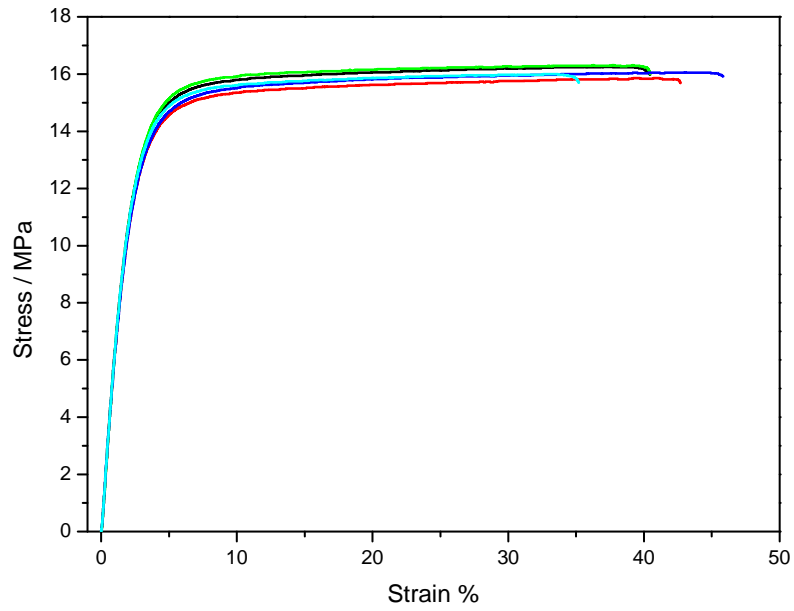


Figure C.3 Stress-strain curves of IPC/Adi-CaSt (1:2)

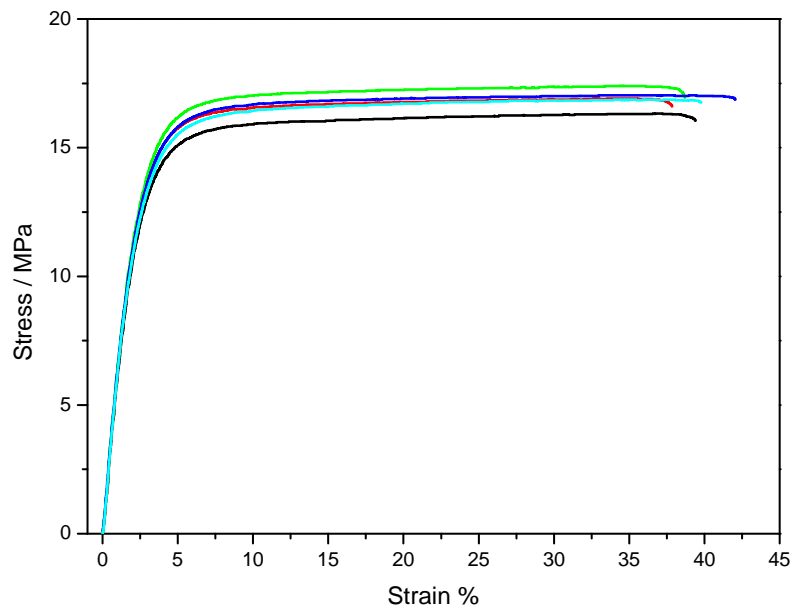


Figure C.4 Stress-strain curves of IPC/Adi-CaSt (1:3)

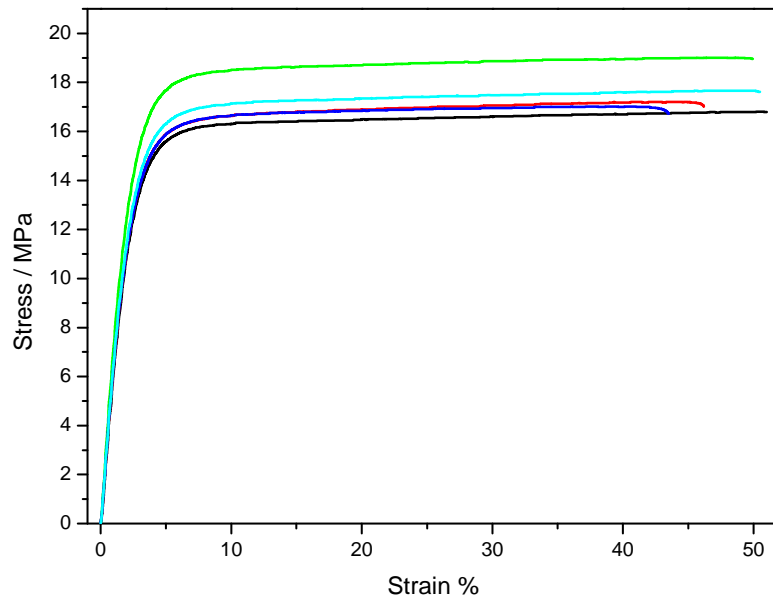


Figure C.5 Stress-strain curves of IPC/CaSt

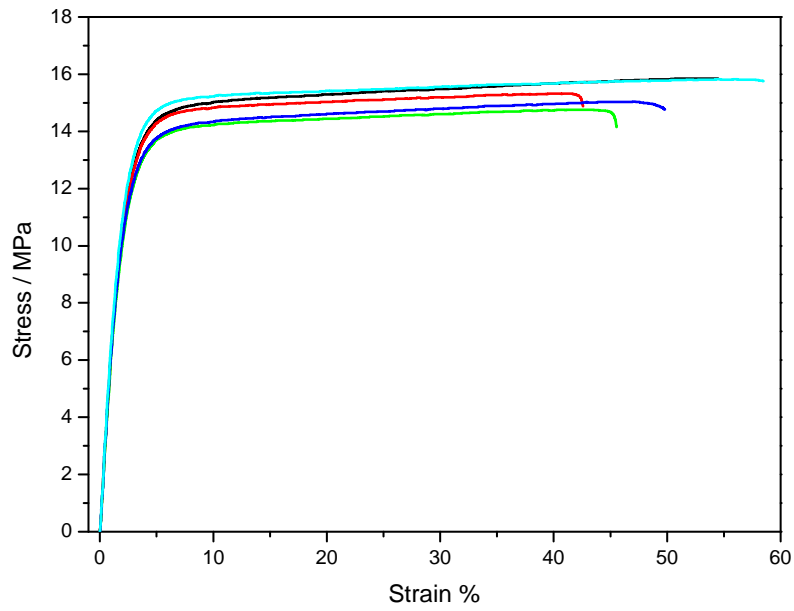


Figure C.6 Stress-strain curves of IPC/Pim

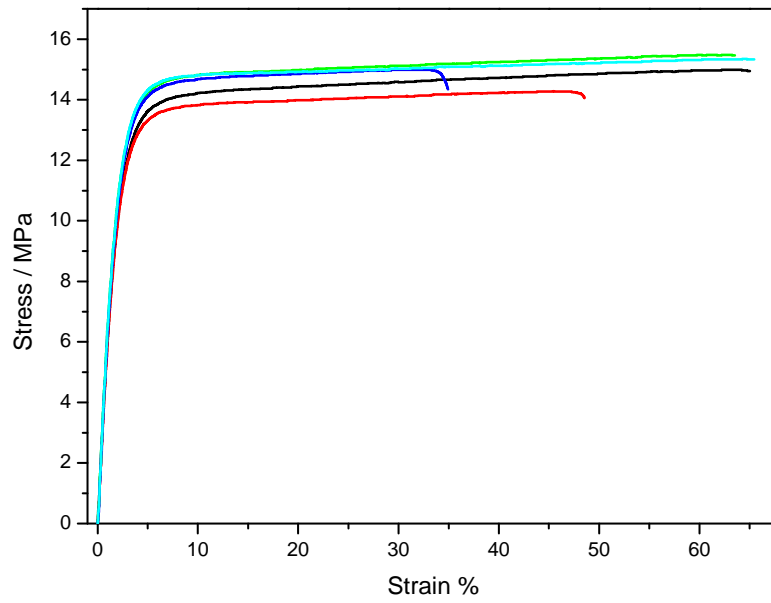


Figure C.7 Stress-strain curves of IPC/Pim-CaSt (1:2)

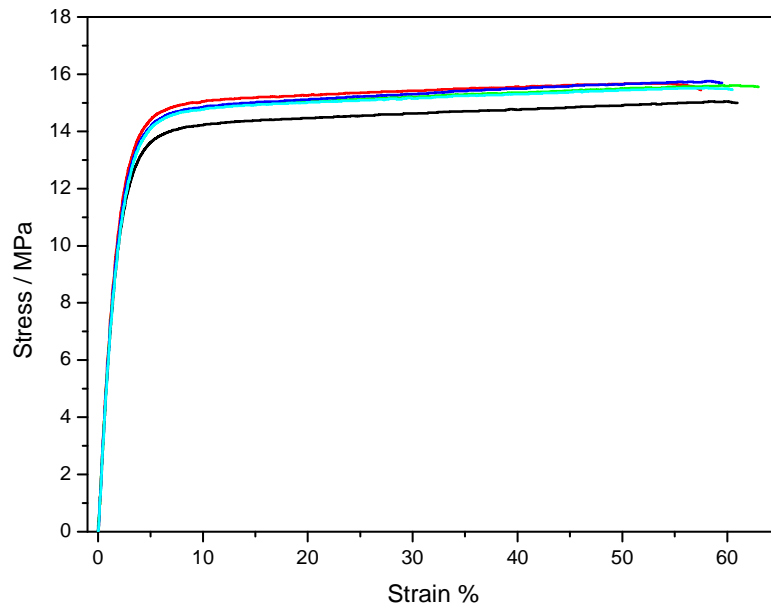


Figure C.8 Stress-strain curves of IPC/Pim-CaSt (1:3)